ADDIS ABABA UNIVERSITY

INSTITUTE OF TECHNOLOGY SCHOOL OF GRADUATE STUDIES

DEPARTMENT OF CIVIL ENGINEERING

THE EFFECT OF LAND USE CHANGE ON HYDROLOGY OF AKAKI CATCHMENT

By

ABDRHMAN BERGA

Advisor: Dr. YONAS MICHAEL

July, 2011

THE EFFECT OF LAND USE CHANGE ON HYDROLOGY OF AKAKI CATCHMENT

By

ABDRHMAN BERGA

A thesis submitted to the School of Graduate Studies of Addis Ababa University Institute of Technology in partial fulfillment of the requirements for the degree of Master of Science in Hydraulics Engineering

Addis Ababa University Institute of Technology

July, 2011

Declaration and Copyright

I, Abdrhman Berga, do here by declare to the Senate of Addis Ababa University that this thesis is entirely original work and all other materials are duly acknowledged. This work has not been submitted for any academic degree award at any University.

Declaration

ADDIS ABABA UNIVERSITY

ADDIS ABABA INSTITUTE OF TECHNOLOGY

SCHOOL OF GRADUATE STUDY

EFFECT OF LANDUSE CHANGE ON HYDROLOGY OF AKAKI CATCHMENT

By Abdrhman Berga

APPROVED BY BOARD EXAMINERS

1. Ato Habtamu Mihrete	……..	……
Chairman	Signature	Date
2. Dr Yonas Michael	……..	……
Advisor	Signature	Date
3. Dr Habtamu Hailu	……..	……..
External Examiner	Signature	Date
4. Dr Daniel F/selassie	……..	……..
Internal Examiner	Signature	Date

ACKNOWLEDGEMENT

First of all, I would like to thank 'Almighty Allah' who made it possible, to begin and finish this work successfully.

I would like express my wholehearted gratitude to my advisors, Dr. Yonas Michael, for his priceless support in supervising my work and providing me with important reference materials.

I thank Africa Muslim Agency (Direct Aid) for awarding me a financial support made through the post graduate program of AAiT.

The data receipt used in this study from Ministry of Water Resource and Energy ,Ethiopian Mapping Authority, National Meteorological Service Agency, Addis Ababa City Administration, HALCROW and Addis Ababa Water and Sewerage Authority (AAWSA) particularly Technical staffs of Akaki Branch office gratefully acknowledged.

My classmates are all acknowledged, especially Abynhe A., Ahmed M., Bogale T., and Daniel T., deserves special thanks.

Last but not least, I would like to thank my family, especially my father for his continuous support and encouragement that Contribute great to my life.

Dedication

To my beloved father Berga Biza

ABSTRACT

The main goal of this study is to assess the past and potential future land cover changes, and their impact on the hydrology of the Akaki catchment which is located in upper-Awash basin with a total area of 1429 km^2. Specifically, the study analyzed the historical land cover changes (1973 to 2000) that have taken place in the catchment and its effect on the hydrology of the catchment. Also land cover change of future scenario was used to determine the potential effect that will happen on the catchment hydrology.

This study contributes a lot on understanding history of development progresses and their impact on land use and land cover change which influences the streamflow directly. This enhances the ability of planners, researchers and city development actors to formulate and implement sound policies to minimize undesirable future impacts and management alternatives. Also the study has significant role on future flood control of the study area.

The land cover changes within the watershed were examined through classification of satellite images with integrated use of ERDAS imagine (Version 9.1) and Arc GIS software. The Soil and Water Assessment Tool (SWAT) model was used to investigate the impact of land cover change on streamflow of the study area. The model was set up using readily available spatial and temporal data, and calibrated against measured discharge.

Land cover change analysis has shown that the Settlement area has increased from 4.5% to 12.5%, Cultivated land from 35% to 44% between 1973 and 2000, while Forest area has decreased from 19% to 15% and Grass land from 41% to28%.

Sensitivity analysis result shown that both Curve Number (CN) and Alpha factor are the most sensitive parameters affecting the hydrology of the catchment. The model was calibrated from 1997-2002 and validated from 2003-2004 at the Big Akaki river which is gauged part of the catchment. The performance of the model was evaluated on the basis of performance rating criteria, coefficient of determination (R^2), Nash and Sutcliff efficiency (NSE), and percent deviation. The R^2 and NSE values for the catchment were 0.87and 0.85 for calibration, 0.81 and 0.76 for validation respectively.

The evaluation of the SWAT model response to these LU/LC changes shows annual stream flow was increased by 9% from 1973 to 1986 and 17% from 1986 to that of 2000. Generally, the analysis indicated that flow during the wet and dry season has increased by 16%, decreased by 4%.Finally, from the results above show that the changes in stream flow characteristics could be relayed to the change of the land cover during the studied period.

TABLE OF CONTENT

LIST OF FIGURES

LIST OF TABLES

LIST OF ABBREVIATIONS

AACA	Addis Ababa City Administration
AAWSA	Addis Ababa Water and Sewerage Authority
AVHRR	Advanced Very High Resolution Radiometer
CAD	Computer Aided Design
DEM	Digital Elevation Model
DN	Digital Number
EMR	Electro Magnetic Radiation
ERDAS	Earth Resources Data Analysis System
ER	Electromagnetic Radiation
ETM+	Enhanced Thematic Mapper
EMA	Ethiopian Mapping Authority
FAO	Food and Agriculture Organization
GIS	Geographic Information System
GLCF	Global Land Cover Facility
GWQ	Groundwater Contribution to Streamflow (main channel)
HRU	Hydrological Response Unit
ISODATA	Iterative Self Organizing Data Analysis Technique
JICA	Japan International Co-operation Agency
LUCC	Land Use and Land Cover Change
LULC	Land Use and Land Cover
LU/LC	Land Use and Land Cover
MDG	Millennium Development Goal
MOWR	Ministry of Water Resource
+masl	Meter Above mean Sea Level

MSS	Multi Spectral Scanner
NSE	Nash Sutcliff Efficiency
NMSA	National Meteorological Service Agency
PET	Potential Evapotranspiration
RS	Remote Sensing
SCS	Soil Conservation System
SURQ	Surface Runoff Contribution to Streamflow (main channel)
SWAT	Soil and Water Assessment Tool
UTM	Universal Trans Mercator
TM	Thematic Mapper
WGEN	Weather Generator

CHAPTER ONE

1 Introduction

1.1Back Ground

The relationship between land use land cover change and hydrology is complex, with linkages existing at a wide variety of spatial and temporal scales; however, land use change unquestionably has a strong influence on global water yield. Land cover and use directly impact the amount of evaporation, groundwater infiltration and overland runoff that occurs during and after precipitation events. These factors control the water yields of surface streams and groundwater aquifers and thus the amount of water available for both ecosystem function and human use (Mustard & Fisher, 2004). Changes in land cover and use alter both runoff behavior and the balance that exists between evaporation, groundwater recharge and stream discharge in specific areas and in entire watersheds, with considerable consequence for all water users (Sahin & Hall, 1996; DeFries & Eshleman, 2004). Climate models have even shown that land use land cover change affects global precipitation and temperature patterns, which drive the global hydrological cycle in the most fundamental ways (Chase *etal*. 2000). For instance river discharge worldwide has increased noticeably since 1900, and study suggests that land use land cover change may be directly responsible for 50% of this increase (Piao, *etal.* 2007).

The study area, Akaki Catchment, is the main part of the Upper Awash basin containing the city Addis Ababa. Addis Ababa is the capital of Africa in general and that of Ethiopia in particular and is the seat of level of governmental and Non-governmental organizations like (UNDP, UNICEF, ECA, AU, etc.). The city has been expanding since its foundation .It definitely as the expense of rapid conversion of land from rural to urban uses more than anywhere else in the country. For the last one hundred years, for example it has been noticed that there is an intensive conversion of rural land to urban development like buildings, transportation network, commercial centers, various type of industry, parks, and recreational area (JICA 1998).

Understanding impacts of land use/land cover change on the hydrologic condition is therefore needed for optimal management of natural resources in the area. So far impacts of LU/LC change on surface components of the hydrologic cycle are less well recognized.

Hence quantifying accurate LU/LC change within a catchment is an important component of monitoring watershed quality. Therefore to estimate and understand the impact of land use/land cover on runoff, it is also important to accurately assess the type and direction of changes occurring within the catchment. This can be accomplished more efficiently through change detection analysis of multi-temporal remotely sensed image and hydrological models.

Landcover is one of the most important products of remote sensing and it is a primary input of many hydrologic models. In this regard, it is imperative to integrate the various quantification methods with the spatial data handling capabilities of Geographic Information Systems (GIS) to process data for hydrological modeling. For this modeling, the Soil and Water Assessment Tool (SWAT) developed by Arnold and Fohrer (1994), is selected for assessing the hydrologic impacts of land use change in the Akaki Catchment. GIS and remote sensing serve to prepare inputs to the SWAT model and can help to predict and quantify the impacts of land use change on the hydrology of any catchment.

1.2 Problem Statement

Since Akaki catchment is exposed to intensive development, significant part of the area is characterized by greater level of impervious surface such as road parking lots sidewalks and roof tops. The catchment remained undisturbed by anthropogenic activities for some decades. But now days it started experiencing huge amount of LU/LC change having great impact on the hydrological condition. Unfortunately this fact was not given due attention (WWDSE, 1999).

According to JICA and Region 14 Administration report (1998), the city has flood pron riparian area especially Kebena, Bantyiketu, Kurtume, Big Akaki and Little Akaki rivers. These areas suffered from serious floods in the year 1978, 1994 and 1995 causing damages to houses, various infrastructures. Even, it led to loss of human lives and paralyze of socio economic activities resulting serious social disturbance.

This report also claims that there are potential risks increased by urban growth in several parts of the town. Addis Ababa city has steep slopes from North end to the Akaki plateau. This elevation ranges between 2800m (at the northern part) and 2200m (at the southern

part). This high elevation difference could favor run off with higher speed and quantity of flow.

Outlining the relationship between LU/LC and hydrological condition of the area enables us to project the possible flood risks through future development progress for appropriate measure. Therefore, the need for a scientific research is unquestionable.

Specifically, this research attempt to understand and estimate the effect of LU/LC changes on the streamflow of Akaki river for contribute a lot on the way toward tackling the above problems.

1.3 General Objectives

The overall objective of the study is to estimate the potential effect of land use and land cover changes on flow of Akaki river using SWAT model.

Specific Objectives includes:-

I) To determine the past space-time changes in the land cover of the catchment:

II) To evaluate the response of a hydrologic model of the catchment to the changes in LULC

III) To see the effect catchment surface flow based on future land cover

To address the aforementioned objectives, the research questions for this study are:

- Is there LULC change in Akaki Catchment over the past three decade?
- What is the trend of LULC look like?
- Does the LULC change affect the catchment hydrology?
- How will the land cover changes affect the hydrologic response of the catchment?

1.4 Overall Framework of the Study

The method to evaluate the impact of land use and land cover change, on hydrological regimes can be achieved through integrating GIS, remote sensing, and hydrological models. Satellite image have great contribution for preparation of land use land cover of the area. LU/LC information is of critical importance in hydrologic modeling, as it helps determine model variables that account for the volume, timing, and quality of runoff. A Physically-based distributed hydrological (Arc SWAT) model that allows several different subunits or objects to be defined within a catchment is utilized. Details of the approach followed are given in Figure 1.1

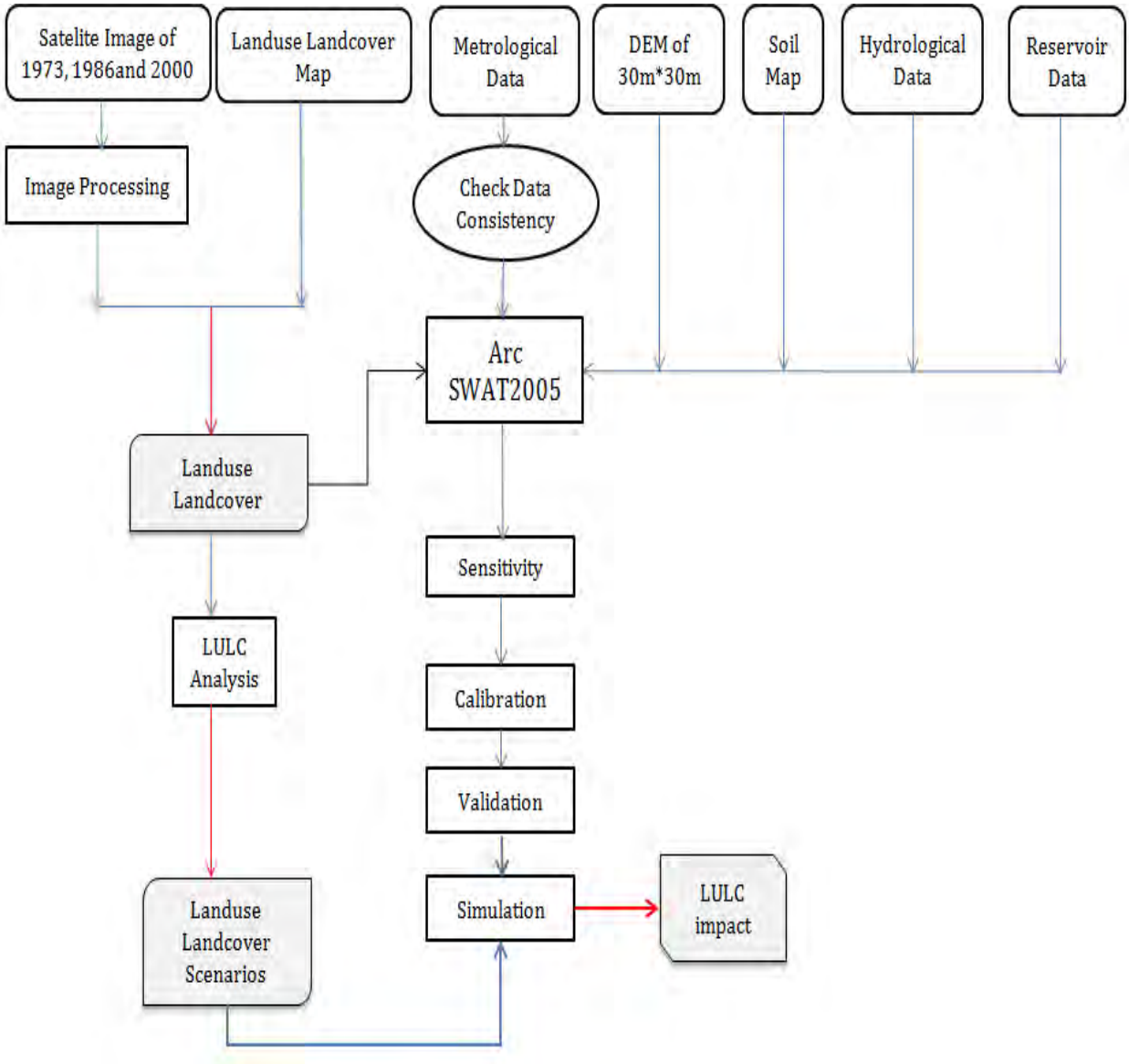

Figure1. 1: Overall frame work of the study

1.5 Thesis Outline

This thesis report consists of seven chapters. The contents of each chapter are organized as follows: In the first chapter, a general introduction about land cover change and hydrological responses is presented. The problem statement, the research objectives and the research questions are also discussed in this chapter. In the second chapter, literature review about the subject matter is presented and it gives a scientific review this study is mainly based on. The reviewed literatures are relevant to land cover classification, change detection and hydrologic impact of land cover change. The third chapter gives a brief introduction of the study area. The location, topography, climate and land cover of the study area are also described in this chapter. The fourth chapter presents the available hydrological meteorological and spatial data used for this study .The fifth chapter describes the procedure how to address the objective using Hydrological model and also Land use Land cover classification using maximum likely algorithm for the Landsat images for the year of 1973, 1986 and 2000. The six chapter present results of hydrological model and a land use change scenario from past data and master plan study of the area; finally chapter seven consist the research conclusion and recommendations based on the study conducted to indicate direction for future studies.

CHAPTER TWO

2 Review of Literature

2.1 Land-Use and Land-Cover Dynamics and Links

Land cover has gone under continuous change for millennia. This change has occurred through the use of fire for game hunting and clearance of patches of land for agriculture and livestock production, since the advent of plant and animal domestication. This is because human's production demands cannot be fulfilled without modification and/or conversion of land covers. In the past two centuries, the impact of human activities on land has grown enormously because of population increase, technological development and the requirements thereafter, altering entire landscapes, and ultimately impacting the biodiversity, nutrient and hydrological cycles as well as climate (de Sherbinin, 2002), especially in the developing world. These diverse roles have been recognized in a large number of research publications and international conferences, symposia, and workshops devoted to the subject over the past few years.

According to de Sherbinin (2002), land use is the term that is used to describe human uses of land, or immediate actions modifying or converting land cover. On the other hand, land cover refers to the natural vegetative cover types that characterize a particular area. Land-use change is the proximate cause of land-cover change. The driving forces to this activity could be economic, technological, demographic, scenic and or other factors. Hence, Land Use and Land Cover dynamics is a result of complex interactions between several biophysical and socio-economic conditions which may occur at various temporal and spatial scales (Reid *et al*., 2000).

2.2 Interaction of Land Use and Land Cover Change and Hydrology

To understand how LULC affects and interacts with global earth systems, information is needed on what changes occur, where and when they occur, the rates at which they occur, and the social and physical forces that drive those changes. Human impact on global land cover change, especially in terms of change from forest cover to other land cover, has been one of the important issues on global change research. In the primitive times when there was little human population and low level of economic activity, deforestation was not a problem because the natural regeneration of forest was adequate to cover for any loss of

forest by the human beings. However, with the advent of modern civilization and industrialization and the increase in population, the forest loss to meet the ever-growing needs of the human population became so huge that it posed a problem for the global environment. The concept of different aspects of an effect of land use change on hydrology at local, regional and global scale is discussed in detail by (Maidment 1993a). Vegetation has a significant impact on infiltration both by providing canopy and litter cover to protect the soil surface from raindrop impacts and by producing organic matter, which binds soil particles and increases its porosity. Higher porosity increases infiltration and percolation rates and the water-holding capacity of the soil. Infiltration rates are positively related to litter and grass basal cover, being up to 9 times faster with 100% litter cover than for bare soil (Maidment 1993a). Therefore deforestation increases surface runoff and reduces recharge by affecting the above condition especially if the area is steeply sloped and recharge zone.

2.3 Overview of Remote Sensing and GIS

Planners and resource managers need a reliable mechanism to assess the consequence of the changes resulted by the stress imposed natural resource by detecting, monitoring and analyzing land use changes quickly and efficiently. The conventional method of environmental data collection and analysis are not efficient in delivering the necessary information in a timely and cost effectively fashion. Hence viewing the Earth from space has become essential to comprehend the cumulative influence of human activities on its natural resource base. Remote sensing technology however can play a vital role in providing accurate and reliable information with cost effective and lesser time compared to other methods. Remote sensing refers the technique of obtaining information about an object or feature through the analysis of data acquired by a device that is not in contact with the object or feature under investigation (Lillesand, 1994).

Remote sensing has helped in the development of various environmental management methodologies, providing the following advantages when compared to conventional ground based methods

Synoptic view: Remote sensing facilitates the study of various features of earth's surface and the spatial relationship between features,

Accessibility: Remote sensing makes it possible to gather information about areas that are not accessible for ground surveys, like mountainous areas or foreign land

Time: Since information about a large area can be gathered quickly, these techniques save time and effort.

2.4 General Principles of Remote Sensing

The sensors on remote sensing platforms usually record electromagnetic radiation. Electromagnetic radiation (EMR) is energy transmitted through space in the form of electric and magnetic waves. Remote sensors are made up of detectors that record specific wavelengths of the electromagnetic spectrum. The electromagnetic spectrum is the range of electromagnetic radiation extending from cosmic waves to radio waves.

The measured and recorded energy is converted and stored as a digital number (DN) value, which ranges from 0-255. Each pixel (picture element or unit area or ground cell) has a single DN value. Most sensors measure reflected sunlight however; some sensors detect energy emitted by the earth itself or provide their own source of energy (active remote sensing) (Ahmed, 2001). The figure below indicates the range of different waves of Electromagnetic Spectrum.

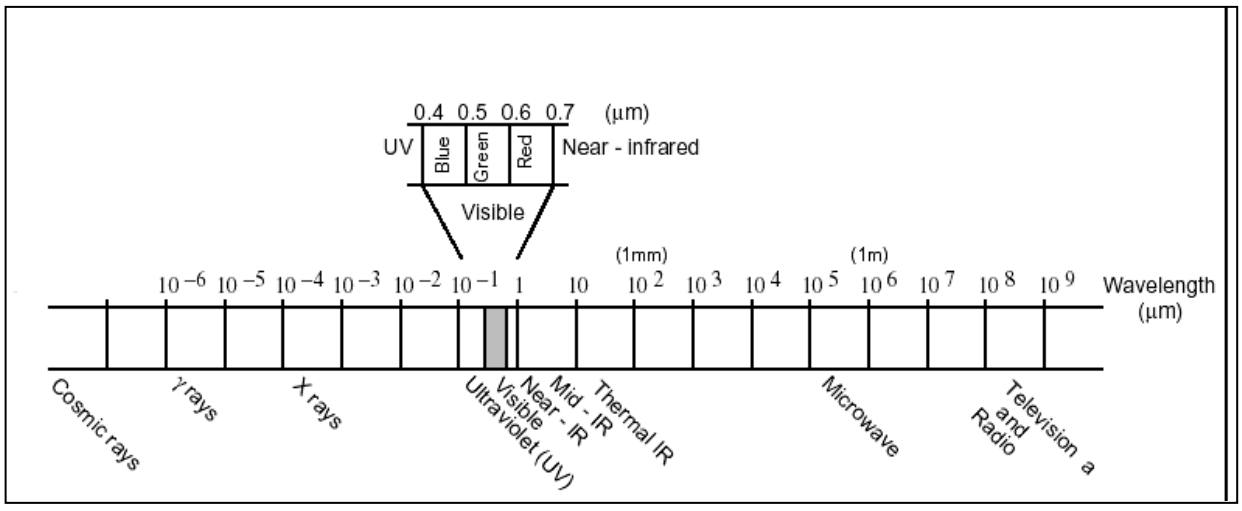

Figure2. 1: The rage of electromagnetic spectrum (ERDAS Filed Guide, 2005)

2.5 Application of Remote Sensing for Different Fields

The utility of different remote sensing data from different satellites have been demonstrated in many fields such as agriculture, cartography, civil engineering, environmental monitoring, forestry, geography, water resources management land

resources analysis and land use planning**.** The use of satellite images in any of fields mentioned above, demand the knowledge of the different bands that each sensor system onboard satellites use to take the imagery and how these bands of the electromagnetic spectrum interact with land surface features and with that of the atmosphere. As there are many satellites in the space providing remote sensing data, their application will vary with their way of data acquisition.

The most popular satellite is the landsat, which operated since early 1970s till 2005. This long period of operation makes landsat very important for environmental systems analysis. All types of satellites vary with their sensors, flight height, bands, and spatial resolution, spectral resolution etc.

2.5.1 ERDAS IMAGINE Model

It is a remote sensing application with raster graphics editor capabilities designed by ERDAS, Inc for geospatial applications. Prior to the ERDAS IMAGINE Suite, ERDAS, Inc. developed various different products to process satellite imagery from AVHRR, Landsat MSS, Landsat TM and SPOT imagery into land cover / land use maps, map deforestation. The latest version ERDAS IMAGINE is aimed primarily at geospatial raster data processing and allows the user to prepare, display and enhance digital images for mapping use in GIS or in CAD software. It is a toolbox allowing the user to perform numerous operations on an image and generate an answer to specific geographical questions.

By manipulating imagery data values and positions, it is possible to see features that would not normally be visible and to locate geo-positions of features that would otherwise be graphical. The level of brightness or reflectance of light from the surfaces in the image can be helpful with vegetation analysis, prospecting for minerals etc. Other usage examples include linear feature extraction, generation of processing work flows ("spatial models" in ERDAS IMAGINE), import/export of data for a wide variety of formats, ortho-rectification, mosaicking of imagery, stereo and automatic feature extraction of map data from imagery(Wikipedia,2010).

2.6 Hydrological Process

The hydrologic cycle is the central focus of hydrology. The cycle has no beginning or end, and its many processes occur continuously. As Shown schematically in figure below water evaporates from the oceans and the land surface to become part of the atmosphere; water vapor is transported and lifted in the atmosphere until it condenses and precipitates on the land or the oceans; precipitated water may be intercepted by vegetation, become overland flow over the ground surface infiltrated; in to the ground, flow through the soil as subsurface flow, and discharge into streams as surface runoff. Much of the intercepted water and surface runoff returns to the atmosphere through evaporation. The infiltrated water may percolate deeper and eventually recharge to ground water, later emerging in spring so seeping into streams to form surface runoff, and finally flowing out to the sea or evaporating into the atmosphere as the hydrologic cycle continues (Chow *et al*., 1988).

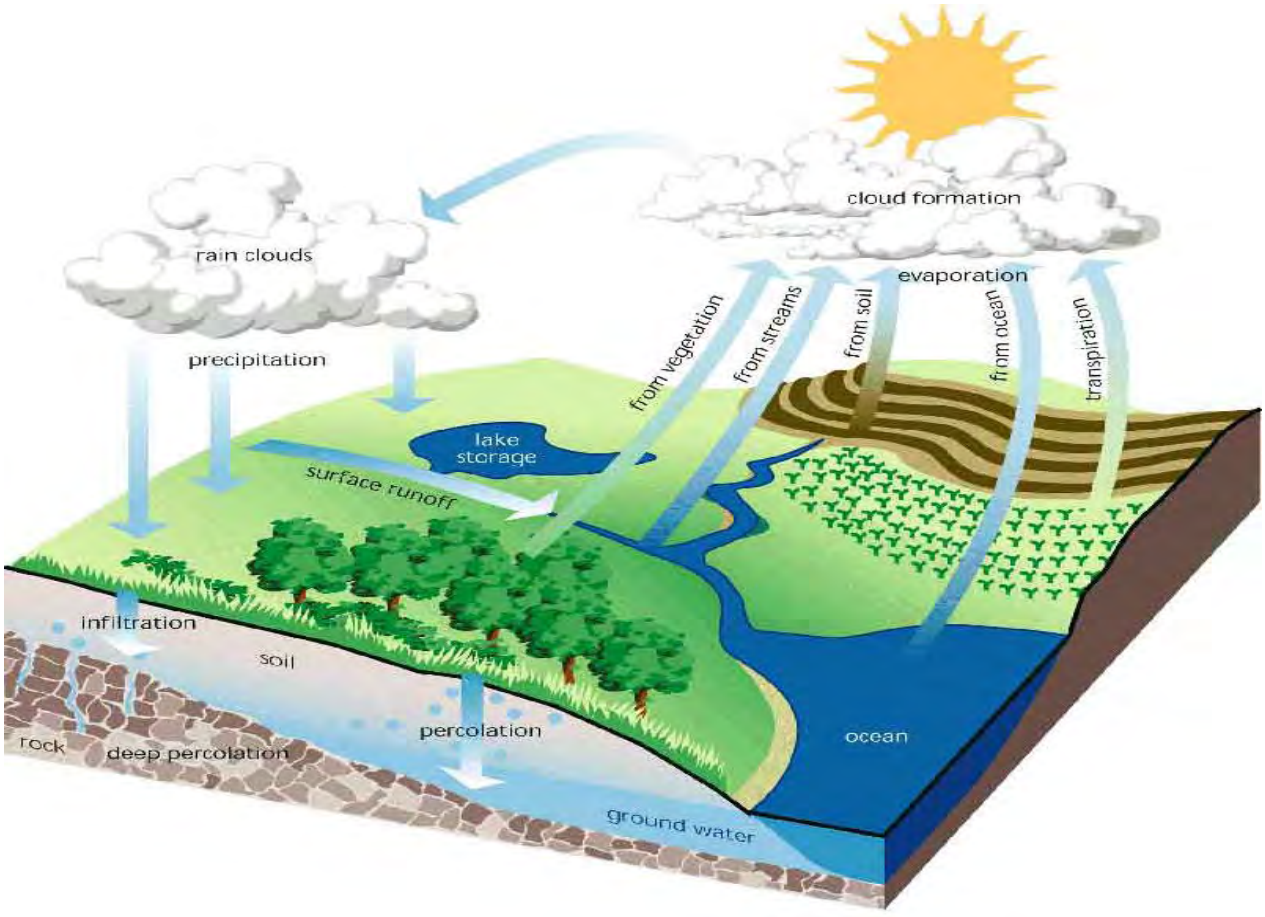

Figure2. 2: Hydrological cycle of a basin (source Loucks 2005)

2.7 Hydrological Model

When design and management decisions are made about environmental and water resources systems, they are based on what the decision-makers believe, or perhaps hope, will take place as a result of their decisions. These predictions are either based on very qualitative information and beliefs in people's minds at least in part, and quantitative information provided by mathematical or computer-based models. Today computer-based modeling is used to enhance mental models. These quantitative mathematical models are considered essential for carrying out environmental impact assessments. Mathematical simulation and optimization models packaged within interactive computer programs provide a common way for planners and managers to predict the behavior of any proposed water resources system design or management policy before it is implemented.

Models are a simplified representation of the real world. What features of the actual system are represented in a model, and what features are not, will depend in part on what the modeler thinks is important with respect to the issues being discussed or the questions being asked. How well this is done will depend on the skill of the modeler, the time and money available, and, perhaps most importantly, the modeler's understanding of the real system and decision-making process (Louks etal 2005).

Hydrological models, which are simplified representation of complex hydrological system, can be: (a) physical, such as a scaled-down reproduction of a full-scale prototype built in a laboratory to assume dynamic similarity between model and real world; (b) abstract, in which the behavior of the system is represented by a set of equations, together with logical statements, expressing relationships between variables and parameters This variable may be functions of space and time, and they may also be probabilistic or random variables which do not have a fixed value at a particular point in space and time instead are described by probability distribution (Chow, 1998).

A model which does not consider randomness and for given input always produces the same output such model is called a deterministic model on the other hand a model output at least partially random called stochastic model.

Hydrologic models can be either lumped or spatially distributed. Lumped models do not take into account spatial heterogeneity across the modeling domain. Rather, they simulate

a spatially averaged hydrologic system. Spatially distributed models however allow for spatially varying precipitation, temperature, and other climatic variables, and the spatial occurrence of watershed characteristics such as soils, slope, and land cover types (Chow *et al*., 1988).

Therefore, spatially distributed models are the best way towards understanding the impacts of land use/land cover changes rather than the lumped ones. Hence, the following spatially distributed models are fall in to consideration during model selection period.

2.7.1HBV-96

The HBV-model (Hydrologiska Byråns Vattenbalansavdelning) is a general-purpose hydrologic model developed at the Swedish Meteorological and Hydrologic Institute (SHMI).

The model is designed to run on a daily time step (shorter time steps are available as an option) and to simulate river runoff in river basins of various sizes. The basin can be disaggregated into sub-basins, elevation zones, and land-cover types. Input data include precipitation, air temperature (if snow is present), monthly estimates of evapotranspiration, runoff (for calibration) and basin geographical information. The treatment of snow accumulation and melt in HBV is based on a simple accounting (degree-day) algorithm. The existence and amount of snowfall is predicted using meteorological input data extrapolated to the mean elevation of each sub-area of the basin. A simple model based on bucket theory is used to represent soil moisture dynamics. There is a provision for channel routing of runoff from tributary basins, using a modified Muskingum method. Outflow from lakes is usually specified by a stage-discharge rating curve but can be given by a lookup table to allow for power station operating rules. The HBV model can be linked with real time weather information and river monitoring systems (Lindström et al.(1997).

2.7.2 HEC-HMS (Hydrologic Modeling System)

HMS is a comprehensive hydrologic model developed by Hydrologic Engineering Center (HEC) of United States Army Corps of Engineers (USACE). It is an event – based model (HEC, 2000). HMS offers several options to model various physical processes occurring in a watershed system. One such process is the direct runoff computations. Most of runoff models available with HMS are lumped in nature except for two which are distributed.

Most of the lumped runoff models derive their roots from the Unit Hydrograph (UH) concept.

This model provides a lumped model option called Clark's UH. To overcome its lumped character, a modified version called ModClark method was developed for HMS (Daniel and Arlen 1998). ModClark's method requires that watershed be further divided into sub-areas by intersecting it with a grid. Each of these sub-areas is assigned individual lag time, instead of one value for the whole watershed, as in the case of Clark's UH. The precipitation excess at each sub-area is transported to the watershed outlet using the corresponding lag time. Thus the inflow contributions due to all the subareas to linear reservoir are computed. These flows are then routed through a linear reservoir (only a single value for storage coefficient being defined for all the sub areas) to obtain the hydrograph at the outlet, which will later be routed through the channels.

2.7.3 TOPMODEL

TOPMODEL is a hydrologic model that bases its distributed predictions on an analysis of basin topography. The development of TOPMODEL was initiated by Michael Kirkby at the School of Geography, University of Leeds. The model allows basins to be divided into a set of subbasins. Evaporation is estimated by using the Penman-Monteith method. Surface runoff is computed based on variable saturated areas.

The subsurface flow is calculated using an exponential function of water content in the saturated zone. Channel routing and infiltration excess are calculated using the Beven and Kirkby method. The spatial component requires a high quality DEM without sinks (Beven etal. (1997)

2.7.4 SWAT Model

SWAT is the acronym for Soil and Water Assessment Tool a river basin, or watershed scale model developed by Dr Jeff Arnold for the USDA Agricultural Research Service (ARS). SWAT is a basin-scale, continuous-time model that operates on a daily time step and is designed to predict the impact of management on water, sediment, and agricultural chemical yields in large complex watersheds. The model is physically based, computationally efficient, and capable of continuous simulation over long time periods. Major model components include weather, hydrology, soil temperature and properties,

plant growth, nutrients, pesticides, bacteria and pathogens, and land management. In SWAT, a watershed is divided into multiple sub watersheds, which are then further subdivided into hydrologic response units (HRUs) that consist of homogeneous land use, management, and soil characteristics. The HRUs represent percentages of the sub watershed area and are not identified spatially within a SWAT simulation. Alternatively, a watershed can be subdivided into only sub watersheds that are characterized by dominant land use, soil type, and management.

2.8 Model Selection

The selection of a particular model is a key issue to get satisfactory answers to a given problem. Currently, there are numerous hydrological models simulating the hydrological process at different spatial and temporal scales. Although there are no clear criteria for making a choice between models, some simple guidelines can be stated (Cunderlik, 2003).

These criteria are always project-dependent, since every project has its own specific requirements and needs. Further, some criteria are also user-dependent (and therefore subjective), such as the personal preference for graphical user interface, computer operation system (OS), input-output (I/O) management and structure, or user's add- on expansibility.

Among the various project-depended selection criteria, there are four common and fundamental ones that must be always answered:

- Required model outputs important to the project and therefore to be estimated by the model (Does the model predict the variables required by the project such as peak flow, event volume and hydrograph, long-term sequence of flows…),
- Hydrologic processes that need to be modeled to estimate the desired outputs adequately (Is the model capable of simulating land use/cover change, regulated reservoir operation, snow accumulation and melt, single-event or continuous processes…),
- Availability of input data (Can all the inputs required by the model be provided within the time and cost constraints of the project?),

- Price (Does the investment appear to be worthwhile for the objectives of the project?) (Cunderlik, 2003).

This study aims for assessing the potential impact of land use/cover change on hydrologic processes in Akaki catchment. More specifically, the hydrologic model for this study needs to have the capability to:

- Represent variable land use/land cover throughout the catchment, and to produce a full hydrograph response from each sub-area
- Simulate different components of the streamflow including surface runoff, lateral flow and base flow
- Route hydrographs through different stream reaches, and identify principal runoff source areas at selected points-of interest.
- Compute sub-area release rates, or provide travel time and peak flow information from which these release rates may be developed.
- Evaluate the impact of land use land cover changes on hydrology
- To be applied over a range of catchment sizes from small to large catchments
- Simulate continuous and long term impact
- Freely available

For this study, SWAT is selected as an appropriate model to meet the simulation requirements set above using available soil, topography, land cover /land use and weather data.

2.9 Previous Work Done in the Pilot Area

Addis Ababa Master Plan Revision Project 2000

This study was conducted mainly by revision of Addis Ababa Master plan of 1986. The plan had also incorporated strategic plans prepared for 5 and 10 years physical and socio-economic studies, detailed plan of the city's key development and investment options, study pertinent to city administration and structuring, implementation policies and directives to address the Millennium Development Goals (MDG).

This research summarizes the growth of built up Area with five periods from 1887 (the city foundation) to the year 1999 (study period) and their major event.

Table2. 1: Physical growth of Addis Ababa City Built-Up Area

Period	Change of built up Area(ha)	% of Built-up Area	Remark
1887-1937	1863.34	12.70	Establishment of Church
1937-1975	4187.39	28.54	Italian incursion
1976-1985	4783.07	32.60	Expansion at central part
1986-1995	2928.73	19.96	"
1996-1999	909.66	6.20	Construction Accelerated
Total	14672	100.00	

Taye Aduna (2009): This study focus on assessing the impact of land cover changes on the hydrology and water quality of Legedadi and Dere catchment. Land use/land covers for the year 1960, 1980 and 2008, temporal and spatial data were used in SWAT hydrological model.

Without climate change, the study concludes that an increase runoff from 3.4-49.9% for Legedadi and 14.9-15.3% for Dere catchment is observed during hypothetical scenarios. Similarly sediment, nitrate and phosphorus through the application of agricultural inputs such as Fertilizers also increase.

Fessahatsion Z (2008): a rainfall runoff model was applied for the impact of urbanization on storm water with 24hr duration IDF curve the return periods for the city of Addis Ababa.

He used HEC-Geo-HMS for data processing, watershed delineation and generation of Basin Model. The Curve number (CN) Grid of the study area was prepared using land use and soil data.

He stated that he could not calibrate HEC-HMS model due to absence of hourly discharge data. After considering the history of land use land cover map between 1975 (baseline) and 2020 (projected), the storm water flow shows increase of 5.97%, 4.94%, 4.56%, 4.24% and 4.04% for every considered return period of 5,10,25,50, and 100 years respectively.

CHPTER THREE

3 Study Area

3.1 Location

The Akaki catchment is located in central Ethiopia along the western margin of the main Ethiopian rift valley. The catchment is situated at the north western Awash River between $8^{0}46'–9^{0}14'$ N and $38^{0}34'–39^{0}04'$E. It is bounded to the north by the Intoto ridge system, to the west by Mt. Menagesha and the Wechecha volcanic range, to the southwest by Mt Furi, to the south by Mt Bilbilo and Mt Guji, to the southeast by the Gara Bushu hills and to the east by the Mt Yerer volcanic centre. The Akaki catchment has an area of about 1429 km^2.

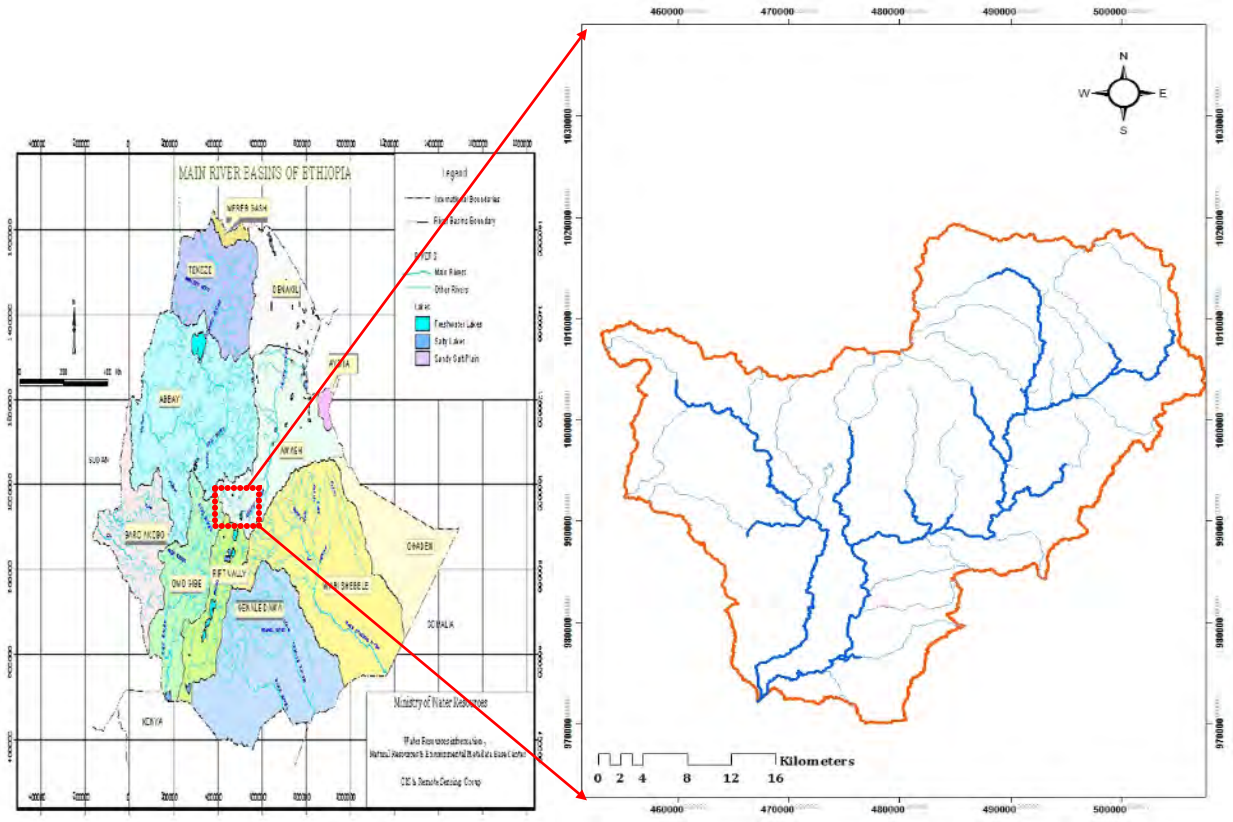

Figure3. 1: Location map of study area

3.2 Climate

The climate of the Akaki catchment is characterized by two distinct seasonal weather patterns. The main wet season, locally known as Kiremt, extends from June to September .A minor rainy season, locally known as Belg, contributes moisture to the region from mid February to mid April (Daniel, 1977).

3.3 Rainfall

The variation in the seasonal distribution of rainfall in Ethiopia can be attributed by the reference to the position of the Inter-Tropical Convergence Zone (ITCZ), the relationship between upper and lower air circulation, the effects of topography and the role of local convection currents and the amount of rainfall (Daniel, 1977).

The range of mean annual rainfall for the stations in the period 1997- 2004 lies between 900 to 1250 mm. During the year there are strong seasonal variations due to the passage of the ITCZ (Inter Tropical Convergence Zone) and westward propagating disturbance from the Indian Ocean (Daniel, 1977).

The mean monthly rainfall between June and September is above 100mm, with monthly maximum rainfall record 337mm in August. While November and December show the lowest mean monthly rainfall.

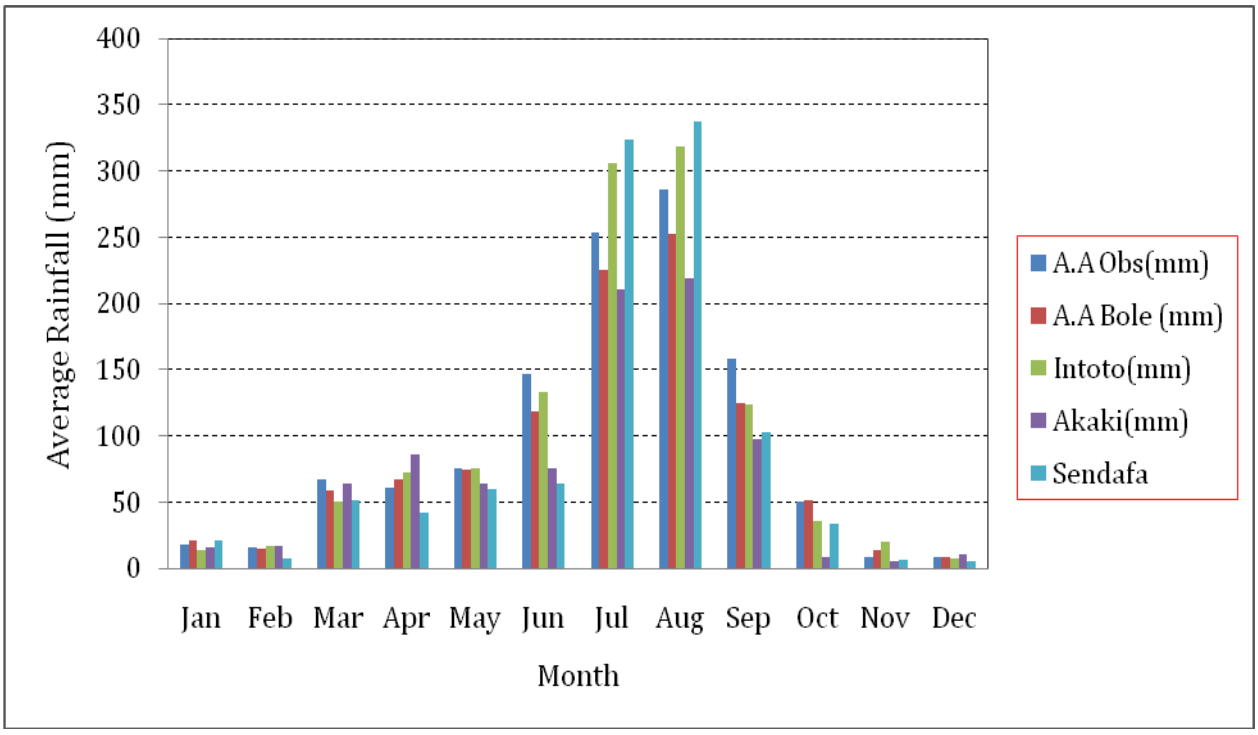

Figure3. 2: Mean monthly rainfall distribution for a period of 1997-2004

3.4 Temperature

Under normal conditions, air temperature decreases with increasing altitude at a mean rate of 0.7^{o}c for every 328 feet (Fetcher, 1998). This works also in Ethiopia where temperature decreases with increasing elevations. The maximum temperature of Addis Ababa ranges between 20^{0}c (in wet season) to 25^{0}c (in dry season), while the minimum falls between 7^{0}c - 12^{0}c in the year.

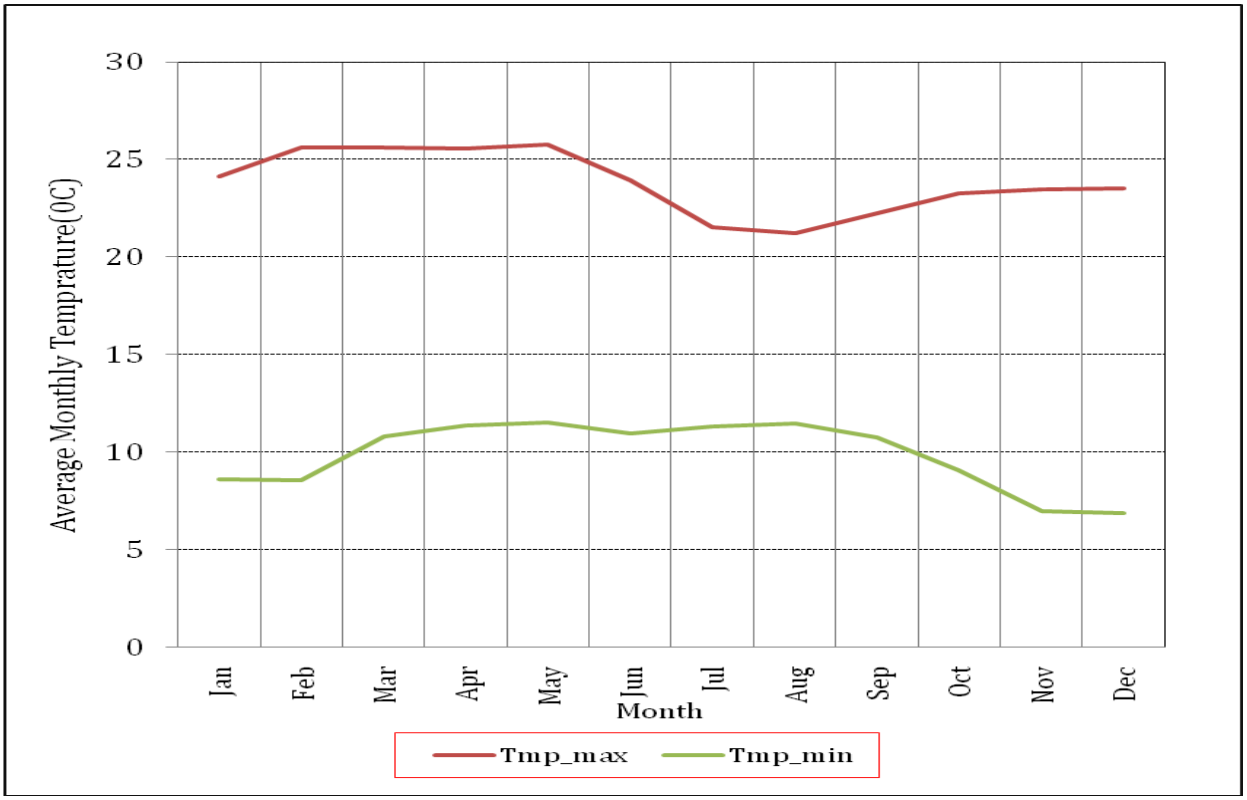

Figure3. 3: Average monthly minimum and maximum temperature for the study area 1997-2006

3.5 Wind Speed, Sunshine and Relative Humidity

The wind flow pattern is influenced by the seasonal variation of the ITCZ. The predominant wind direction during June to September is south to southwest. The wind speed pattern is distinctly bimodal in the region with peaks occurring in March and September and minimum speeds being recorded in July and August. The mean annual wind speed is 0.6m/s. The monthly variation closely follows the rainfall pattern as would be expected with more sunshine hours in the dry months than in the wet months. Sunshine hours vary from a daily mean of 9.4 hours in December to 3 hours in July. The mean annual relative

humidity of the basin is 60.2% measure. The monthly variation in relative humidity at ranges from 47.9% in March to 76.5% in August.

3.6 Topography

The study area found at the southern flank of Entoto ridge (3199m a.s.l.) and expanded in all directions. This ridge marks the northern boundary of the city following the east-west trending major fault (Ambo-Kassam). Other prominent volcanic features surrounding the city are Mt. Wochacha in the west (3385m a.s.l.), Mt. Furi (2839m a.s.l.) in the southwest and Mt. Yerer (3100 a.s.l.) in the southeast. (AAWSA, AAU, 2003).

The topography is undulating and form plateau in the northern, western and southwestern parts of the city, while gentle morphology and flat land areas characterize the southern and southeastern parts of the city (JICA and Region 14 Administration, 1998).

3.7 Geology

The north and north eastern area (the Entoto Mountain, the northern and north eastern Addis Ababa) is covered with trachytes, rhyolites, basalts and several episodes of pyroclastic materials of older volcanism occur on the upper part and foothill sides of Entoto ridge. Overlying these, younger basaltic rocks (Addis Ababa Basalt) are found covering the central and southern part of the city. Outcrops of ignimbrites north of Bole area (Eastern Addis) and Lideta area (Central Addis) have been observed underlying the Addis Ababa basalt. Younger volcanic of trachy-basalt, trachytes, ignimbrites and tuff belonging to the wochecha, Furi and Yerer volcanoes are recognised overlying un-conformably on the Addis Ababa basalt in the western, south-western and eastern part of the catchment.

3.8 Hydrology

The total catchment area of Akaki is divided into two sub-catchments. These are Big Akaki sub-catchment (Eastern) and the Little Akaki sub catchment (Western).

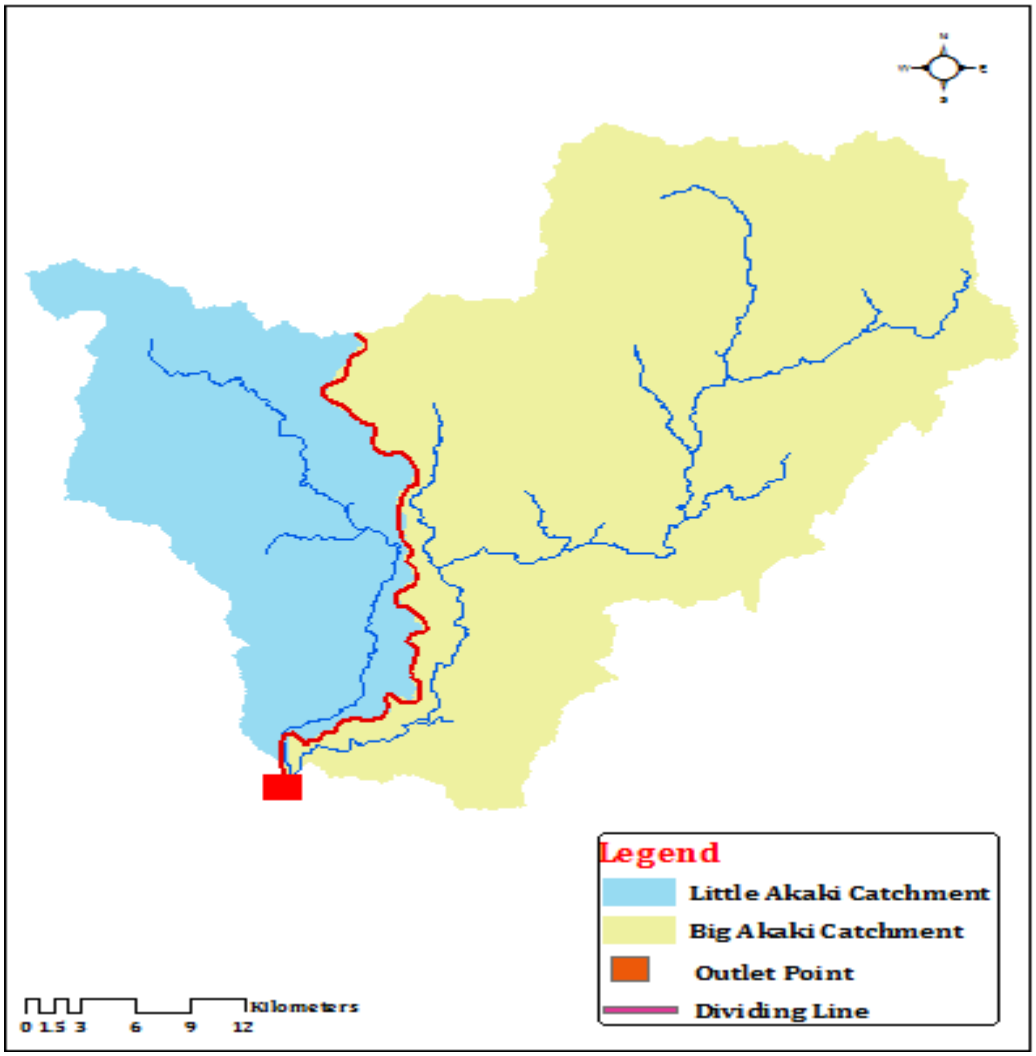

Figure3. 4: Sub-Catchments of Akaki River

3.8.1 Little Akaki Sub-catchment

Most parts of the Little Akaki Sub-catchment is characterized by undulating topography steeper in the North, moderate in the middle and West; and relatively gentle and flat-laying in the South. In the South West, a flat grassland plain covered with thick black cotton soil covers the East of Addis Ababa –Jimma road and it is swampy and extends in the Southeast direction. The catchment has been highly eroded by little Akaki river and its tributaries but in the Northern and Western parts the removal of topsoil is reduced due to the Eculpatus

tree that covers the area. Groundwater in this cacthment occurs in confined, unconfined and or semi-confined condition.

The northern and Western part of this catchment is densely vegetated and dominantly constituted by highly weathered rocks and fractured volcanic rocks. Basalts and siliceous rocks infiltrate the precipitated water and recharge the aquifers located beneath. Rivers that started from Entoto ridge, Mt.Wachecha, and Mt.Furi also recharge the ground water in the catchment.

3.8.2 Big Akaki sub -catchment

It is about 62% of the area of the whole catchment. The topography is rugged and steep mostly between Entoto and Filwoha but it is gentle and flat lying in south and southwest parts of the catchment.

The surface water reservoir, Legadadi and Dere, found in this catchment and they are the major water supply to Addis Ababa. The presences of massive, fractured and porous units at different depths produce a multi-layer aquifer system in Big Akaki catchment. Due to this hand-dug wells and boreholes located in most parts of this catchment, tap groundwater from different aquifers and it is common to use springs in this catchment for human consumption specially when there is shortage of municipal water supply.

The special characteristic of Big Akaki sub catchment is the occurrence of thermal water in Filwoha and its surrounding. The boreholes drilled at Hilton, Filwoha, Ghion, National palace and st. Joseph school tap thermal groundwater that occur in pheratic and confined conditions.

Since 1981, the Big Akaki catchment is gauged at Addis-Debrezeit Road Bridge, commanding a catchment area of 885km^2. The station is equipped with an automatic hydrometric record and seven staff gauges to measure manually.

3.9 Water Reservoirs

In the outskirts of the city four water reservoirs were built for two main purposes. Gefersa, Legadadi, and Dere dam were built for public water supply, while Aba Samuel dam was built for hydroelectric power generation. As a consequence, Lake Gefersa in the northwest, Lake Dere and Legedadi in the northeast and Lake Aba Samue (due to siltation and

pollution it is not functional at present) in the southern outskirts of the city were formed at different times.

Gefersa was the first dam built in 1944 about 18 kms west of Addis Ababa. At present the dam has a reservoir capacity of 6.5 million cubic meters and the maximum capacity of the treatment plant is 30,000 m^3 of water per day. Due to rapid growth of the population and expansion of the city from year to year, there is a serious shortage of water in different parts of Addis Ababa. To alleviate the problem Legedadi and Dire dams were built in 1970 and 1999 at about 33 kms east of Addis Ababa. The treatment capacity of Legedadi plant was upgraded from 50,000 m^3 to 150,000 m^3 of water per day. The Dire dam supplies 42,000 m^3 of water per day for Legedadi plant, since 1999.

3.10 Demography of the Study Area

Central Statistical Agency of Ethiopia (CSA) 2007 reported that Addis Ababa has a total population of 2,738,248, of whom 1,305,387 are men and 1,434,164 women. This report also shows that population of the city grow at an average rate of 2.1 percent than that of 1994 Census. This change has occurred due not only to natural increase but continues attraction between 90,000 to 120,000 new residents every year. In general, it appears that much of this growth (probably up to 70 percent of the total), taken place in the slums and squatter settlements of the city (UN-HABITAT 2007).

Table3. 1: Average annual population and growth rate of Addis Ababa from 1961 to 2007

Year	Population	Growth Rate
1961	443,728	
1967	683,530	7.60%
1978	1,167,315	4.99%
1984	1,423,111	3.63%
1994	2,112,737	3.57%
2007	2,738,248	2.10%

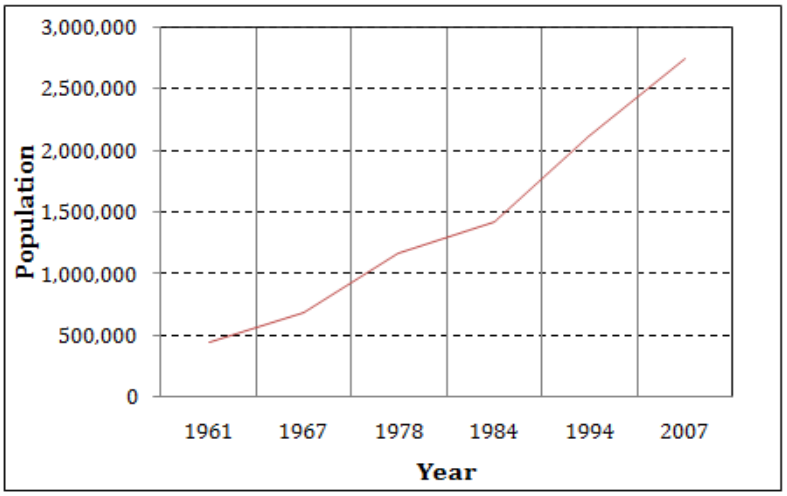

CHABTER FOUR

4 Data Source and Analysis

4.1 Meteorological Data

Daily data for five stations was collected from National Meteorological Agency (NMA). Data like daily precipitation, daily maximum and minimum temperature were collected in a soft copy format and other weather information like wind speed, sunshine hours and relative humidity were collected in a hard copy format which later encoded to soft copy format. The location of meteorological stations and monthly precipitation is available in Appendix C.

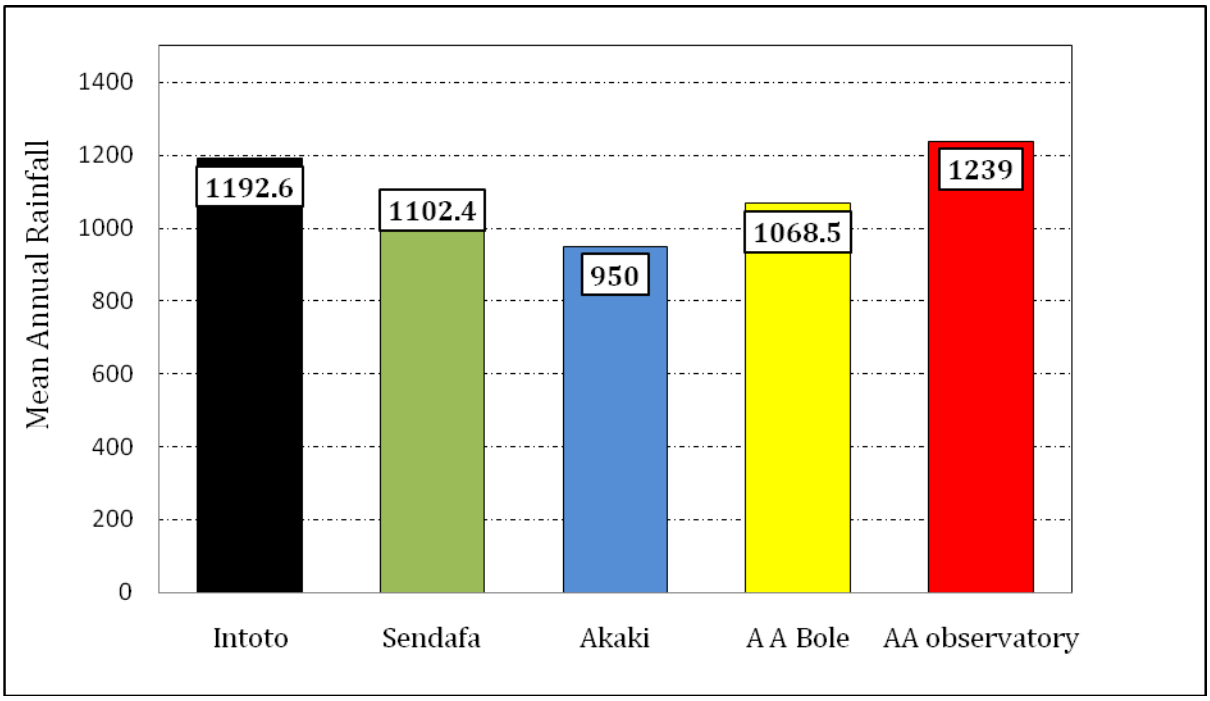

Figure4. 1: Mean annual rainfall from a period of 1997-2004

4.2 Filling Missing Weather Data

The climatic data collected from the five meteorological stations in the study area however, have missing data. Since SWAT has a built in weather generator called WGEN that is used to fill the gaps, all the missing values were filled with a missing data identifier, -99. The weather generator first independently generates precipitation for the day. Maximum temperature, minimum temperature, solar radiation and relative humidity are then generated based on the presence or absence of rain for the day. Finally, wind speed is generated independently.

For the sake of data generation, weather parameters were developed by using the weather parameter calculator WXPARM (Williams, 1991) and dew point temperature calculator DEW02 (Liersch, 2003), which were downloaded from the SWAT website (http://www.brc.tamus.edu/swat/soft_links.html). The WXPARM program reads daily values of solar radiation (calculated from daily sunshine hours), maximum and minimum temperatures, precipitation, relative humidity, and wind speed data. It then calculates monthly daily averages and standard deviations of all variables as well as probability of wet and dry days, skew coefficient, and average number of precipitation days in the month. The DEW02 programs reads daily values of relative humidity, and maximum and minimum temperature values and calculates monthly average dew point temperatures. In this study weather generated parameters were calculated for Addis Ababa Bole and Addis Ababa observatory stations. The weather generator parameters used and their values are shown in Appendix B.

4.3 Solar Radiation

Once water is introduced to the system as precipitation, the available energy, specifically solar radiation, exerts a major control on the movement of water in the land phase of the hydrologic cycle. Processes that are greatly affected by temperature and solar radiation include snow fall, snow melt and evaporation. Since evaporation is the primary water removal mechanism in the watershed, the energy inputs become very important in reproducing or simulating an accurate water balance. ArcSWAT need daily solar radiation but the data acquired from National Meteorological Agency (NMA) is sunshine hour, and hence a conversion of this variable was made using Angstrom (1924) empirical equation

$$Qs = Qext(a + b(\frac{n}{N}) \quad \text{---------- Eq.4.1}$$

Where *Qs* is the solar radiation in (MJm-2day-1), *Qext* is the daily total extraterrestrial radiation in (MJm-2day-1), *a* and *b* are constants which depend on the location, season, and state of the atmosphere, *n* is the actual number of hours of bright sunshine (sunshine hour), and *N* is the number of day light hours (since Ethiopia is near the Equator, *N* is assumed to be 12).

4.4 Checking the Consistency of Data

The most common method of checking for inconsistency of record is Double Mass Curve analysis (DMC). The curve is a plot on arithmetic graph paper, of cumulative rainfall collected at a gauge where measurement condition may have changed significantly against the average of the cumulative rainfall for the same period of record collected at several gauges in the same region. The data is arranged in the reverse order that is the latest record as the first entry and the oldest record as the last entry in the list. A change in the proportionality between the measurements at the suspect station and those in the region is reflected in a change in the scope of the trend of the plotted points.

The data series, which is inconsistent, adjusted to consistent values by proportionality. Double mass curve plot made for all five stations figure 4.2 shows only for Addis Ababa Observatory For the rest station available in Appendix D. From the double mass curve figure the stations are consistent each other.

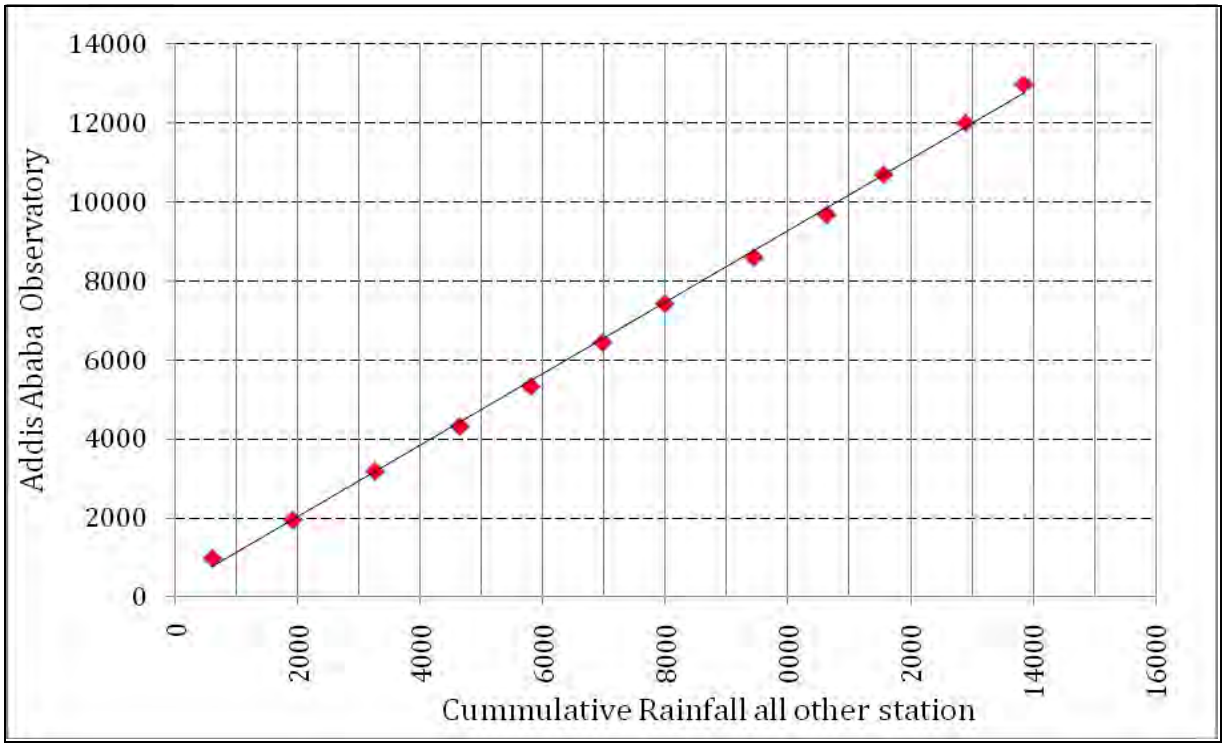

Figure4. 2: Double mass curve for Addis Ababa Observatory Meteorological stations

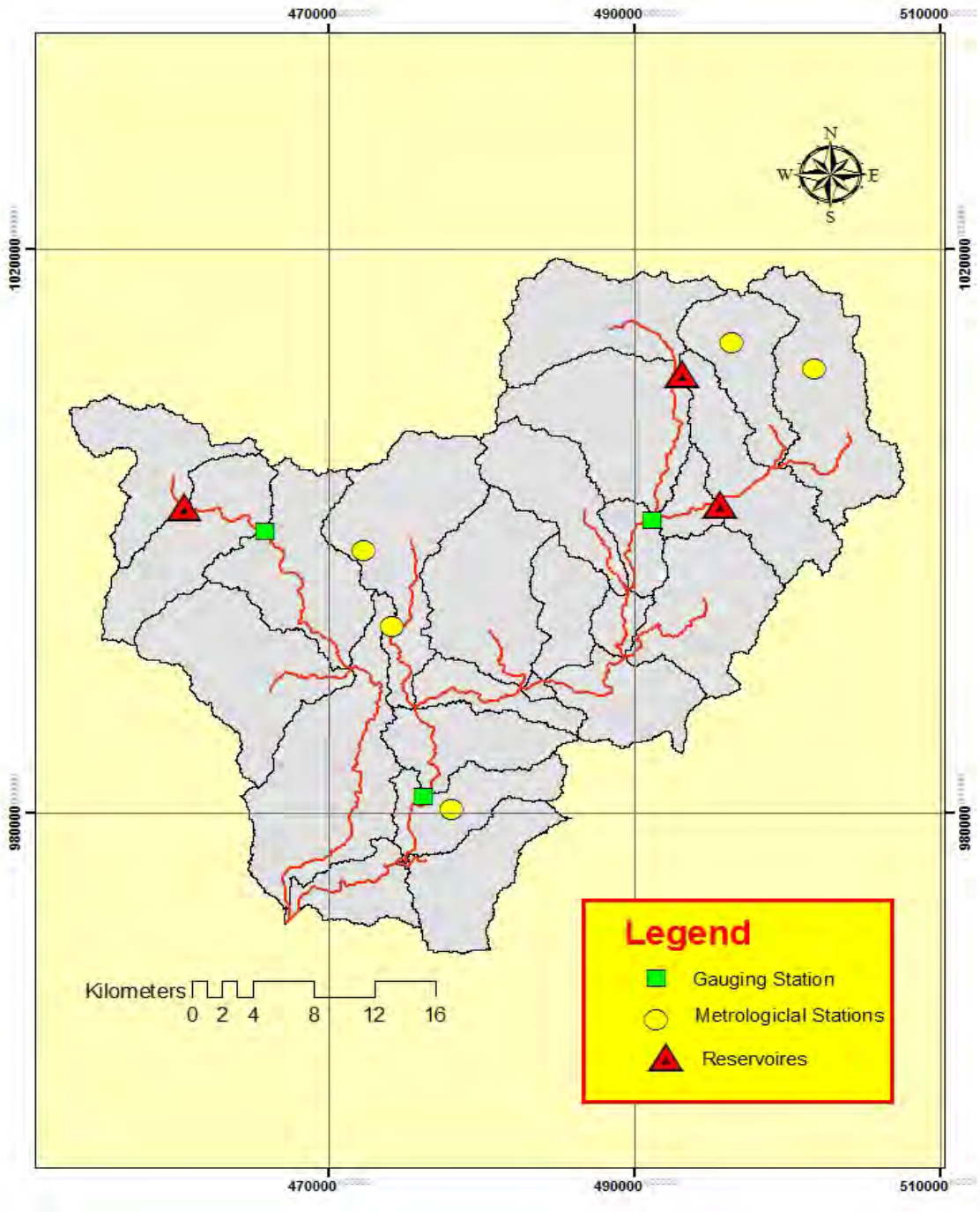

Figure4. 3: Distribution of Meteorological, Reservoirs and gauging station

4.5 Hydrological Data Availability

The study area is gauged at three stations. These are Mutincha (d/s of Legedadi Dam), Little Akaki (d/s of Geffersa Dam) and Big Akaki near Akaki town on Addis Ababa - Debrezeit road. The first two stations gauge about 9% and 12% of the total area and are aimed to control the dam out flow only. Also they have high percentage missing data. But 62% of the total catchment area is gauged by the third gauging station (Big Akaki). It is equipped with an automatic water level recorder and is capable of discharge measurement.

The hydrological data for Big Akaki collected from the Ethiopian MoWE (Ministry of Water and Energy), is used for sensitivity analysis, calibration and validation of the model. Hence, daily flow data from 1997-2002 was used for model calibration and from 2003-2004 for model validation. The mean monthly discharges of at Big Akaki gauging station is shown in the figure below

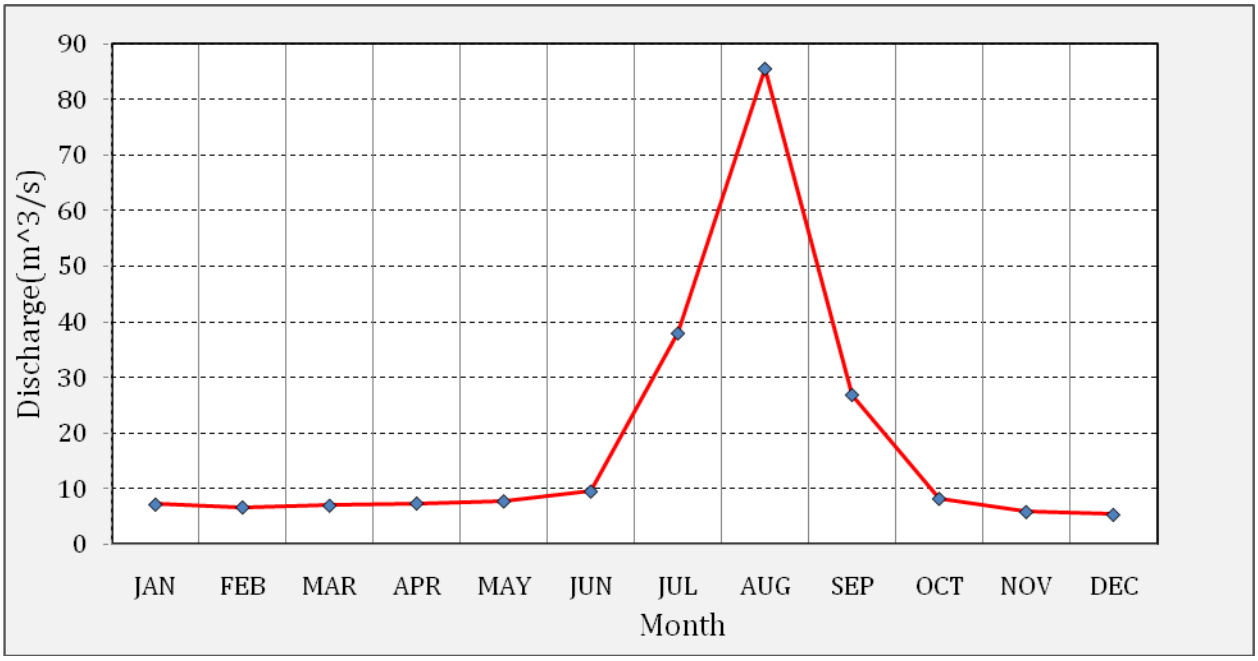

Figure4. 4: Mean monthly flow at Big Akaki for a period of (1997-2004)

4.6 Reservoirs

Impoundments play an important role in water supply and flood control. SWAT models four types of water bodies: ponds, wetlands, depressions/potholes, and reservoirs. Ponds, wetlands, and depressions/potholes are located within a subbasin off the main channel.

Water flowing into these water bodies must originate from the subbasin in which the water body is located. Reservoirs are located on the main channel network. They receive water from all subbasins upstream of the water body. In the study area there are three reservoirs which are the sole of water supply system.

Table4. 1: Major water source and there catchment area

Dams	Catchment Area(km^2) SWAT Delineation	Catchment Area(km^2) AAWSA
Legedadi	210	210
Geffersa	60	57
Dere	75.9	75

SWAT model requires different physical properties for each dam and the main required parameters and the data used are shown in Table Below

Table4. 2: SWAT parameters and data used (data sources Bathymetric survey2000)

SWAT parameters	**Legedadi (ha)**	**Geffersa (ha)**	**Dere (ha)**	**Description**
RES-ESA	490	135	133	Surface Area at maximum water level
RES-PSA	280	100	115	Surface Area at principal level
SWAT parameters	Legedadi (10^4m^3)	Geffersa (10^4m^3)	Dere (10^4m^3)	Description
RES-EVOL	4380	623	2350	Volume at maximum water level
RES-PVOL	2350	250	2000	Volume at principal level

4.7 Digital Elevation Model (DEM

Topography is defined by a Digital Elevation Model (DEM), which describes the elevation of any point in a given area at a specific spatial resolution as a digital file. Digital elevation

model is one of the essential inputs required by SWAT to delineate the watershed in to a number of sub watershed or sub basins.

DEM is used to analyze the drainage pattern of the watershed, slope, stream length, width of channel within the watershed. The digital elevation model used in this study was obtained from the Ministry of Water Resource with a resolution of 30m*30m.

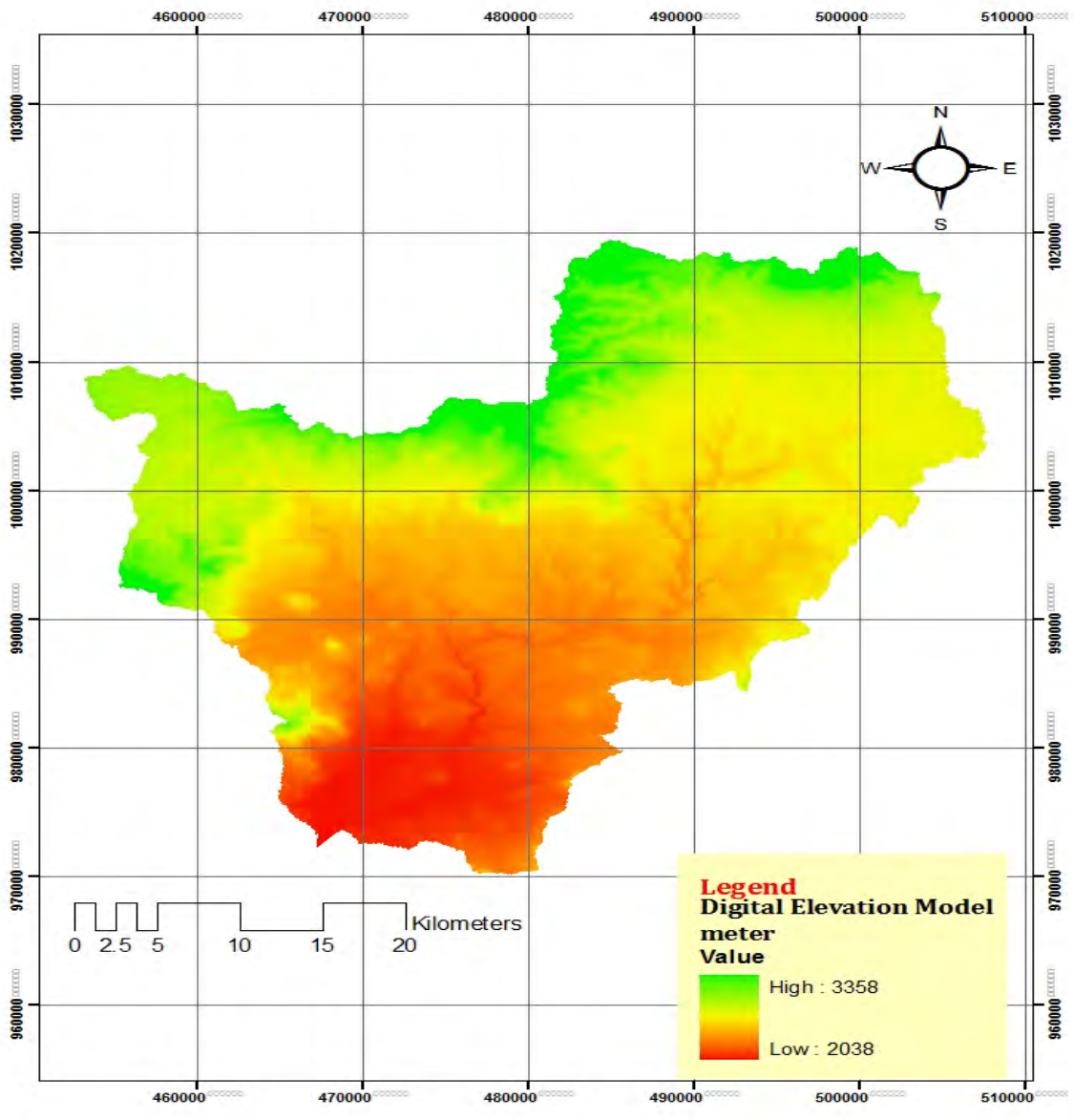

Figure4. 5: Digital Elevation Model for the study area

4.8 Land Use Land Cover Data

The land use is one of the most important factors that affect runoff, evapotranspiration and surface erosion in a catchment. The land cover data was obtained from MOWR which is done by Halcro for Awash basin Master Plan Project was used as a benchmark in producing the of land cover/land use map of the study area.

A look up table that identifies the 4-letter SWAT code for the different categories of land use/land cover were prepared so as to relate the grid values to SWAT land cover/land use classes. Detail analysis on land use land cover for the year 1973, 1986 and 2000 was given in next chapters of this report.

4.9 Soil Data

To have the SWAT model inputs concerning catchment's soil physical and chemical properties, first the shape file format of soil type distribution through the catchment was collected from Ethiopian MoWR GIS department. Using this shape file, soil texture, available water content, hydraulic conductivity, bulk density and organic carbon content for different layers (up to 4layers) of each soil type were extracted from Major Soils of the world database FAO (1995) and Digital soil map of the world database and Derived Soil Properties from FAO (1998)

Major soil types in the catchment are Chromic Luvisols, Eutric Vertisols, Vertic Cambisol ,Humic Nitisols and Lithic Leptosols.

Table4. 3: Major soil type of the study area

Soil Type	Symbol	SWAT Name	Area(ha)	% Watershed Area
Vertic Cambisol	CMv	ACMv	3536.01	2.48
Chromic Luvisol	LVx	ALVx	32018.13	22.44
Lithic Leptosol	LPq	ALPq	1211.49	0.85
Eutric Vertisol	Vre	AVRe	82257.11	57.65
Humic Nitisols	NTu	ANTu	22257.72	15.6
Water	WATR	WATE	1415.54	0.99
Total			142,696	100

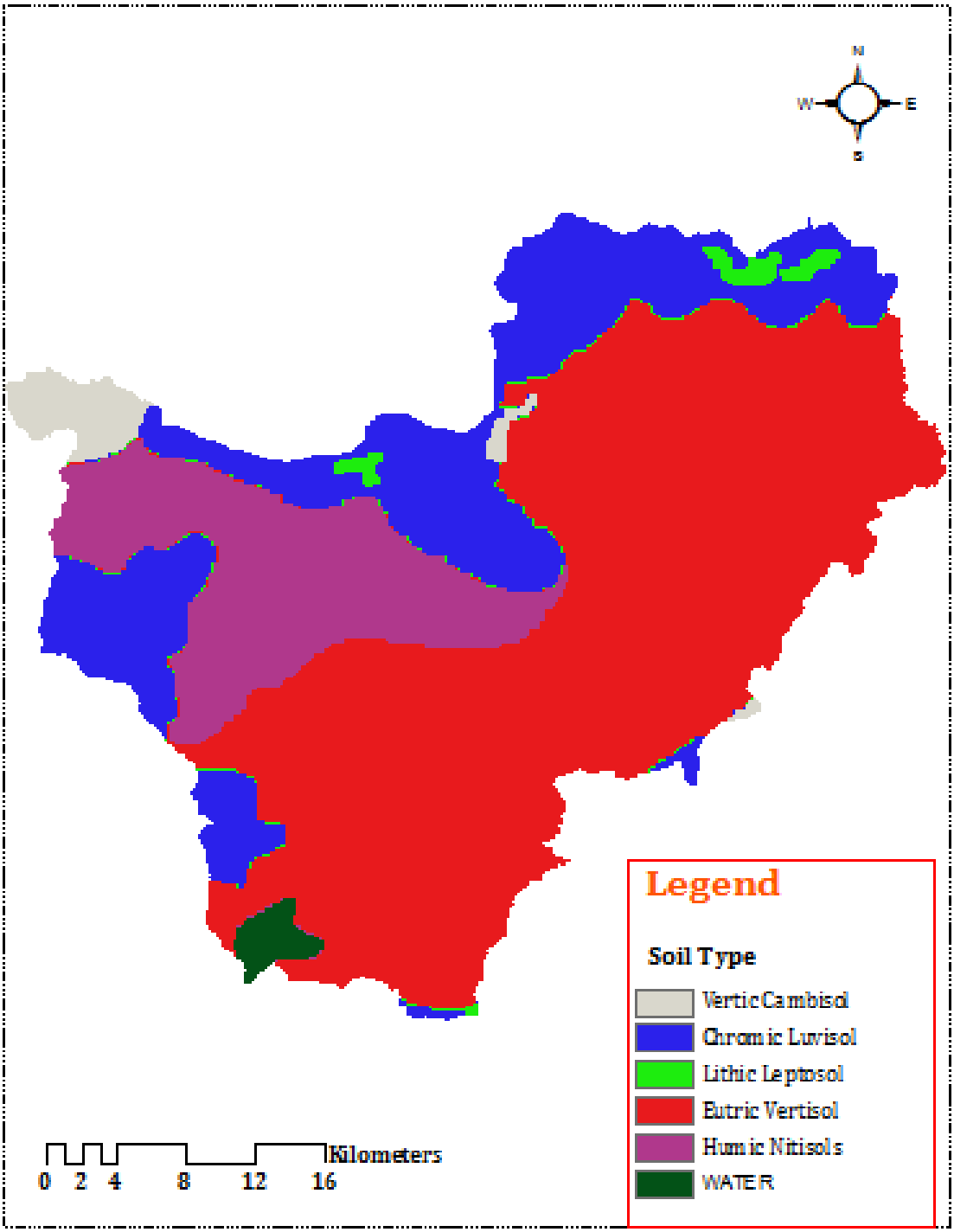

Figure4. 6: Soil Map of the study area

CHAPTER FIVE

5 Methodology

5 .1 Land Cover Classification

Landsat satellite imageries were used to identify changes in LU/LC distribution in the Akaki catchment over a 27 years period from 1973-2000. Landsat MSS, TM and ETM+ were selected to represent the land cover conditions in the years 1973, 1986 and 2000 respectively. The images are particularly acquired for the dry season to capitalize on

- The pronounced difference in reflectance between forested and non forested areas,
- Decreasing confusion at forest edges between dense forest vegetation and small scale agriculture plots.

The Landsat MSS imagery is in four channels (2 visible, 2 near-infrared) at 57-meter resolution. Landsat Thematic Mapper (TM) imagery provides seven multispectral channels (3 visible, 1 near-infrared, 2 mid-infrared, 1 thermal-infrared) at 30-meter resolution (120-meter resolution for the thermal-infrared band). Enhanced Thematic Mapper Plus (ETM+) adds an extra 15-meter resolution panchromatic band and improved resolution for the thermal- infrared map of 60m resolution.

Since the image had different file format, all images were imported in the tagged file formats (TIF). The acquisition dates, sensor, path/row, resolution of the Images are shown below.

Table5. 1: Profile of satellite image

Sensors (Instrument)	Satellite Name	Path	Row	Date of acquisition	Spatial Resolution(m)
Landsat MSS	Landsat_1	181	54	1/31/1973	57
Landsat TM	Landsat_5	168	54	1/28/1986	30
Landsat ETM+	Landsat_7	168	54	12/5/2000	30

To prepare land use/Land cover map for the hydrological model input, the software ERDAS 9.1 (Earth Resources Data Analysis System) was used to perform image analysis and image classification. This analysis was done to provide information on LU/LC trends and for generation of land cover scenario.

5.2 Image Analysis

5.2.1 Satellite Images Spectral Band Selection

Landsat imagery is acquired in a very precise manner, to better emphasize particular land cover aspects. Some of the parameters of this precision involve a scene's radiometry, providing distinct characteristics to components of the image scene. These measures help determine what the images are good for, from a science perspective. For example, Bands 1, 2 and 3 are used together to approximate how the real world appears. Bands 4, 5 or 7 from ETM+ are used in combination with 1, 2 or 3 to demonstrate vegetation conditions. It is sometimes necessary to convert the radiometric values from the initial at sensor measures, to compensate for atmospheric interference. Basic information that were used for image interpretation and band combinations for Landsat images as referred from GLCF site is provided in the table below .

Table5. 2: Landsat MSS image Spectral Bands and their application (ERDAS Filed Guide 2005)

Band N.O	Band	Band Name	Application
1	0.60-0.70	Red	. This band scans the region between the blue and red chlorophyll absorption bands. It corresponds to the green reflectance of health vegetation, and it is also useful for mapping water bodies
2	0.76-0.90	NIR	. Green vegetation mapping and cultural/urban features green vegetation and represents one of the most important bands for vegetation represents one of the most important bands for vegetation discrimination. It is also useful for discrimination of soil boundary and geological boundary delineation and cultural features.
3	0.70-0.80	MIR	This band is essentially responsive to the amount of vegetation biomass present in a scene. It is useful for crop identification and emphasizes soil/crop and land water contrasts.
4	0.8-1.10	MIR	This band is useful for vegetation survey and for penetrating haze.

Table5. 3: Landsat TM and ETM image Spectral Bands and their application (ERDAS Filed Guide, 2005)

Band N.O	Band	Band Name	Application
1	0.45-0.56	Blue	. Soil and vegetation discrimination
			. Bathymetry and coastal mapping
			. Cultural/ urban features
2	0.52-0.66	Green	. Green vegetation mapping and cultural/urban features
3	0.63-0.69	Red	. Vegetated and non vegetated mapping
			. Cultural/urban features
4	0.76-0.9	NIR	. Delineation of water body
			. Soil moisture discrimination
5	1.55-1.75	MIR	. Vegetation moisture discrimination
			. Soil moisture discrimination
			. Differentiation of snow and ice
6	10.4-12.5	TIR	. Vegetation and soil moisture analysis
			. Thermal mapping
7	2.08-2.35	NIR	. Discrimination of minerals and rocks
			. Vegetation moisture analysis

5.2.2 False Color Composite Image Preparation

To enhance the visualization of the land cover and to prepare the image for the future classification various false color composite were made. The applications of bands for different feature identification were used according to the information provided in above table. Different band combinations both TCC and FCC are used to select for classification. According to the information extracted the spectral response for different features and land cover types was analyzed. The spectral profile graph below shows the response of each land cover for different spectral bands.

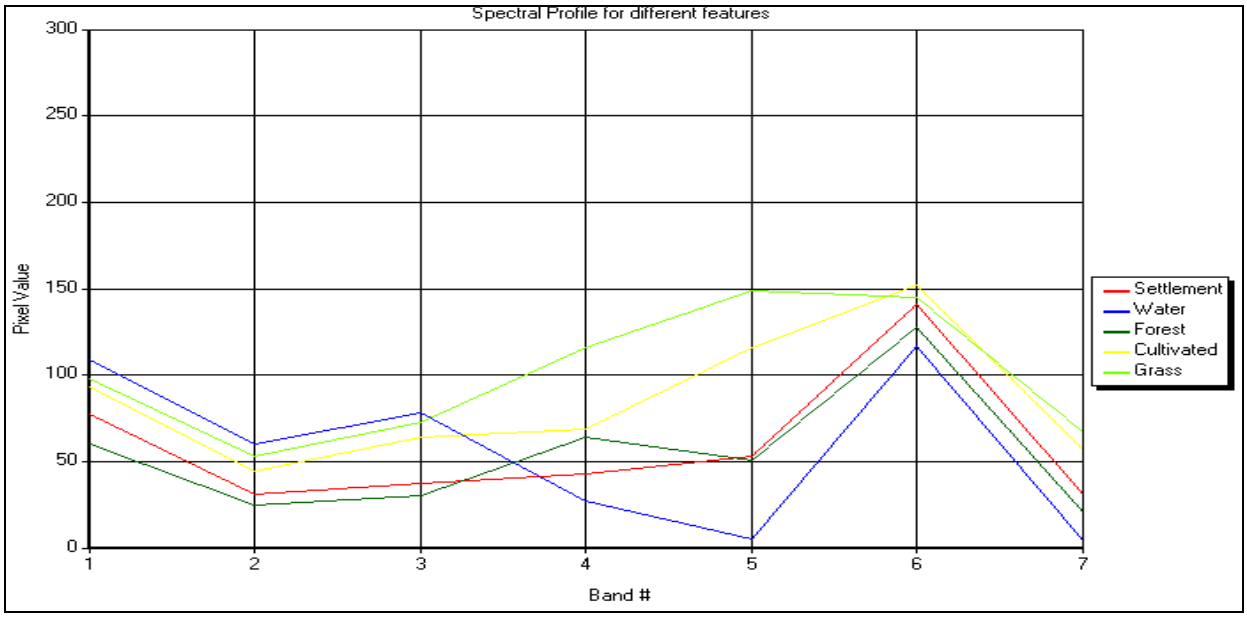

Figure5. 1: Spectral response of Land sat TM for different cover classes

The best image combination used for land cover identification and LU/LC mapping were the FCC prepared using bands 4, 3 ,2 (RGB) for both Landsat TM and ETM+, and 4-2-1 for MSS satellite imageries.

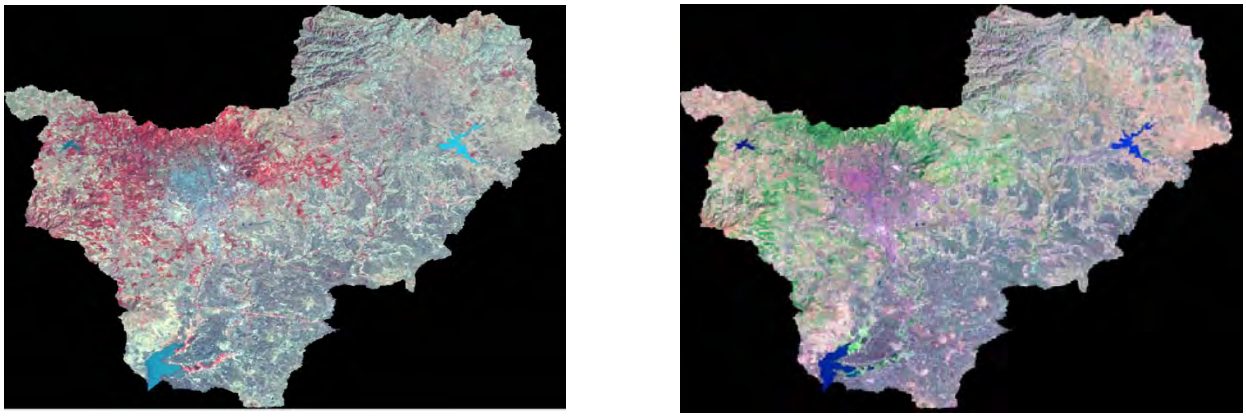

A:-Landsat MSS B: - Landsat TM

Figure5. 2: Band combinations for Landsat MSS and Landsat TM

5.3 Image Classification

5.3.1 Unsupervised Classification

Unsupervised classification is used to cluster pixels in a data set into classes based on statistics only. These classes are spectral classes and their identity is not initially known, until they are compared with some reference data. This method calculates class means evenly distributed in the data space and then iteratively clusters the remaining pixels using minimum distance techniques. Each iteration recalculate means and reclassifies pixels with respect to the new means. All pixels are classified to the nearest class unless a standard deviation or distance threshold is specified. If some pixels do not meet the selected criteria, they will be unclassified. This process continues until the number of pixels in each class changes by less than the selected pixel change threshold or the maximum number of iterations is reached. The final clusters are used to classify the image with classifiers such as the minimum distance or maximum likelihood. The output however requires post classification operations to make the results more meaningful.

Image classification was first done by unsupervised classification using the ISODATA algorithm. This produced a map with 10 classes which was then displayed over color

composite images, and classes assigned to a specific land cover category. The output of this method is used in the process of supervised classification.

In this study, total outputs of 10 classes were found; but reduced to five classes after information and statistics obtained from MOWR, HALCRO, AACA, AAWSA and EMA. The description of these land cover classes can be stated as follows:

The five land cover classes were considered namely; Forest land, Grass land, cultivated land, Settlement (urban) and Water body.

- **Forest Land**: Area with high density of trees which include deciduous forest land, ever green forest land, mixed forest land and plantation forests that mainly are eucalyptus, junipers and conifers.
- **Grass land**: Area covered with grass that is used for grazing and that covered for a considerable period of the year (half of the year).
- **Water body**: Area which remains water logged throughout the year, in this study refer to manmade reservoirs.
- **Cultivated Land** : Areas used for both annual and perennial crop cultivation
- **Settlement (Urban):** areas where there is a permanent concentration of people building, and other man-made structures and other activities.

5.3.2 Supervised Classification

This method is used to cluster pixels in a data set into classes corresponding to user-defined area of interest (AOIs) or training classes which are selected as representative areas to be mapped in the output. Supervised classification done using Maximum Likelihood algorithm. Training classes were defined prior to performing supervised classification.

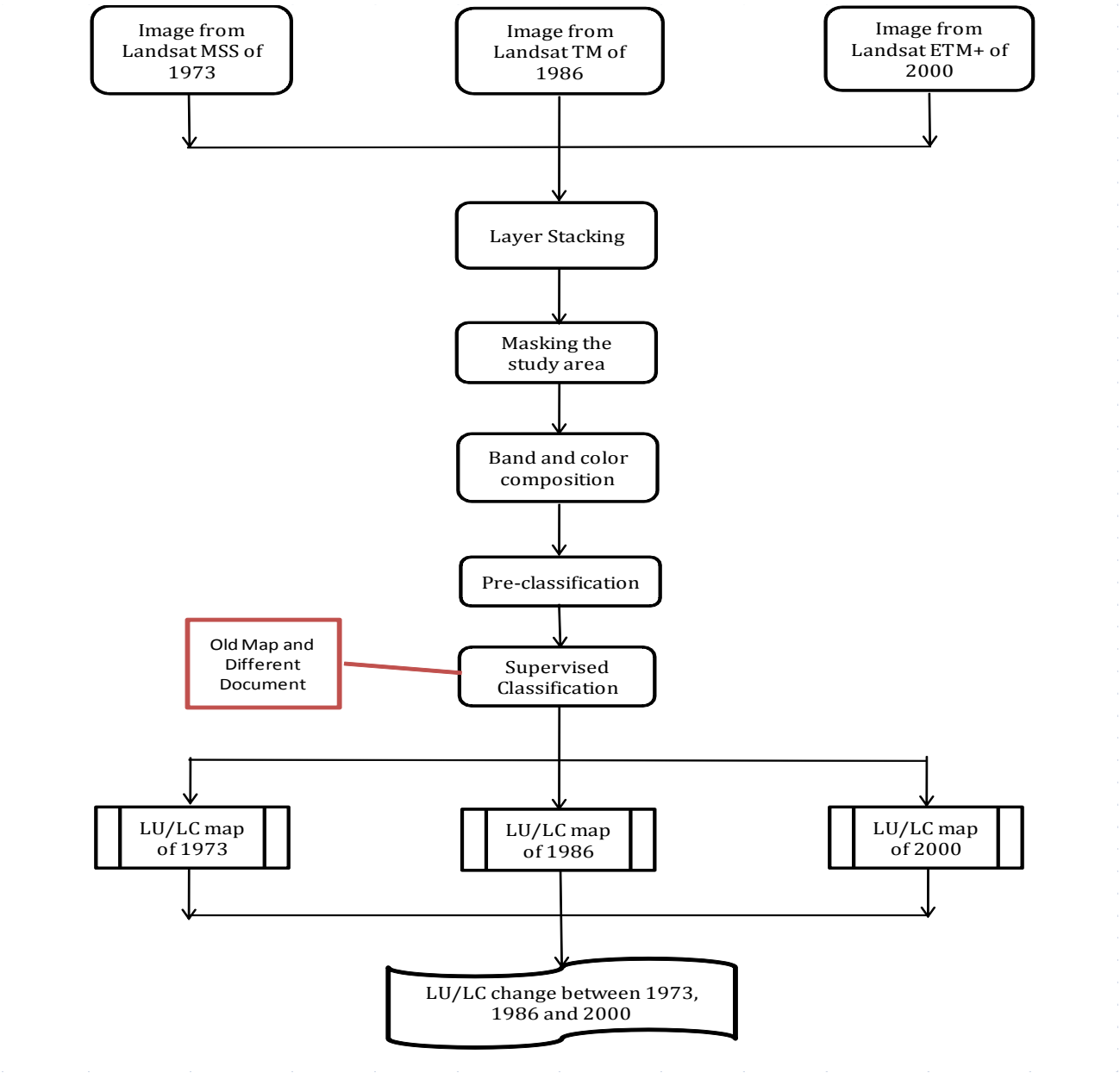

Figure5. 3: Flow chart showing the methodology of the Land use Land cover map preparation

5.4 Land use and Land cover Scenario

Scenario analysis is a process of evaluating possible future events by considering alternative possible outcomes. This analysis is designed to facilitate decision-making and assessment through a complete consideration of possible outcomes and their implications.

In September 2000, UN member states held a Millennium Summit in New York declare that eight Millennium Development Goals (MDGs), each of which has its own specific targets. All of the eight goals are interrelated, with the achievement of any one of them contributing

considerably towards the achievement of the others. Nonetheless, the MDG that specifically aims at improving the living conditions of the urban population is Goal 7, Target 11 that aims at achieving "a significant improvement in the lives of at least 100 million slum dwellers" by 2020.

To address the goal Addis Ababa municipal authority launched a massive urban renewal and new development programs in order to upgrade the view of the city. It has planned to construct more than 400,000 residential units over five years in the predominantly in 103 building sites across the city two-thirds of these units are currently completed. Real estate developers are now becoming increasingly ever since currently above 2700ha of land is was leased to developers (access capital, 2010).

This will lead to change more and more land features (forest and grass land) to impervious area before. Impervious cover in a watershed has a high influence in runoff process by reducing the infiltration to increase in volume and velocity of runoff and larger peak flood discharges.

The scenario was created for the year 2020 by changing patches of selected land cover type one into target land cover type two. Land cover classifications derived from mainly Addis Ababa Master Plan study (AAMP 1999) and Landsat image of 2000 were used as a baseline. The land cover was defined by assigning changed areas to the baseline classification, selected randomly by computer simulation within the selected land cover type, and spread evenly over the target catchment. The total land cover area for this scenario was done by linear extrapolation of classified Satellite images.

5.5 Hydrological Modeling

5.5.1 Hydrological Component of SWAT

The simulation of the hydrology of a watershed is done in two separate divisions. One is the land phase of the hydrological cycle that controls the amount of water, sediment, nutrient and pesticide loadings to the main channel in each sub-basin. Hydrological components simulated in land phase of the hydrological cycle are canopy storage, infiltration, redistribution, evapotranspiration, lateral subsurface flow, surface runoff, ponds, tributary channels and return flow. The second division is routing phase of the hydrologic cycle that

can be defined as the movement of water, sediments, nutrients and organic chemicals through the channel network of the watershed to the outlet.

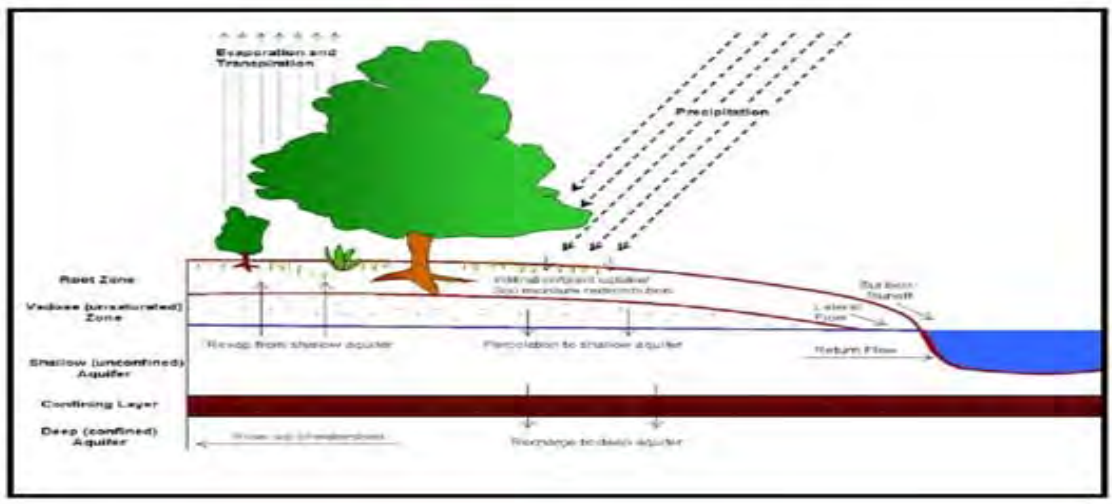

Figure5. 4: Hydrological components of SWAT model

The hydrologic cycle as simulated by SWAT is based on the water balance equation:

$$SW_t = SW_0 + \sum_{i=1}^{t}(R_{day} - Q_{surf} - E_a - W_{seep} - Q_{gw}) \quad \text{----------} \quad \text{(Eq).5.1}$$

In which SW_t is the final soil water content (mm), SW_o is the initial soil water content on day i (mm), t is the time (days), R_{day} is the amount of precipitation on day i (mm), Q_{surf} is the amount of surface runoff on day i (mm), E_a is the amount of evapotranspiration on day i (mm), W_{seep} is the amount of water entering the vadose zone from the soil profile on day i (mm), and Q_{gw} is the amount of return flow on day i (mm).

5.5.2 Surface Runoff Generation

Surface runoff or overland flow is a flow that occurs along a sloping surface and it occurs whenever the rate of water application to the ground surface exceeds the rate of infiltration. It is the major component of the hydrologic cycle.

SWAT2005 provides two surface runoff computation methods; a modification of the Soil Conservation Service (SCS) Curve Number (CN) method (USDA SCS, 1972) or the Green and Ampt infiltration method (Green and Ampt, 1911). The CN method was initially developed for small agricultural watersheds and the CN varies non-linearly with the moisture content of the soil. It drops to zero as the soil approaches the wilting point and increases to near 100 as the soil approaches saturation, with higher CNs associated with higher runoff

potential watershed. In this study, the SCS curve number method was used to estimate surface runoff because of the unavailability of sub daily data for Green & Ampt method.

The method is an empirical model, which is based on the following equation:

$$Q_{surf} = \frac{(R_{day} - I_a)^2}{(R - I_a + s)}$$ ---------- Eq.5.2

Where: Q_{surf} is accumulated runoff or rainfall excess (mm water), R_{day} is rainfall depth for the day (mm water), I_a *is* an initial abstraction which includes surface storage, interception and infiltration prior to runoff (mm water),S is a retention parameter (mm water).

The retention parameter varies spatially due to changes in soils, land use, management and slope and temporally due to changes in soil water content. It is mathematically expressed as:

$$S = 25.4\left(\frac{100}{CN} - 10\right)$$ ---------- Eq.5.3

Where: CN is the curve number for the day. CN = f (land use, practice, soil permeability, soil hydrologic group) For the definition of the soil hydrologic groups, the model uses the U.S. Natural Resource Conservation Service (NRCS) classification, which classifies soils into four hydrologic groups (A, B, C, & D) based on infiltration characteristics of the soils. Group A, B, C and D soils have high, moderate, slow, and very low infiltration rates with low, moderate, high, and very high runoff potential, respectively. The initial abstraction, Ia, is commonly approximated as 0.2S and the equation becomes

$$Q_{surf} = \frac{(R_{day} - 0.2S)^2}{(R_{day} + 0.8S)}$$ ---------- Eq.5.4

5.5.3 Peak Runoff Rate

The peak discharge or the peak surface runoff rate is the maximum volume flow rate passing a particular location during a storm event. SWAT calculates the peak runoff rate with a modified rational method. In rational method it assumed that a rainfall of intensity i begins at time t = 0 and continues indefinitely, the rate of runoff will increase until the time of concentration, t = tconc. The modified rational method is mathematically expressed as

$$q_{peak} = \frac{\alpha_{tc} * Q_{surf} * Area}{3.6 * t_{conc.}}$$ ---------- Eq.5.5

Where: q_{peak} is the peak runoff rate (m^3/s),α_{ct} is the fraction of daily rainfall that occurs during the time of concentration, Q_{surf} is the surface runoff (mm), Area is the sub-basin area (km^2), t_{conc} is the time of concentration (hr), and 3.6 is a conversion factor.

SWAT estimates the value of α using the following equation:

$$\alpha_{tc} = 1 - \exp[2 * t_{conc} * \ln(1 - \alpha_{0.5})]$$ ---------- Eq.5.6

Where: t_{conc} is the time of concentration (hr), and $\alpha_{0.5}$ is the fraction of daily rain falling in the half-hour highest intensity rainfall.

5.5.4 Time of Concentration

The time of concentration, t_{conc}, is a time within which the entire sub basin area is discharging at the outlet point. It is calculated by summing up both the overland flow time of the furthest point in the sub basin to reach a stream channel (t_{ov}) and the upstream channel flow time needed to reach the outlet point (t_{ch}):

$$t_{conc} = t_{ov} + t_{ch}$$ ---------- Eq.5.7

The overland flow time (tov) is computed as:

$$t_{ov} = \frac{L_{slp}}{3600 * V_{ov}}$$ ---------- Eq.5.8

Where: L_{slp} is the average sub basin slope length (m), V_{ov} is the overland flow velocity (m/s), and 3600 is a unit conversion factor.

The overland flow velocity for a unit width along the slope is calculated by using the

Manning's equation:

$$V_{ov} = \frac{q_{ov}^{0.4} * S_{lp}^{0.3}}{n^{0.6}}$$ ---------- Eq.5.9

Where: q_{ov} is the average overland flow rate (m^3/s), Slp is the average slope of the sub basin (m/m), n is Manning's roughness coefficient of the sub basin.

Assuming an average flow rate of 6.35 mm/hr and substituting the equation of V_{ov} into t_{ov}, the simplified equation of the overland flow becomes:

$$t_{ov} = \frac{L_{slp}^{0.6} * n^{0.6}}{16 * slp^{0.3}} \quad \text{---------- Eq.5.10}$$

Channel flow time is computed as:

$$t_{ch} = \frac{L_c}{3.6 * V_c} \quad \text{---------- Eq.5.11}$$

Where: Lc is the average flow channel length (km), Vc is the average flow velocity (m/s), and 3.6 is a unit conversion factor.

The average flow channel length is calculated as:

$$L_c = \sqrt{L * L_{cen}} \quad \text{---------- Eq.5.12}$$

Where: L is the channel length from the furthest point to the sub basin outlet (km),Lcen is the distance along the channel to the sub basin centroid (km).

Assuming Lcen = 0.5L, and using the Manning's equation for Vc for a trapezoidal channel with side slope of 2:1 and bottom width to depth ratio of 10:1, channel flow time becomes:

$$t_{ch} = \frac{0.62 * L * n^{0.75}}{Area^{0.125} * slp_{ch}^{0.375}} \quad \text{---------- Eq.5.13}$$

Where: tch is the time of concentration for channel flow (hr), L is channel length from the most distant point to the sub basin outlet (km), n is Manning's roughness coefficient for the channel, Area is the sub basin area (km^2), and Slpch is the channel slope (m/m).

5.5.4 Urban Area

Most large watersheds and river basins contain areas of urban land use. Estimates of the quantity and quality of runoff in urban areas are required for comprehensive management analysis.

In urban areas, surface runoff is calculated separately for the directly connected impervious area and the disconnected impervious/pervious area. For directly connected impervious area, a curve number of 98always used. For disconnected impervious/pervious areas, a composite curve number is calculated and used in the surface runoff calculations. The equations used to calculate the composite curve number for disconnected impervious/pervious areas are (Soil Conservation Service Engineering Division, 1986)

$$CN\ c = CN\ p + imp_{tot} \cdot (CN_{imp} - CN\ p) * \left(1 - \frac{impdco}{2 * imptot}\right) \quad \text{---------- (Eq). 5.14} \quad \text{if } imp_{tot} < 0.2$$

$$CN\ c = CN\ p + imptot \cdot (CN\ imp - CN\ p) \quad \text{----------(Eq). 5.15} \quad \text{if } imp_{tot} > 0.30$$

where CNc is the composite moisture condition II curve number, CNp is the pervious moisture condition II curve number, CNimp is the impervious moisture condition II curve number, imptot is the fraction of the HRU area that is impervious (both directly connected and disconnected), and impdcon is the fraction of the HRU area that is impervious but not hydraulically connected to the drainage system.

5.5.5 Computation of Evapotranspiration

The combination of two separate processes where by water is lost on the one hand from the soil surface by evaporation and on the other hand from the crop by transpiration is referred to as evapotranspiration (ET).

Evaporation: is the process whereby liquid water is converted to water vapour (vaporization) and removed from the evaporating surface (vapour removal). Water evaporates from a variety of surfaces, such as lakes, rivers, pavements, soils and wet vegetation.

Transpiration:-consists of the vaporization of liquid water contained in plant tissues and the vapour removal to the atmosphere. Crops predominately lose their water through stomata. These are small openings on the plant leaf through which gases and water vapour pass (FAO 56).

SWAT2005 offers three models for estimating PET: the Penman-Monteith model (Monteith, 1965), Priestley-Taylor model (Priestley and Taylor, 1972), and Hargreaves model (Hargreaves and Samani, 1985). In this study daily potential evaporation is calculated by

using Penman-Monteith formula. The Penman approach of estimating evapotranspiration combines the mass transfer and energy balance approach because of which it gained strong physical base (Dingman, 2002). The Penman Monteith requires radiation, air temperature, air humidity, and wind speed data.

$$ET_O = \frac{0.408\Delta(R_n - G) + \gamma \frac{900}{T+273} u_2 (e_s - e_a)}{\Delta + \gamma(1 + 0.34u_2)}$$ ---------- Eq.5.16

Where:

ETo reference evapotranspiration [mm day-1], Rn net radiation at the crop surface [MJ m-2 day-1], G soil heat flux density [MJ m-2 day-1], T mean daily air temperature at 2 m height [°C], u_2 wind speed at 2 m height [m s-1], e_s saturation vapour pressure [kPa], e_a actual vapour pressure [kPa], e_s-e_a saturation vapour pressure deficit [kPa], Δ slope vapour pressure curve [kPa °C-1],and γ psychrometric constant [kPa °C-1].

5.5.6 Groundwater

The simulation of groundwater is partitioned into two aquifer systems i.e. an unconfined aquifer (shallow) and a deep-confined aquifer in each sub basin. The unconfined aquifer contributes to flow in the main channel or reach of the sub basin. Water that enters the deep aquifer is assumed to contribute to stream flow outside the watershed (Arnold et al., 1993). In SWAT2005 the water balance for a shallow aquifer is calculated with equation

$$aq_{sh,i} = aq_{sh,i} + W_{rchrg} - Q_{gw} - W_{revap} - W_{deep} - W_{pump,sh}$$ ---------- (Eq). 5.17

Where: $aq_{sh,i}$ is the amount of water stored in the shallow aquifer on day i (mm), $aq_{sh,i-1}$ is the amount of water stored in the shallow aquifer on day i-1 (mm), W_{rchrg} is the amount of recharge entering the aquifer on day i (mm), Q_{gw} is the groundwater flow, or base flow, into the main channel on day i (mm), W_{Revap} is the amount of water moving into the soil zone in response to water deficiencies on day i (mm), W_{deep} is the amount of water percolating from the shallow aquifer into the deep aquifer on day i (mm), and $W_{pump,sh}$ is the amount of water removed from the shallow aquifer by pumping on day i (mm).

5.6 Routing Phase of the Hydrological Cycle

The second phase of the SWAT hydrologic simulation, the routing phase, consists of the movement of water, sediment and other constituents (e.g. nutrients, pesticides) in the stream network. The rate and velocity of flow is calculated by using the Manning equation. The main channels or reaches are assumed to have a trapezoidal shape by the model. Two options are available to route the flow in the channel networks: the variable storage and Muskinghum methods. Both are variations of the kinematic wave model. While calculating the water balance in the channel flow, the transmission and evaporation are also well considered by the model. The variable storage method uses a simple continuity equation in routing the storage volume, whereas the Muskinghum routing method models the storage volume in a channel length as a combination of wedge and prism storages. In the latter method, when a flood wave advances into a reach segment, inflow exceeds outflow and a wedge of storage is produced. As the flood wave recedes, outflow exceeds inflow in the reach segment and a negative wedge is produced. In addition to the wedge storage, the reach segment contains a prism of storage formed by a volume of constant cross-section along the reach length. For this study, the variable storage method was adopted. The method was developed by (Williams, 1969) and used in the ROTO (Routing Outputs to Outlet) (Arnold etal*., 1*995) model. Storage routing is based on the continuity equation

$$\Delta V_{storage} = V_{in} - V_{out} \quad \text{----------} \quad \text{(Eq). 5.18}$$

Where: Vin is the volume of inflow during the time step (m^3 water), V_{out} is the volume of outflow during the time step (m^3 water), and V_{stored} is the change in volume of storage during the time step (m^3 water). Detail of the equation was given in SWAT manual.

5.7 Impoundment Water Routing

Impoundments play an important role in water supply and flood control. SWAT models four types of water bodies: ponds, wetlands, depressions/potholes, and reservoirs. Ponds, wetlands, and depressions/potholes are located within a subbasin off the main channel. Water flowing into these water bodies must originate from the subbasin in which the water body is located. Reservoirs are located on the main channel network. They receive water from all subbasins upstream of the water body. The features of an impoundment are shown in figure below

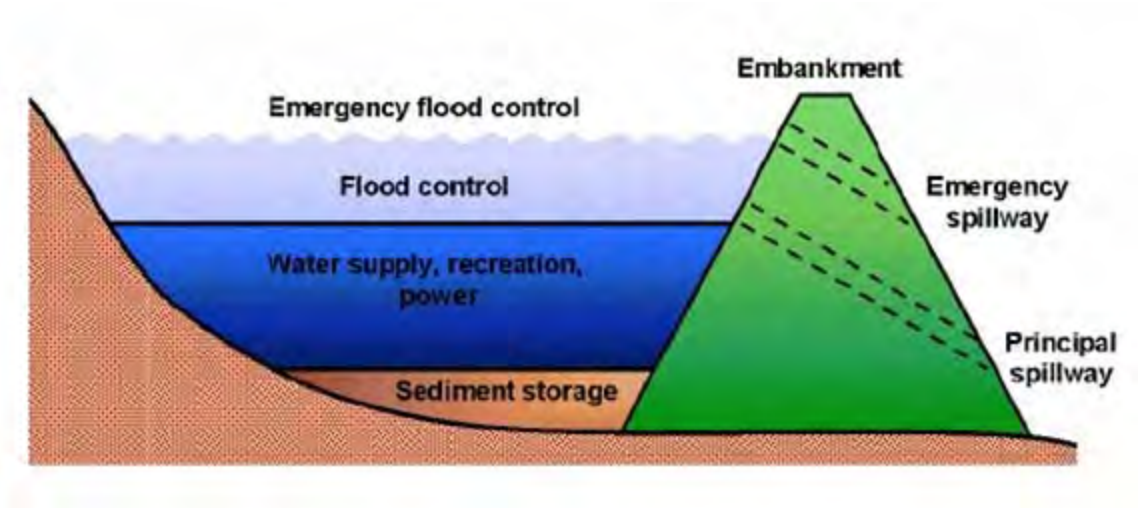

Figure5. 5: Components of a reservoir with flood water detention features (After Ward andElliot, 1995).

The water balance for a reservoir is:

$$V = Vstored + Vflowin - Vflowout - Vevap + Vpcp - Vseep$$ ---------- (Eq). 5.19

Where V is the volume of water in the impoundment at the end of the day (m^3 H2O), Vstored: is the volume of water stored in the water body at the beginning of the day (m^3 H2O), Vflowin: is the volume of water entering the water body during the day (m^3 H2O), Vflowout : is the volume of water flowing out of the water body during the day (m^3 H2O), Vpcp: is the volume of precipitation falling on the water body during the day (m^3 H2O), Vevap: is the volume of water removed from the water body by evaporation during the day (m^3H_2O), and Vseep: is the volume of water lost from the water body by seepage(m^3H_2O).

More detailed on the reservoir component like surface area, volume of precipitation, volume of evaporation, volume of seepage and volume of flowout on the reservoir are available on theoretical documentations are found in Neitsch etal (2005) for SWAT2005. SWAT use four methods to calculate the volume of out flow from reservoirs

A: - Measured daily outflow,

B: - Measured monthly outflow,

C:-Average annual release rate for uncontrolled reservoir,

D:-Controlled outflow with target release.

Because of gating either daily or monthly outflow data this research used controlled outflow with target release options, it tries to mimic general release rules that may be used by reservoir operators. Although the method is simple and cannot account for all decision criteria, it can realistically simulate major outflow and low flow periods.

For the controlled outflow with target release approach, the principal spillway volume corresponds to maximum flood control reservation while the emergency spillway volume corresponds to no flood control reservation. The model requires the beginning and ending month of the flood season. In the non-flood season, no flood control reservation is required, and the target storage is set at the emergency spillway volume. During the flood season, the flood control reservation is a function of soil water content. The flood control reservation for wet ground conditions is set at the maximum. For dry ground conditions, the flood control reservation is set at 50% of the maximum. The target storage may be specified by the user on a monthly basis or it can be calculated as a function of flood season and soil water content. If the target storage is specified:

$V_{targ} = V_{starg}$ ---------- (Eq).5.20

Where Vtarg is the target reservoir volume for a given day (m^3 H2O), and Vstarg is the target reservoir volume specified for a given month (m^3 H2O). If the target storage is not specified, the target reservoir volume is calculated:

$V_{targ} = V_{em}$ ---------- (Eq). 5.21

if mon fld ,beg < mon < mon fld ,end

$$V_{t\arg} = V_{pr} + \frac{\left(1 - \min\left[\frac{SW}{FC}, 1\right]\right)}{2} * \left(V_{em} - V_{pr}\right)$$ ---------- (Eq). 5.22

if mon ≤ mon fld ,beg or mon ≥ mon fld ,end

where Vtarg :- is the target reservoir volume for a given day (m3 H2O), Vem:- is the volume of water held in the reservoir when filled to the emergency spillway (m^3 H2O), Vpr:- is the volume of water held in the reservoir when filled to the principal spillway (m^3

H2O), SW:- is the average soil water content in the subbasin (mm H2O), FC:- is the water content of the subbasin soil at field capacity (mm H2O), Mon:- is the month of the year, mon fld,beg:- is the beginning month of the flood season, and mon fld,end:- is the ending month of the flood season. Once the target storage is defined, the outflow is calculated:

$$Vflowout = \frac{V - Vtarg}{NDtarg}$$ ---------- (Eq).5.23

Where

Vflowout :- is the volume of water flowing out of the water body during the day (m^3 H2O), V is the volume of water stored in the reservoir (m^3H2O), Vtarg: is the target reservoir volume for a given day (m^3 H2O), and NDtarg, is the number of days required for the reservoir to reach target storage.

5.8 Flow Separation

The automated base flow separation and recession analysis techniques (Arnold *et al.* 1999), are among the several methods available to separate base flows. Due its simplicity, this technique was applied.

The automated base flow separation and recession analysis technique uses a dos based software called Base flow-program found from the SWAT website. It is developed based on the recursive digital filter techniques (Nathan and McMahon 1990), and filters surface runoff (high frequency signals) from base flow (low frequency signals). The filter can be passed over the stream flow data three times (forward, backward, and forward). The details of the methodology are explained in Arnold *et al.* (1995).

Furthermore, they suggested that in general the fraction of water yield contributed by base flow should fall somewhere between the value for the fraction of stream flow contributed by base flow that is estimated in first pass (Fr1) and in second pass (Fr2). This is true if the base flow in the watershed is from aquifers recharged by precipitation falling in the watershed. So the value between these two was adopted for the calibration of SWAT simulated flow. In addition to the alpha factor, the base flow days (number of days for the base flow recession to decline through one log cycle) was also calculated.

5.9 Arcswat Model

In conjunction with the SWAT model, ArcSWAT was used to preprocess GIS data. ArcSWAT is an extension to the SWAT model that runs within ArcGIS. It provides a graphical user-interface that allows for GIS data to be easily formatted for use in SWAT model simulations. ArcSWAT breaks preprocessing into three main steps: Watershed Delineation, Hydrologic Response Unit (HRU) Analysis, and Weather Data Definition with that of sensitivity Analysis and calibration.

In order to understand how each section works within the modeling process, it is important to understand the conceptual framework of each step, as well as what data are used and how they are integrated into ArcSWAT. Therefore, the major steps of ArcSWAT preprocessing will be covered in depth.

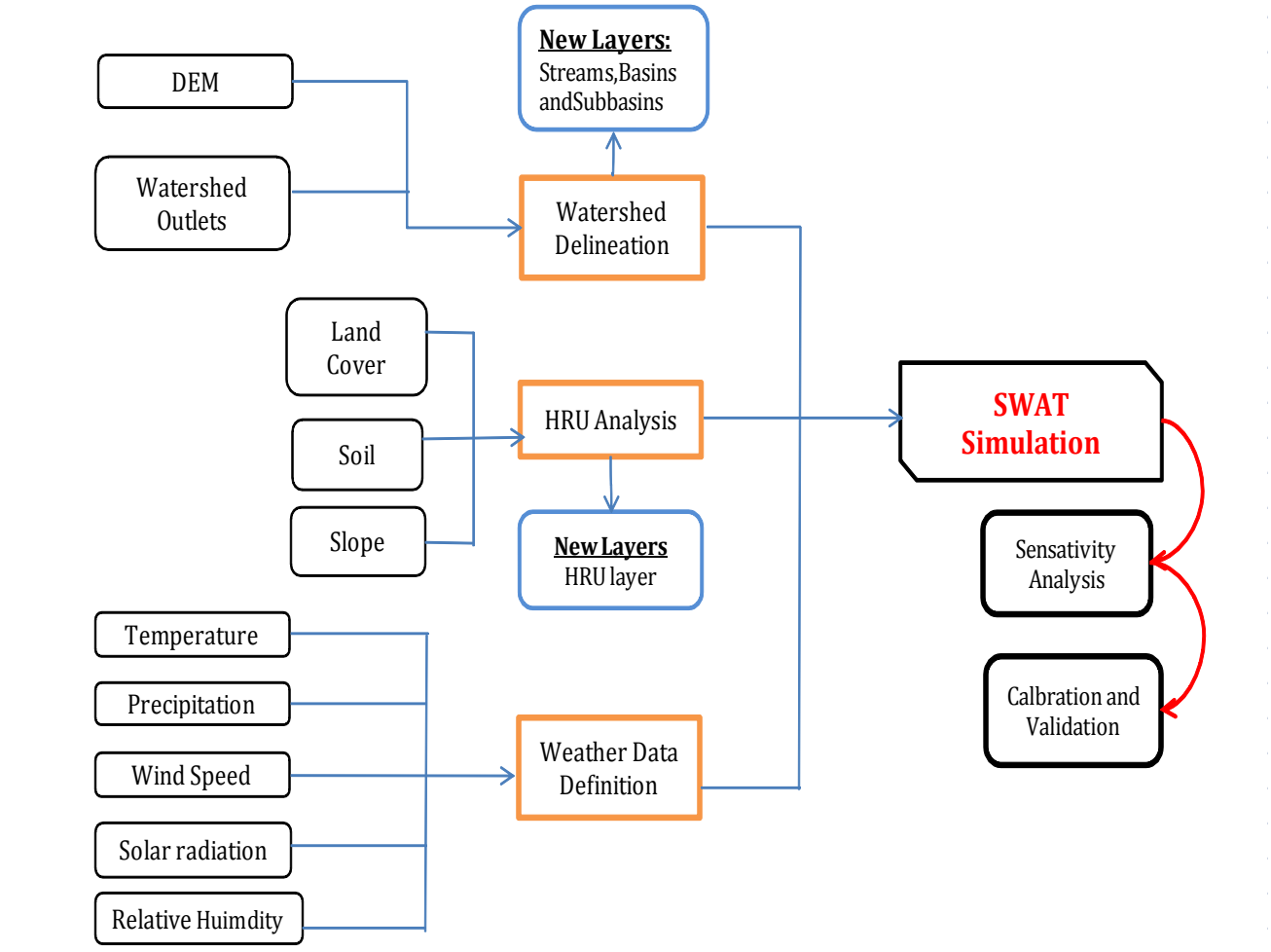

Figure5. 6: Flowchart of ArcSWAT processing Steps

5.9.1 Watershed Delineation

The Watershed Delineation section of ArcSWAT data processing allows for the formatting of data in preparation for dividing the watershed into subunits. This is particularly useful when there are distinct areas within the watershed that are primarily of one land use or soil type. Subdivision allows for the differentiation of these areas, so that the associated impact on hydrology can be more accurately measured and studied (Neitsch 2005). The primary division made is on the subbasin level, and is determined based on the relative spatial location of each subbasin, the direction of hydrologic flow and the natural divisions of stream networks determined by elevation. A digital elevation model (DEM) is the only required dataset for this step.

Reach and Monitoring Point layers are created for the ArcSWAT-determined stream network and the inlet/outlets, respectively. Outlet and inlet definition, along with reservoir placement, is the last major section of Watershed Delineation. User-supplied table of outlet locations was imported and integrated into the ArcSWAT determined points layer. These outlet locations were determined based on the most downstream points of watershed boundaries that were intersected by a major stream channel. All stream gauging stations which were collected from MOWR are imported in a dbase format added to the Monitoring Point layer.

5.9.2 HRU Analysis

The HRU Analysis section takes land use, soil and slope data, and divides each subbasin into hydrologic response units, with specific combinations of the three layers respective characterizations. The layer produced by this process is crucial to the ultimate analysis performed by the SWAT model, because it determines the land, soil and slope category assigned to each HRU. This category determines how land will respond to precipitation, runoff, infiltration and other hydrologic processes during the simulation. Each subbasin can then have one or more major HRUs defined within it.

ArcSWAT requires that land cover and soil data be accompanied by a look-up table with attribute information for each specific land cover and soil type, and provides these tables for each layers. The last layer needed for the HRU Analysis setup is slope, which is determined from the DEM supplied during watershed delineation.

Once each layer is loaded, they must be overlaid to determine the HRU features. For every unique combination of slope, land use and soil class an HRU will be created, although within the study area there can be multiple HRUs with the same combination.

The last step is to define how HRU classifications will be aggregated or transferred to the subbasin level. The Multiple HRU option was chosen for defining HRU. This option allows the user to select a threshold for each category individually, starting with land use, then soil class, and finally ending with slope.

According to (Luzio *et al.* 2002) user manual, the threshold levels set for multiple HRUs is a function of the project goal and the amount of detail desired by the modeler. For most applications, the default settings for land use threshold (20 %) soil threshold (10 %) and 20% slope are applied in this research work.

5.9.3 Weather Data Definition

Another major section of ArcSWAT is Weather Data. Weather data necessary for running a basic SWAT simulation are precipitation, wind speed, relative humidity, solar radiation as well as maximum and minimum temperatures. Once database setup is complete in ArcSWAT, the designated weather station locations are added to the Monitoring Point layer created during Watershed Delineation. The last step before a SWAT simulation can be run is to write all of the input files required by SWAT and produced from the preprocessed data from ArcSWAT. Once they are written, individual files can be edited through ArcSWAT, or externally. Because it is cumbersome to edit information for each subbasin, reservoir, etc. individually in ArcSWAT, tables were linked to an Access database, and automatically updated based on predetermined queries. Making edits to a selection of these files is crucial to producing more accurate SWAT simulations and outputs.

5.9.4 Sensitivity Analysis

Sensitivity analysis is a technique of identifying the responsiveness of different parameters involving in the simulation of a hydrological process. For big hydrological models like SWAT, which involves a wide range of data and parameters in the simulation process, calibration is quite a cumbersome task. Sensitivity analysis is a method of minimizing the number of parameters to be used in the calibration step by making use of the most sensitive parameters largely controlling the behavior of the simulated process. This

appreciably eases the overall calibration and validation process as well as reduces the time required for it. Besides, as (Lenhart etal, 2002) indicated, it increases the accuracy of calibration by reducing uncertainty.

SWAT model has an embedded tool to perform sensitivity analysis and provides recommended ranges of parameter changes. SWAT2005 uses a combination of Latine Hypercube Sampling and One-At-a-Time sensitivity analysis methods (LH-OAT method) (van Griensven, 2005). The concept of the Latin-Hypercube Simulation is based on the Monte Carlo Simulation to allow a robust analysis but uses a stratified sampling approach that allows efficient estimation of the output statistics while the One-Factor-At-a-Time is an integration of a local to a global sensitivity method (van Griensven, 2005). In local methods, each run has only one parameter changed per simulation which aides in the clarity of a change in outputs related directly to the change in the parameter altered (Green and van Griensven, 2007).

This, therefore, justified the need for the sensitivity analysis made in the study area. The analysis involved a total of 27 parameters. For the study area the sensitivity analysis should be carried out for a period of six years, (from January 1, 1997 to December 31, 2002)

Table5. 4: Sensitivity class for SWAT model

Sensitivity Class for SWAT model Class	Index	Sensitivity
I	0.00 /1/<0.05	Small to Negotiable
II	0.05 /I/<0.2	Medium
III	0.02 /I/<1	High
IV	/I/ 1	Very high

5.9.5 Calibration

Calibration is tuning of model parameters based on checking results against observations to ensure the same response over time. This involves comparing the model results, generated with the use of historic meteorological data, to recorded stream flows. In this process, model parameters varied until recorded flow patterns are accurately simulated. Model calibration of SWAT run can be divided in to several steps. Among these Water balance and stream flow generation are the most important part is also considered. (Refsgaard and Storm, 1996) distinguished three types of calibration methods:

A: The manual trial-and-error method,

B: Automatic or numerical parameter optimization method; &

C: A combination of both the above methods

For this research work the measured stream flow data of Big Akaki were manually calibrated from a period of 1997-2002.

5.9.6 Model Validation

In order to utilize the calibrated model for estimating the effectiveness of future potential management practices, the model tested against an independent set of measured data. This testing of a model on an independent set of data set is commonly referred to as model validation. As the model predictive capability was demonstrated as being reasonable in both the calibration and validation phases, the model was used for future predictions under different management scenario.

For this research work the measured stream flow data of Big Akaki were validate from a period of 2002-2004 were used to validate the model.

5.10 Model Evaluation

The performance of SWAT was evaluated using statistical measures to determine the quality and reliability of predictions when compared to observed values. Coefficient of determination (r^2) and Nash-Sutcliffe simulation efficiency (ENS) were the goodness of fit measures used to evaluate model prediction. The r^2 value is an indicator of strength of relationship between the observed and simulated values. The Nash-Sutcliffe simulation efficiency (ENS) indicates how well the plot of observed versus simulated value fits the 1:1

line. If the measured value is the same as all predictions, ENS is 1. If the ENS is between 0 and 1, it indicates deviations between measured and predicted values. If ENS is negative, predictions are very poor, and the average value of output is a better estimate than the model prediction (Nash and Sutcliffe, 1970). The r^2 and ENS values are explained in equations below.

$$r^2 = \frac{[\sum_{i=1}^{n}(q_{si} - q_s)(q_{oi} - q_o)]^2}{\sum_{i=1}^{n}(q_{si} - q_s)^2 \sum_{i=1}^{n}(q_{oi} - q_o)^2}$$ ---------- (Eq).5.24

Where:

q_{si} :- is the simulated value , q_{oi} :- is the measured values, $q_{s:-}$ is the average simulated value and $q_{o:-}$ is the average measured value

The E_{NS} simulation efficiency for n time steps is calculated as:

$$\sum_{NS} = 1 - \frac{\sum_{i=1}^{n}(q_{oi} - q_{si})^2}{\sum_{i=1}^{n}(q_{oi} - q_o)^2}$$ ---------- (Eq).5.25

Where: q_{si} is the simulated value and q_{oi} is the measured value

The percent difference for a quantity (D) over a specified period with total days is calculated from measured and simulated values of the quantity in each model time step as:

$$D = 100 * [\frac{\sum_{i=1}^{n} q_{oi-} \sum_{i=1}^{n} q_{si}}{\sum_{i=1}^{n} q_{oi}}]$$ ---------- (Eq). 5.26

Where: q_{si} is the simulated value and q_{oi} is the measured value

A value close to 0% is best for D. A negative value indicates model over estimation and a positive value indicate model under estimation.

Observation standard deviation ratio (RSR) is also another performance rating which standardizes Root mean square error (RMSE) using the observations standard deviation and it combines both an error index (McCabe 1999, Cited in D.N Moriasi, 2007). RSR is calculated as the ratio of the RMSE and standard deviation of measured data, as shown in equation below:

$$RSR = \frac{RMSE}{STDEV_{obs}} \qquad RSR = \frac{((\sum_{i=1}^{n}(Q_{obs} - Q_{sim})^2)^{1/2})}{((\sum_{i=1}^{n}(Q_{obs} - Q''_{obs})^2)^{1/2})}$$ ---------- (Eq). 5.27

Where: Q_{obs} is the observed flow, Qsim is the simulated flow and Q"obs is means observed flow.

RSR incorporates the benefits of error index statistics and includes a scaling / normalization factor, so that the resulting statistic and reported values can apply to various constituents. RSR varies from the optimal value of 0, which indicates zero RMSE or residual variation and therefore perfect model simulation, to a large positive value. Note: NSE= 1-(RSR) [2]

Table5. 5: General performance ratings for recommended statistics for a monthly time step. (D. N Moriasi, et al. 2007)

Performance Rating	For Stream Flow		
	RSR	NSE	%D
Very good	0.0<=RSR<=0.5	0.75<NSE<=1	D <=±10
Good	0.5<RSR<=0.6	0.65<NSE<=0.75	±10 <=D < ±15
Satisfactory	0.6<RSR<=0.7	0.5<NSE<=0.65	±15<=D<± 25
Unsatisfactory	RSR>=0.7	NSE<=0.5	D >= ± 25

CHAPTER SIX

6 Result and Discussion

6.1 Land Use Land Cover Map

Spatial analysis was carried out to describe land use land cover change pattern and overall land use changes with time. This is done after image classification of the three land use land cover maps (1973, 1986 and 2000) whose results for each analysis can be expressed as follows:

6.1.1Land use land Cover Map of 1973

The land cover map of 1973 in figure 6.2 and the histogram of the land class coverage in figure 6.1 shows that about 41% of the Akaki catchment was covered by Grass Land, 19% by Forest land, 35% by cultivated land, 4.5% by Settlement and 0.5% by water. The distribution of land cover class as it is shown in the figure 6.2, Grass cover was found in most parts of the catchment; especially the north eastern and south western part of the catchment is more dominantly covered by Grass.

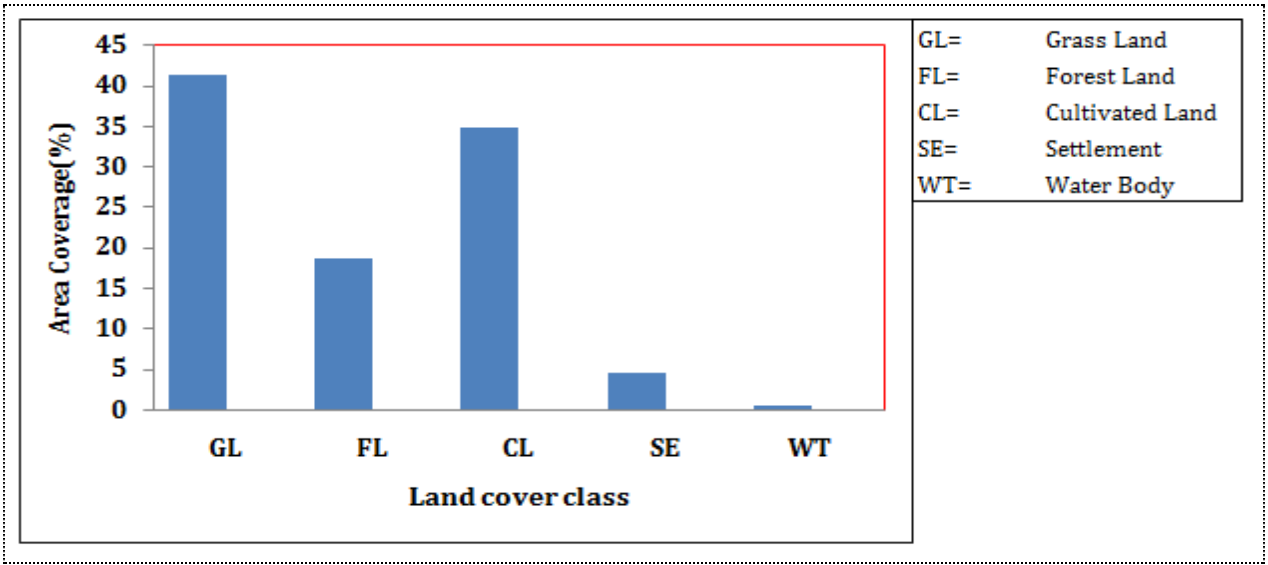

Figure6. 1: Percentage cover comparison of LU/LC classes 1973

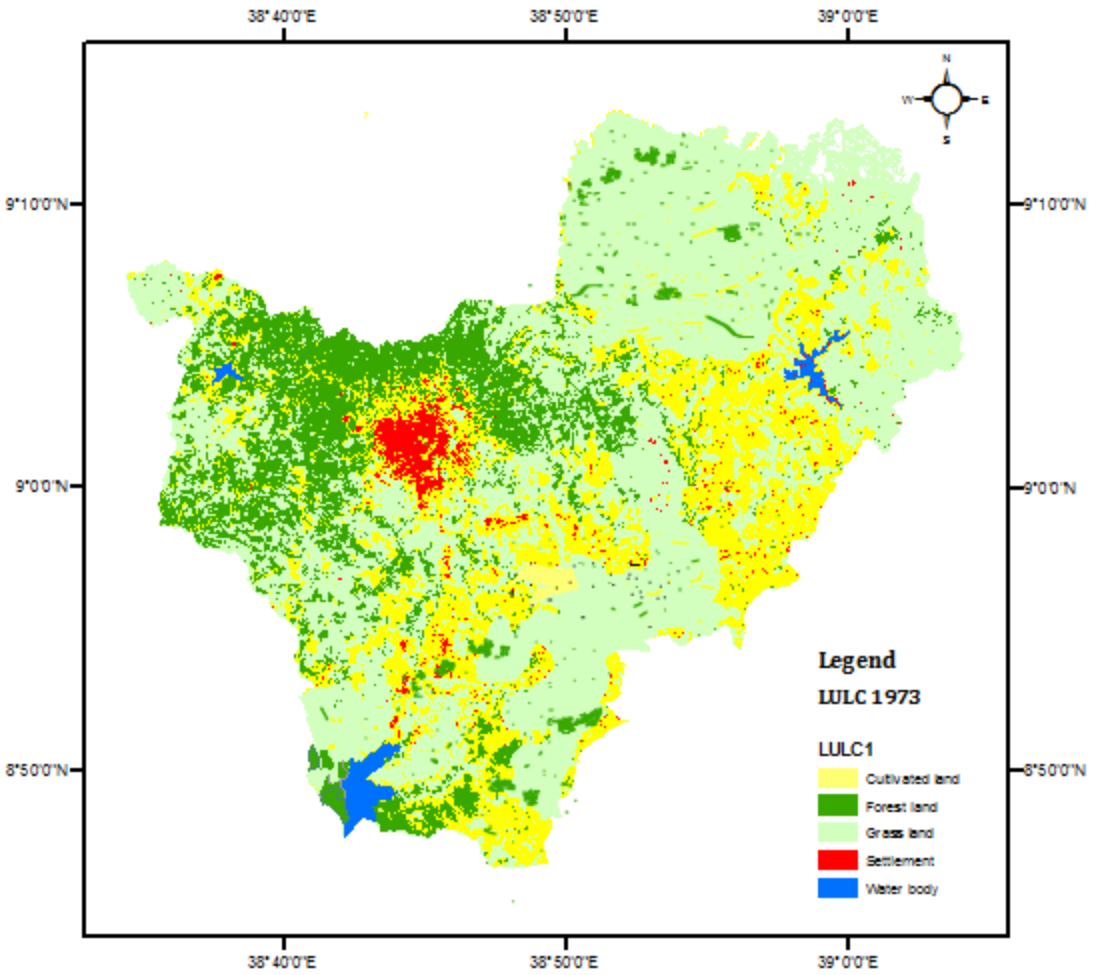

Figure6. 2: Land use land cover map of Akaki catchment in the year 1973

6.1.2 Land use land Cover Map of 1986

The land cover map of 1986 in figure 6.3 and the percentage coverage of each land cover class in figure 6.4 show that the catchment was covered by 38% Grass, 17% Forest, 36.5 % Cultivated land, 8% Settlement , and 0.5% of water body. During this period, mainly the forest land in the Southern, and Grass land in, South-Eastern and the central part of the catchment was reduced. On contrast the cultivated land was expanded in most parts of the catchment.

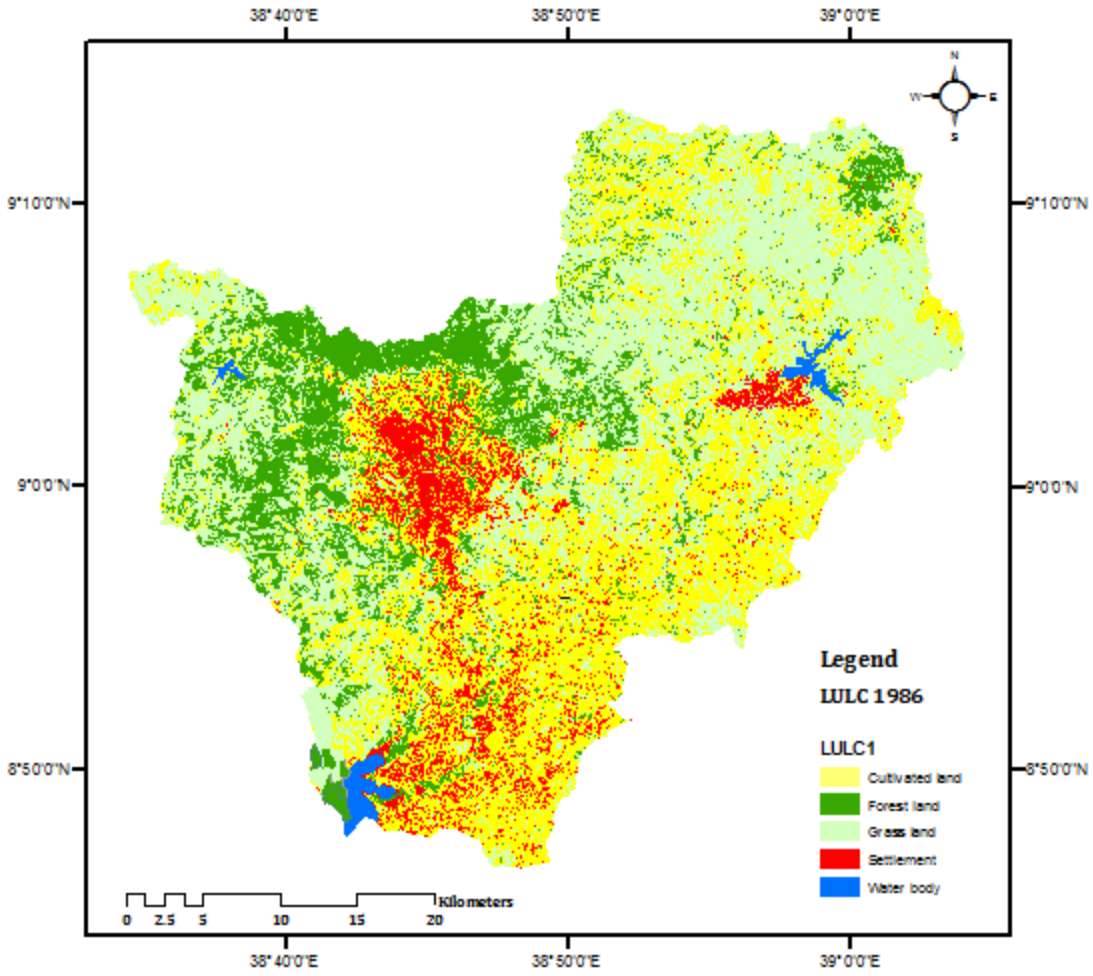

Figure6. 3: Land use land cover map of Akaki catchment in the year 1986

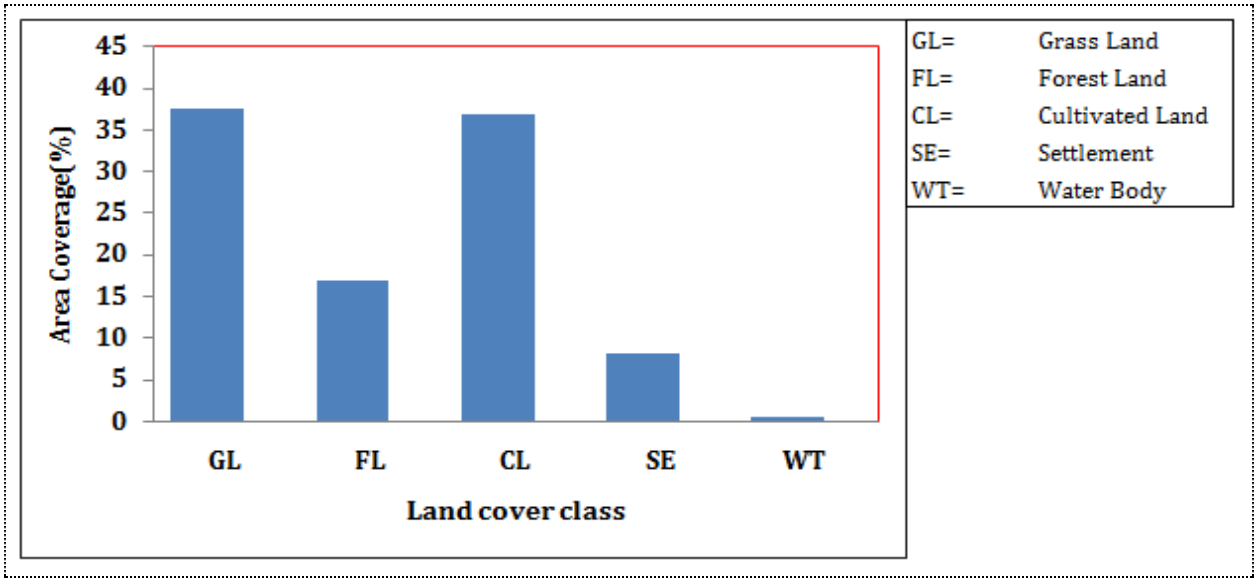

Figure6. 4: Percentage covers comparison of LU/LC classes of 1986

6.1.3 Land use Land Cover Map of 2000

For the year 2000 the land cover map is shown in figure 6.5. The percentage coverage of each class is shown in figure 6.6 and indicates that cultivated land covered some 43.5% while forest, Grass land, Settlement and water covered 15%, 28%, 12.5% and 0.8% respectively. During this period and due to high increase of population density, this needed to built additional water supply structure called Dere dam and also most of the catchment area was transformed into cultivated lands and Settlement in the central and outskirts part of the catchment, and only little forest cover remains through the Northern part of the catchment.

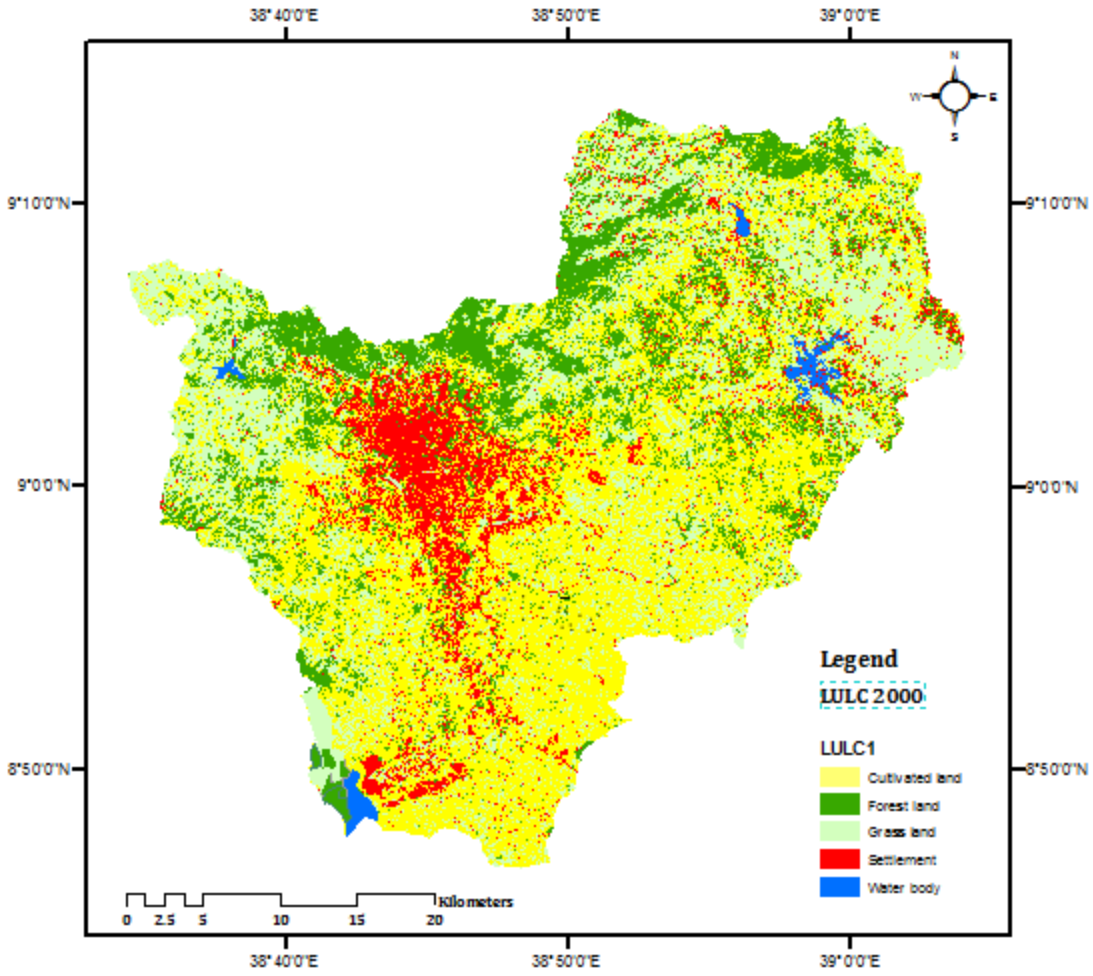

Figure6. 5: Land use land cover map of Akaki catchment in the year 2000

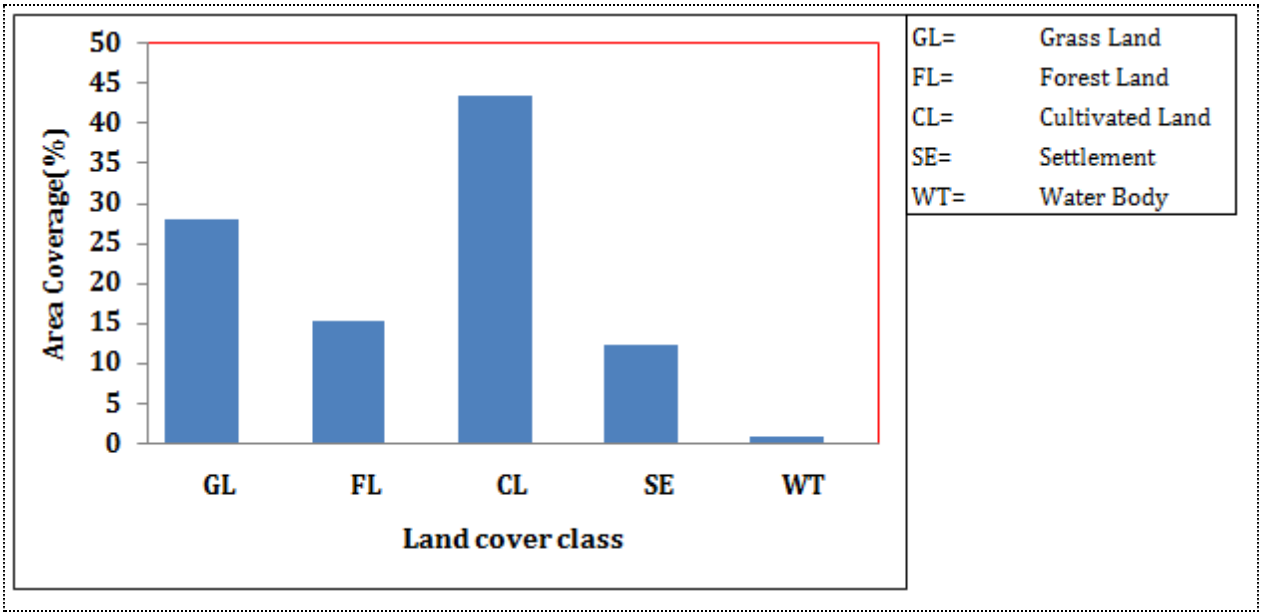

Figure6. 6: Percentage covers comparison of LU/LC classes of 2000

Land cover classification maps of the study area were generated for three reference years 1973, 1986 and 2000 and reflect land cover for the given periods. The overall land use /cover changes at watershed level are summarized in table below

Table6. 1: Land use and Land cover types and changes from1973-2000

Landuse and Landcover type	Landuse and Landcovers						Landuse andLandcover change(LUCC)		
	1973		1986		2000		Landuse and		
	Area		Area		Area		Landcover type	(1973-1986)	(1986-2000)
	(km^2)	%	(km^2)	%	(km^2)	%		%	%
Grass Land	590.8	41.34	537.8	37.63	400.6	28.03	Grass Land	-9.04	-25.49
Forest Land	266.6	18.66	241.5	16.90	219.3	15.35	Forest Land	-9.20	-9.43
Cultivated Land	499.3	34.94	526.1	36.82	620.9	43.45	Cultivated Land	5.31	18.24
Settlement	64.4	4.51	115.7	8.10	176.7	12.37	Settlement	79.87	52.07
Water Body	7.9	0.55	7.9	0.55	11.5	0.80	Water Body	0.00	45.61
Total	**1429**	**100**	**1429**	**100**	**1429**	**100**			

Both increases and decrease linear regression results were used for 2020(projected) Scenario development. The result of this scenario for each class is summarized below:

Table6. 2: Land cover scenario for 2020 (% cover)

	LULC 2000 %	LULC 2020 %
Settlement(Urban)	12.33	18.97
Cultivated Land	43.5	49.23
Grass Land	28.02	19
Forest Land	15.34	12
Land category not changed in scenario		
Water	0.8	0.8

It should be noted that from this point onwards, the above mentioned land cover classes were later regrouped for use in the hydrological model according to Table below.

Table6. 3: Land cover classes regrouped into SWAT classes

Land use Land cover	SWAT Class
Grass Land	RNGE
Forest Land	FRSE
Settlement	URBN
Water Body	WATR
Cultivated Land	AGRR

6.2 Hydrological Modeling

Using the SWAT Model Akaki catchment was divide in to 33 sub–basin and 253 HRU determined by unique inter section of the LU/LC, slope and soil within the catchment.

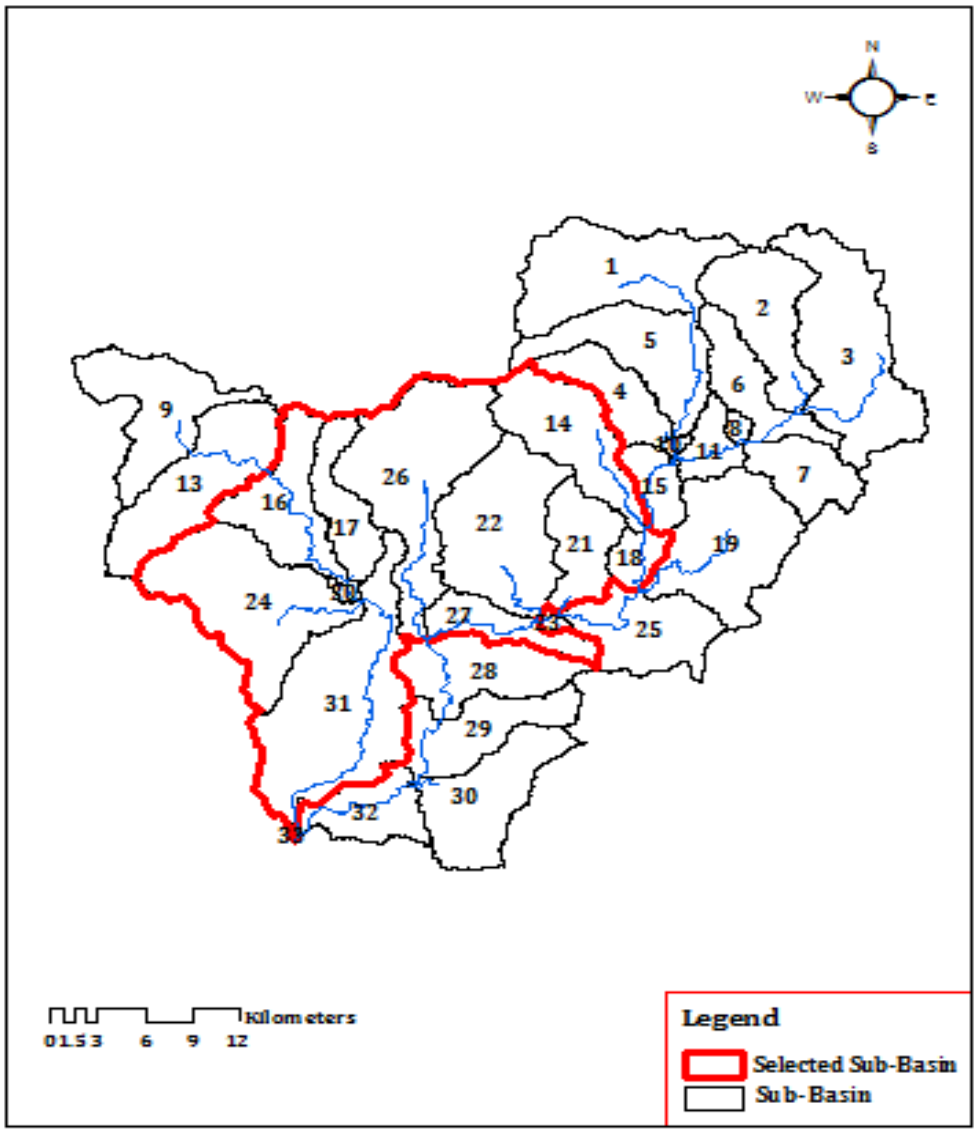

Figure6. 7: Sub-basin for the Akaki Catchment

6.2.2 Sensitivity Analysis

The SWAT2005 model outputs depend on many input parameters related to the soil, land use, management, weather, channels and aquifer. Therefore, modeling LUCC impact with SWAT2005 necessitates evaluation of the sensitivity of flow output to the selected parameters. The sensitivities to the model performance give insight in to parameter using the available information daily stream flow data. In this research, sensitivity analysis,

which is incorporated in SWAT2005, is used to perform sensitivity analysis for all the 27 models parameters. After set-up the SWAT2005 model and incorporating all the input parameters simulations were carried out and sensitivity analysis was run for the period 1997-2002. The result of the analysis indicates that ten parameters namely; Curve number (CN), Soil Available Water Capacity (SOL_AWC), Threshold depth of water in the shallow aquifer (Gwqmn), Soil depth (SOL_Z), Soil Evaporation Compensation factor (ESCO), Effective hydraulic conductivity in main channel alluvium (ch_K2), Groundwater coefficient (GW_REVAP) and Groundwater recession factor (ALPHA_BF) are the most crucial parameters for the studied in the watershed.

Table6. 4 : The most sensitive parameters

Rank	Parameters	Max	Min	Relative Sensitive Value	Class	Description
1	Alpha_Bf	1	0	1.34	Very High	Ground water recession factor
2	Cn II	25%	25%	1.01	Very High	SCS runoff curve number for moisture condition II
3	Gwqmn	5000	0	0.456	High	shallow aquifer required for return flow to occur (mm H2O)
4	Revapmn	500	0	0.19	High	Threshold depth of water in the shallow aquifer for revap or percolation to the deep aquifer to
5	Esco	1	0	0.0965	High	Soil evaporation compensation factor
6	Sol_Z	3000	0	0.0786	Medium	Depth from soil surface to bottom of layer (mm)
7	Ch_K2	150	0	0.0727	Medium	Effective hydraulic conductivity in main channel alluvium(mm/hr)
8	Gw_Revap	0.2	0	0.0683	Medium	Groundwater "revap" coefficient
9	Sol_Awc	1	0	0.0646	Medium	Available water capacity of the soil layer (mm/mm soil)
10	Blai	1	0	0.06	Medium	Maximum potential leaf area index

6.2.3 Base Flow Separation

The base flow separation using the base flow separator program based on the daily flow data measured at the outlet of the sub watershed at Big Akaki showed that the base flow recession constant (alpha factor), which is the rate at which groundwater is returned to the stream, is found to be 0.0167.The base flow days, which is the number of days for the base flow recession to decline through one log cycle, has a value of about 141.1days.

Base flow data file: this file summarizes the fraction of stream flow that is contributed by base flow for each of the 3 passes made by the program

Table6. 5: Flow separation parameters for Akaki catchment at Big Akaki

Fr1	Fr2	Fr3	NPR	Alpha Factor	Days
0.59	0.49	0.45	11	0.0167	141.16

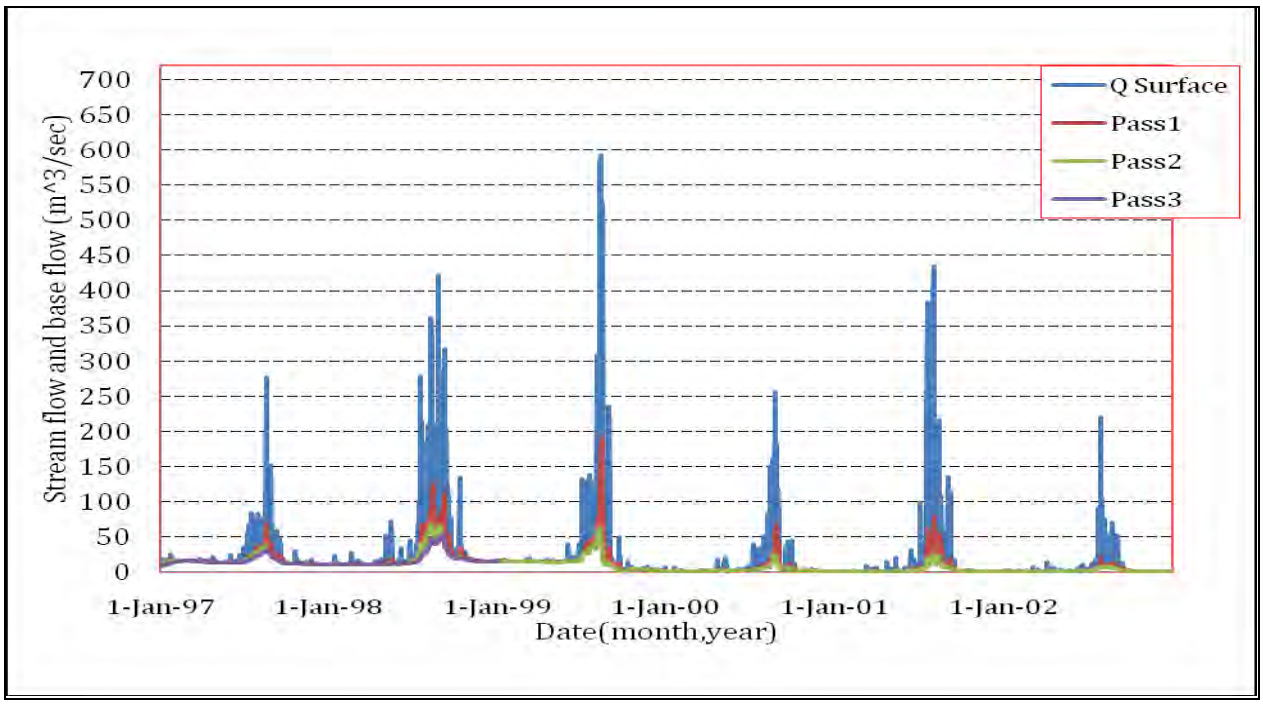

Figure6. 8: Comparison between baseflow estimated using automated digital filter (Pass 1, 2 and 3)

6.2.4 Model Calibration and Validation

Flow calibration was performed a period of six years from January 1997 to December 31, 2002 and also flow validation was performed from 2003-2004 for monthly stream flow using the sensitive parameters identified above. As discussed previously in section five of this report, the flow was calibrated manually using the observed flow gauged at the outlet of the sub watershed at Big Akaki.

Manipulation of the parameter values were carried out within the allowable ranges recommended by SWAT developers. The initial/default and finally adjusted parameter values are shown in table below.

Table6. 6: Initial/Default and finale adjusted parameters

S.No	Parameters	Description	Effect on Simulation	Range	Initial value	Adjusted value
1	Cn2	SCS runoff curve number for moisture condition II	To increase surface runoff	-25%-25%	default	10%
2	Esco	Soil evaporation compensation factor	To increase surface runoff	0-----1	default	0.95
3	Alrha Bf	Baseflow alpha factor (days)		0-----1	default	0.0167
4	GW_Revap	Groundwater "revap" coefficient	To decrease ground flow contribution	0.02----0.2	default	0.2
5	SOL-WAC	soil available water capacity	To increase surface runoff	0-----1	default	0.4

6.2.5 Monthly Calibration and Validation

After the water-balance was calibrated for the annual simulation period, a seasonal calibration and verification on a monthly basis was done. A time-series plot of monthly catchment streamflow indicates an acceptable agreement between the measured and simulated catchment monthly flows as indicated by the value of the Nash and Sutcliffe efficiency criteria.

Table6. 7: Monthly average statistics for calibration and validation

Average Monthly	Observed (m^3/sec)	Simulated (m^3/sec)	Error %	R^2	NSE	D	RSR
Calibration(1997-2002)	18.72	14.5	22.8	0.87	0.81	23	0.43
Validation(2003-2004)	14.1	16.7	-18.4	0.85	0.76	-18	0.48

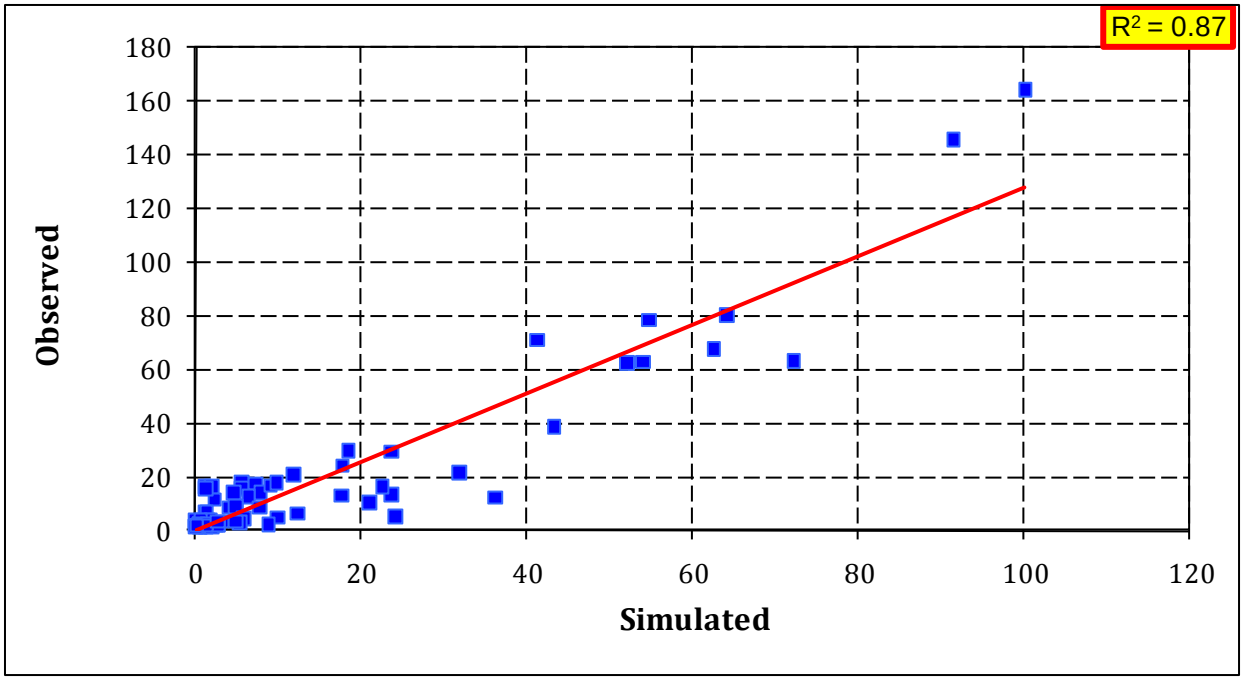

Figure6. 9: Scatter plot of observed and simulated discharge, for a period of (1997-2002)

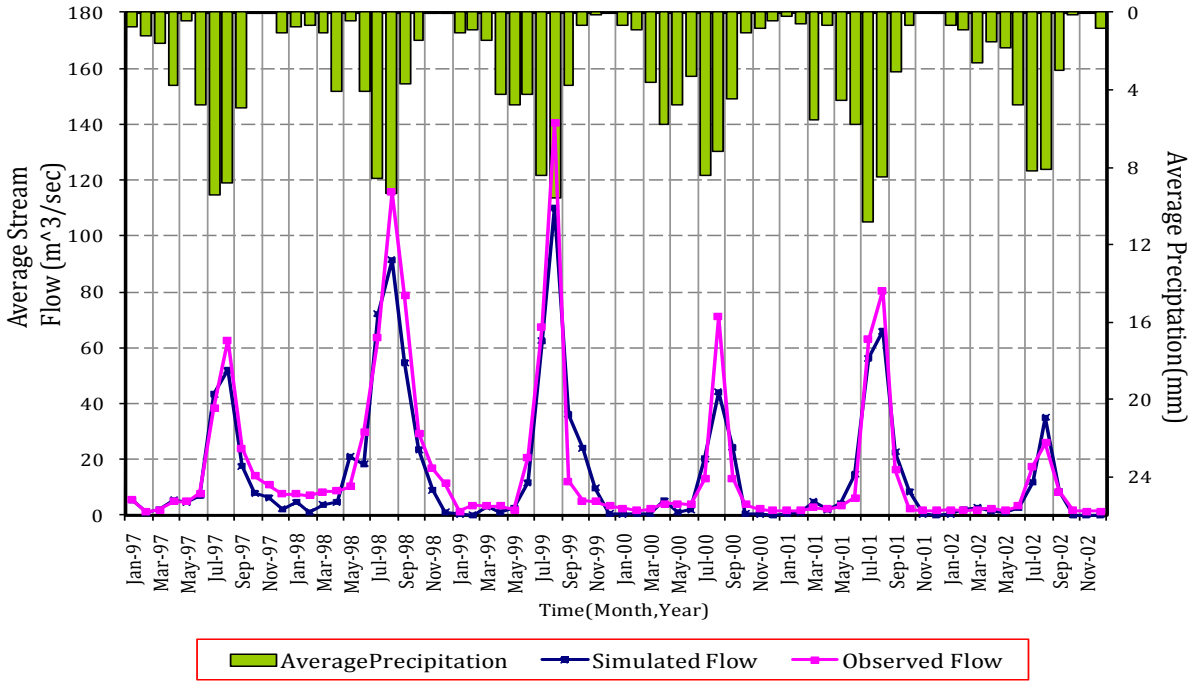

Figure6. 10: Calibration of observed and simulated monthly flow hydrograph, for a period (1997-2002)

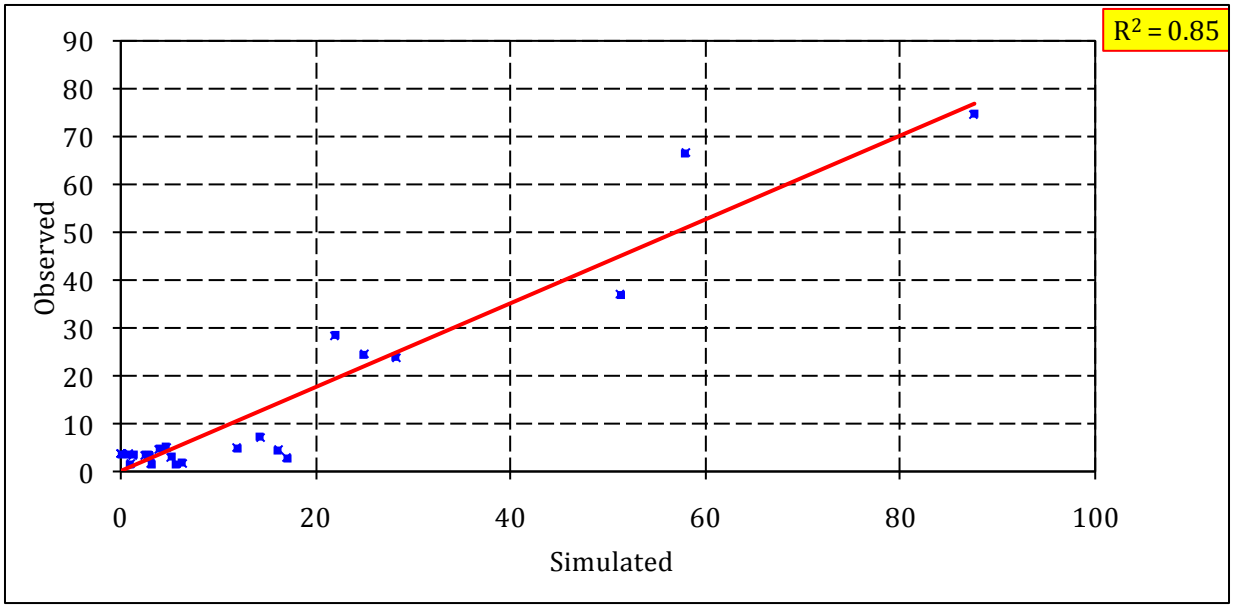

Figure6. 11: Scatter plot of observed and simulated discharge, for a period of (2003-2004)

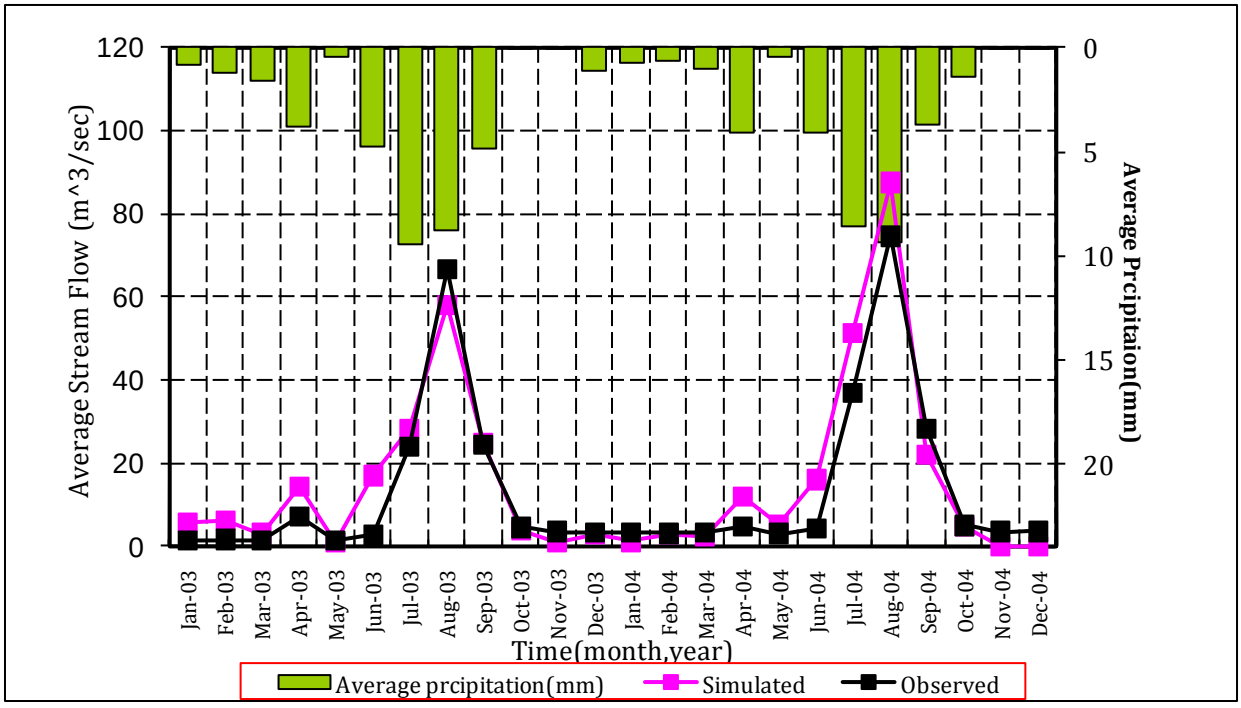

Figure6. 12: Validation of observed and simulated monthly flow hydrograph, for a period (2003-2004)

The validation and calibration results of Big Akaki watershed demonstrate that NSE for monthly stream flow values ranges from 0.81 to 0.76. Based on the model performance criteria, the model simulated the stream flow trend for both case very good performances.

The residual variation (RSR) ranges from 0.43 to 0.48, during calibration and validation indicates that the model simulated residual variation as very good in both validation and calibration periods. The volumetric fit which ranges from 22.86 % to -18.4% indicates, an under estimation of the volume during calibration period and over estimation the model in validation period but it fit satisfactory performance for both calibration and validation periods respectively.

There are two reservoirs (Legedadi and Dere) at the upper part of Big Akaki which are used as a source for the surface water supply of the city. The data and model output for the reservoirs during calibration is given at Appendix E.

6.3 Model Responses to Land Cover Change

The hydrological impacts of land use have received a considerable amount of interest in hydrology. LUCC is an important characteristic in the runoff process that affects infiltration, erosion, and evapotranspiration. Understanding of the effects historic land use changes have had on river flow is required to understand the future effects of land use and land cover on hydrological regimes at a watershed level. Along with these changes, considerable consequences are expected in the hydrological cycles and subsequent effects on water resources (Githu, 2007).

The SWAT model simulated for the three time periods corresponding to the land cover of 1973, 1986 and 2000. The 2002 – 2004 meteorological data served as an input to the SWAT model. This allows studying the effect of land cover on the model response which is not affected by changes in the meteorological data and reservoir characteristics. Simulation runs were conducted on an annual, monthly and daily basis to compare the modeling outputs using the 1973, 1986 and 2000 land covers.

A comparison of the average annual streamflows generated using 1973, 1986 and 2000 land covers respectively is presented in Table 6.8, while Figure 6.13 presents mean annual catchment streamflows. The result indicated that the mean annual surface flow for 2000

land cover was increased by 28% than 1973 land cover. Similarly the 1986 land cover mean annual surface flow was higher by 9% than 1973 land cover.

Table6. 8: Parameters from annual simulations for 1973, 1986 and 2000 land covers

Item	LULC1973	LULC1986	LULC2000
Mean annual SURQ(mm)	194.02	211.64	248.38
Mean total Water Yields	614.45	654.17	710.56

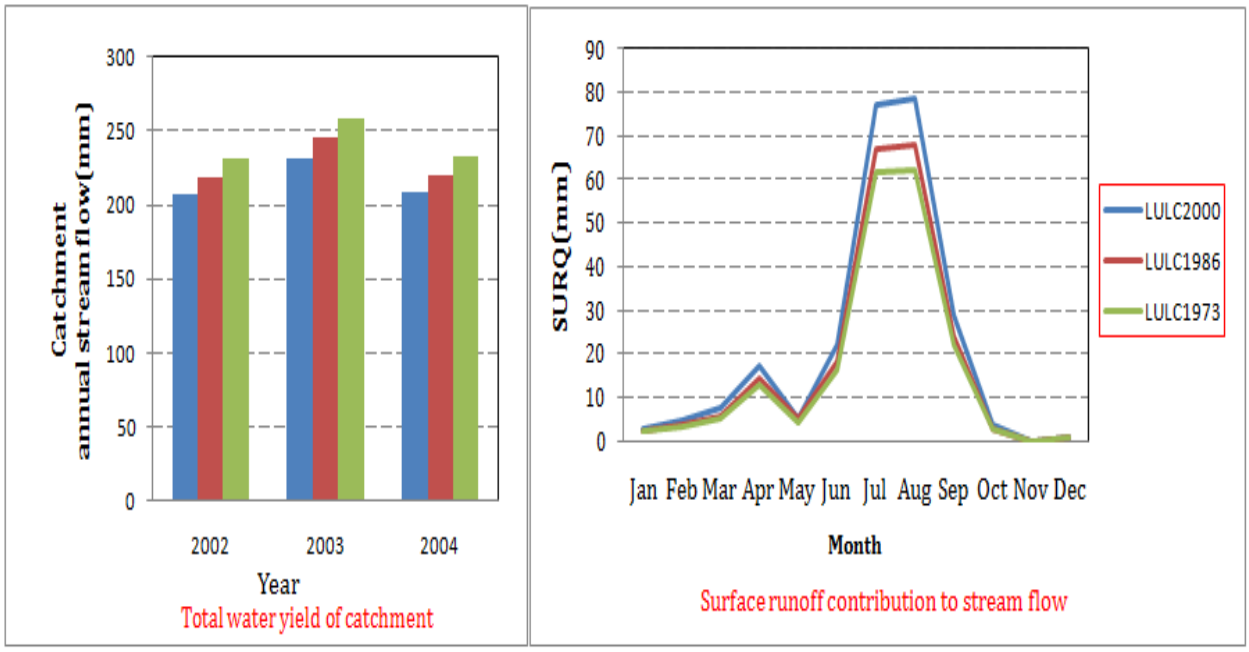

Figure6. 13: Simulated annual catchment stream flow for LU/LC of 1973, 1986 and 2000

Average annual catchment streamflows are directly related to land cover type, soil characteristics and annual precipitation. In the study area, urban and cultivated areas have increased between 1973, 1986 and 2000 with most of the increase occurring in previously vegetated areas of Grass and Forest land. Urban land has the highest potential for runoff because the land is impervious cover in a watershed and reduces infiltrations.

To understand the flow processes during different seasons under different land cover conditions, the average monthly streamflows were plotted for the wet and dry season and compared. In the Akaki River catchment, there are two seasons - wet weather occurs from June to August and dry weather events occur between November and January (Master Plan

Study for Awash by HLCROW, 1989). This two season climate creates significant differences in streamflow. Seasonal variations predicted from the three land cover classifications (1973, 1986 and 2000) are presented in Figure 6.14.

The average dry monthly stream flow shows differences between simulations. For the 1973 and 1986 land cover average monthly stream flow was 15.5 m^3/ s ,14.9 m^3 /s, while that of 2000 land cover data was between 14.7 m^3 /s . For that of wet month's average stream flow were 50 m^3/ s, 54 m^3/ s and 58.5 m^3/ s.

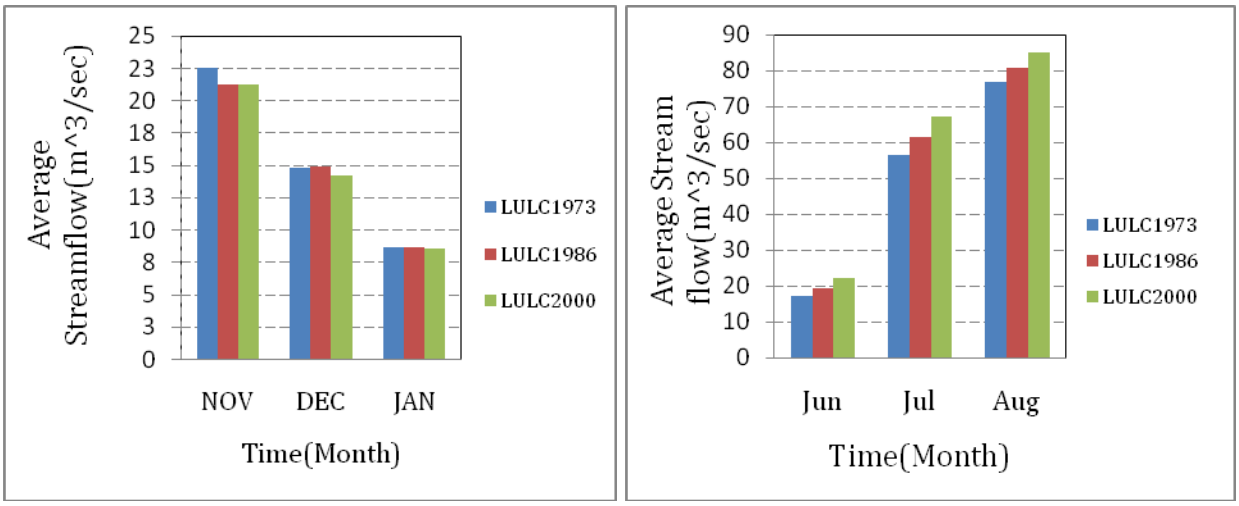

Figure6. 14: Simulated monthly catchment stream flow for LU/LC of 1973, 1986 and 2000

The result indicates that the mean wet monthly flow for 2000 land cover was increased by 16% than 1973 land cover. Similarly the 1986 landcover mean month flow higher by 7% than the 1973 land cover flow of wet months. On the other hand dry average monthly flow was decreased by 4 %, 2.6 % for land cover of 2000 and 1986 than that of 1973 land cover.

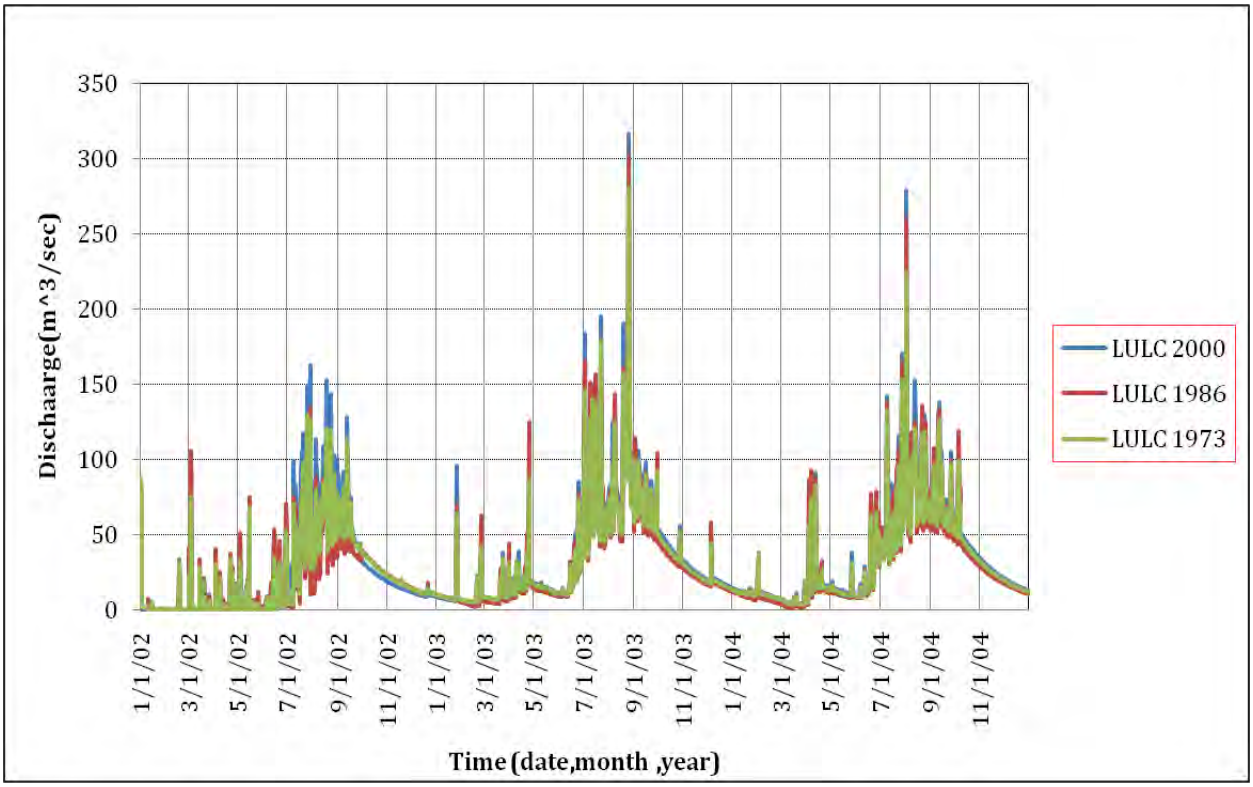

Figure6. 15: Simulated daily catchment streamflow for LU/LC 1973, 1986 and 2000

A comparison of daily catchment stream flow generated for the three land covers. The result obtained difference in daily peak flows between 1973,1986 and 2000 land covers The hydrographs generated for 1973 land cover produce the highest peak flow 280 m^3/s 1986 land cover produce 302 m^3/s whereas the 2000 land cover produce with the highest daily flow of 316 m^3/s. The majority of the peak flows occur during the month of June to August which is the rainy season in the study area.

Total stream flow is composed of surface run-off and base flow (lateral flow and shallow ground water discharge to streams). Comparisons were also done to evaluate differences in surface flow and base flow from different land cover types classified from the 1973, 1986 and the 2000 land cover data sets.

The dominant land cover changes were observed in central part of the study area which is coded in figure 6.7 as 14, 16, 17, 18, 20, 21, 22, 24, 26, 27 and 31. Differences in surface run-off, base flow and their percentage changes are listed in tables 6.9 and 6.10 below:

Table6. 9: Surface runoff simulated for central part of the study area for LULC of 1973, 1986 and 2000

	Simulated annual avergae surface runoff(mm)			Change b/n LULC1973 and LULC 1986	Change b/n LULC1973 and LULC 2000	Percentage change (%)(b/n 1973 and 1986)	Percentage change (%)(b/n 1973 and 2000)
Subbasin	LULC1973	LULC1986	LULC2000				
14	116.92	130.90	156.65	13.98	39.74	11.96	33.99
16	84.59	121.17	202.28	36.58	117.70	43.24	139.14
17	179.65	224.03	365.29	44.38	185.64	24.70	103.34
18	192.58	249.73	258.17	57.15	65.59	29.68	34.06
20	183.09	222.37	332.75	39.28	149.66	21.45	81.74
21	163.83	267.63	268.21	103.81	104.38	63.36	63.71
22	165.86	184.17	292.46	18.31	126.60	11.04	76.33
24	106.55	136.29	173.33	29.75	66.78	27.92	62.68
26	124.71	122.22	208.64	-2.49	83.93	-2.00	67.30
27	258.13	273.09	268.11	14.96	9.98	5.79	3.87
31	207.29	243.97	305.18	36.67	97.88	17.69	47.22
Average						**23.17**	**64.85**

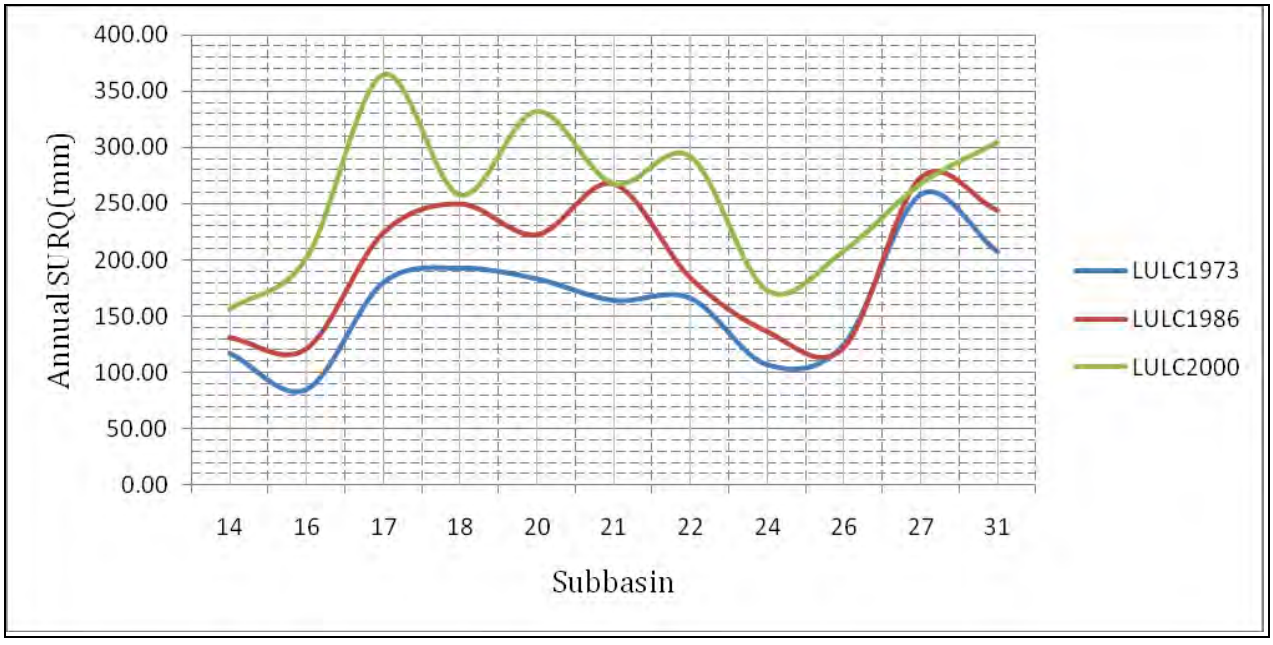

Figure6. 16: Surface runoff simulated for central part of the study area for LU/LC of 1973, 1986 and 2000

The highest annual surface runoff 365.3mm was generated in sub basin 17 .The dominant land cover in this sub basin was Forest in 1973 and had changed to mostly urban and cultivated land in 2000.Thus surface runoff increases by 103% .Generally the surface

runoff of the selected sub basin was change on average by 23% and 64 % of 1986 and 2000 land cover respectively.

Table6. 10: Base flow simulated for central part of the study area for LULC of 1973, 1986 and 2000.

	Simulated annual avergae Base flow(mm)			Change b/n LULC1973 and LULC 1986	Change b/n LULC1973 and LULC 2000	Percentage change (%)(b/n 1973 and 1986)	Percentage change (%)(b/n 1973 and 2000)
Subbasin	LULC1973	LULC1986	LULC2000				
14	447.37	400.38	291.78	-46.99	-155.59	-10.50	-34.78
16	471.92	403.03	244.26	-68.88	-227.66	-14.60	-48.24
17	382.75	308.18	103.98	-74.57	-278.77	-19.48	-72.83
18	527.47	441.90	338.30	-85.57	-189.17	-16.22	-35.86
20	558.23	492.89	301.04	-65.34	-257.19	-11.70	-46.07
21	573.24	444.16	360.51	-129.07	-212.73	-22.52	-37.11
22	561.53	511.47	326.30	-50.06	-235.24	-8.92	-41.89
24	594.93	533.44	418.17	-61.49	-176.76	-10.34	-29.71
26	423.37	390.78	234.01	-32.59	-189.35	-7.70	-44.73
27	469.60	421.78	331.44	-47.82	-138.16	-10.18	-29.42
31	455.10	387.35	246.93	-67.75	-208.17	-14.89	-45.74
Average						**-13.37**	**-42.40**

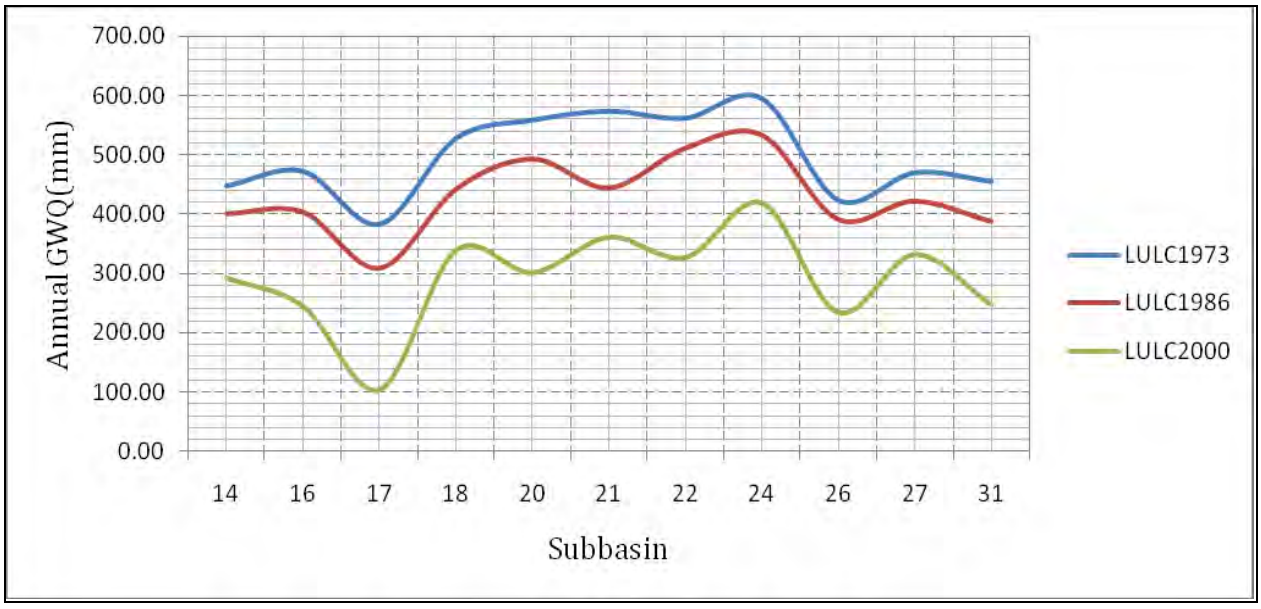

Figure6. 17: Base flow simulated for central part of the study area for LU/LC of 1973, 1986 and 2000

Similar observations have been noted in sub-basins 14, 17, 18, 20, 21, 22, 24, 26, 27, and 31 where dominant land cover has changed from forest(FRST), grass land (RNGB) to mostly

urban land (URBN) cultivation(AGRL) and Under the simulated conditions of a fixed climatic scenario, with only the measured land cover changes inserted, simulated surface run-off increased by 34%, 103%, %, 34%, 82%, 64%, 76%, 63%, 67%, 4%, and 47% in sub-basins 14, 17, 18, 20, 21, 22, 24, 26, 27, and 31 respectively. Proportionately, base flow decreased by -35%, -48%, -73%, -36%, -46%, -37%, -42%, 30%, 45%, 30% and -46% respectively.

6.4 Model Responses Future Scenario

To understand the hydrological response of land use land cover change at the catchment outlet, average annual, monthly and daily flows comparison was done between the two scenarios (baseline and future). The baseline Scenario was simulated using measured climate data for the period (2002 to 2004) and that of land cover data of 2000. Similarly, future Scenario was simulated using the same climate data and land cover data for the year 2020.

The analysis indicated that the annual average peak flow of the future scenario is increased by 12.7% as compared with the baseline scenario. For more illustration of the model response to the effect of land cover change, the comparison of the annual average flow is shown below.

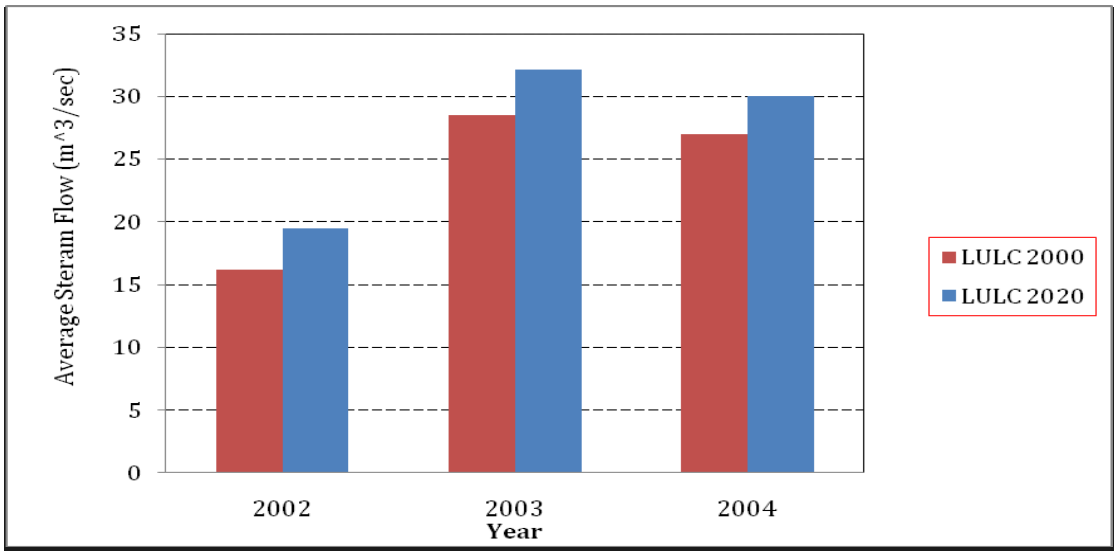

Figure6. 18: Annual average stream flow for baseline and for future scenario

For assessing change in contribution of stream flow components due to LUCC, analyses were made on Surface runoff (SURQ), Ground water flow (GWQ) and Lateral flow (LATQ).

The SURQ, GWQ and LATQ components of the stream simulated using the 2000 land use and land cover map for the same period were 43.2%, 55% and 1.8% while using the 2020 land use and land cover map were 50%, 48% and 2% respectively. The contribution of surface runoff has increased from 43% to 50% due to the LUCC occurred and base flow decreased by 7% between the period 2000 to 2020. An example of this change due to LUCC is given in figure below.

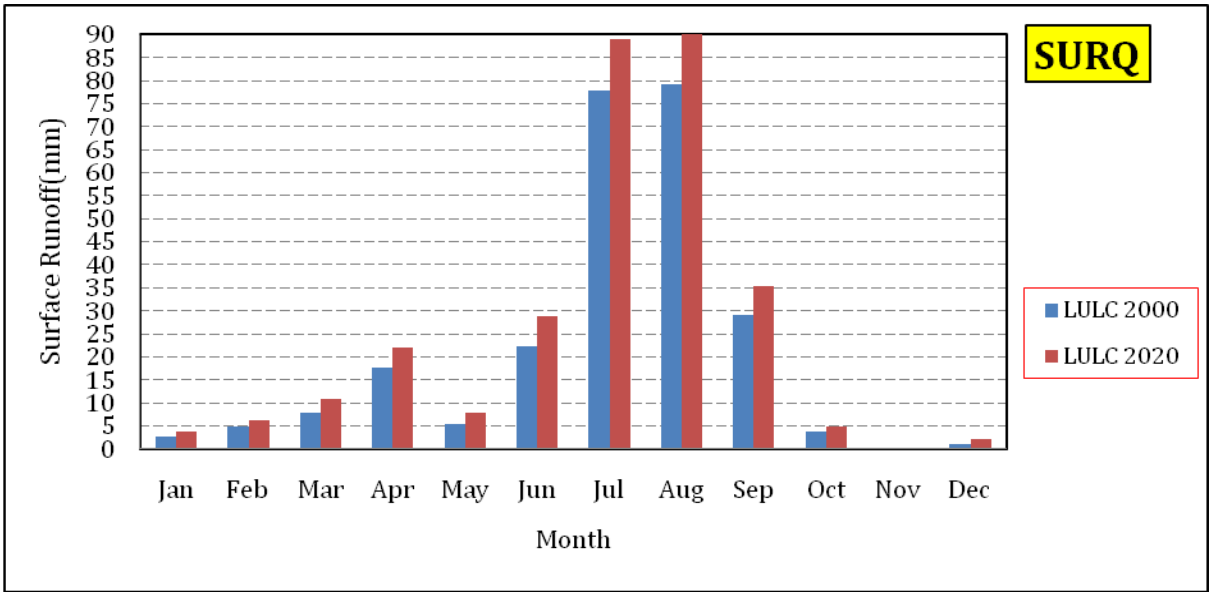

Figure6. 19: Monthly value of SURQ of the basin

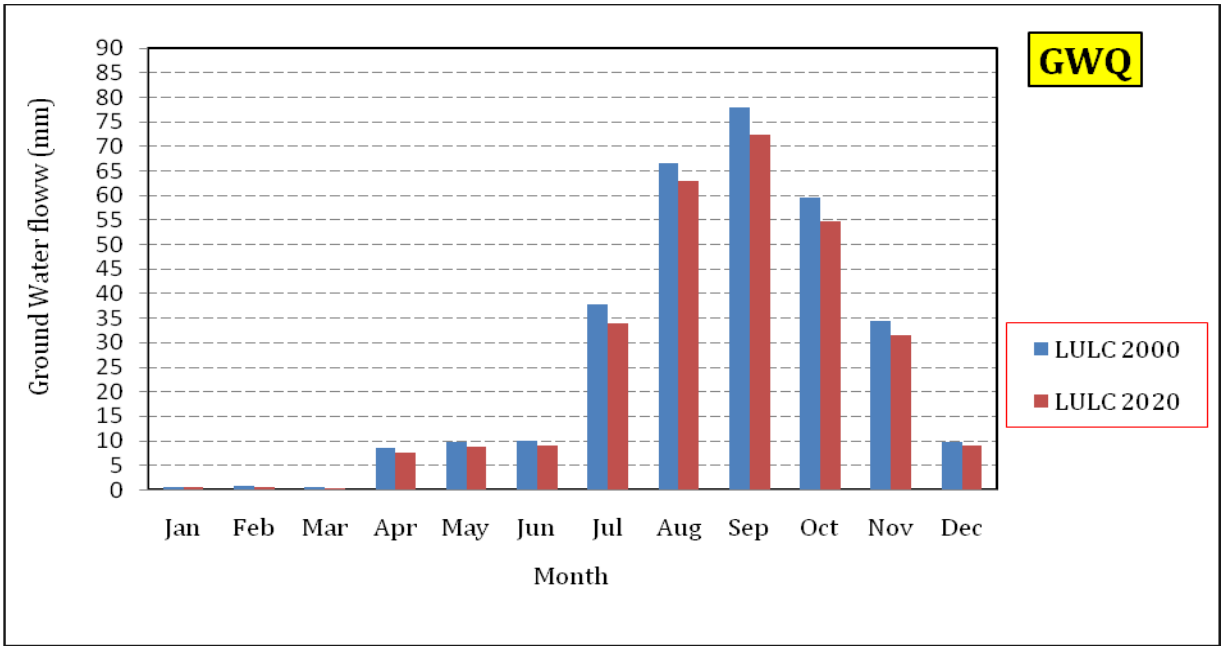

Figure6. 20: Monthly value of GWQ of the basin

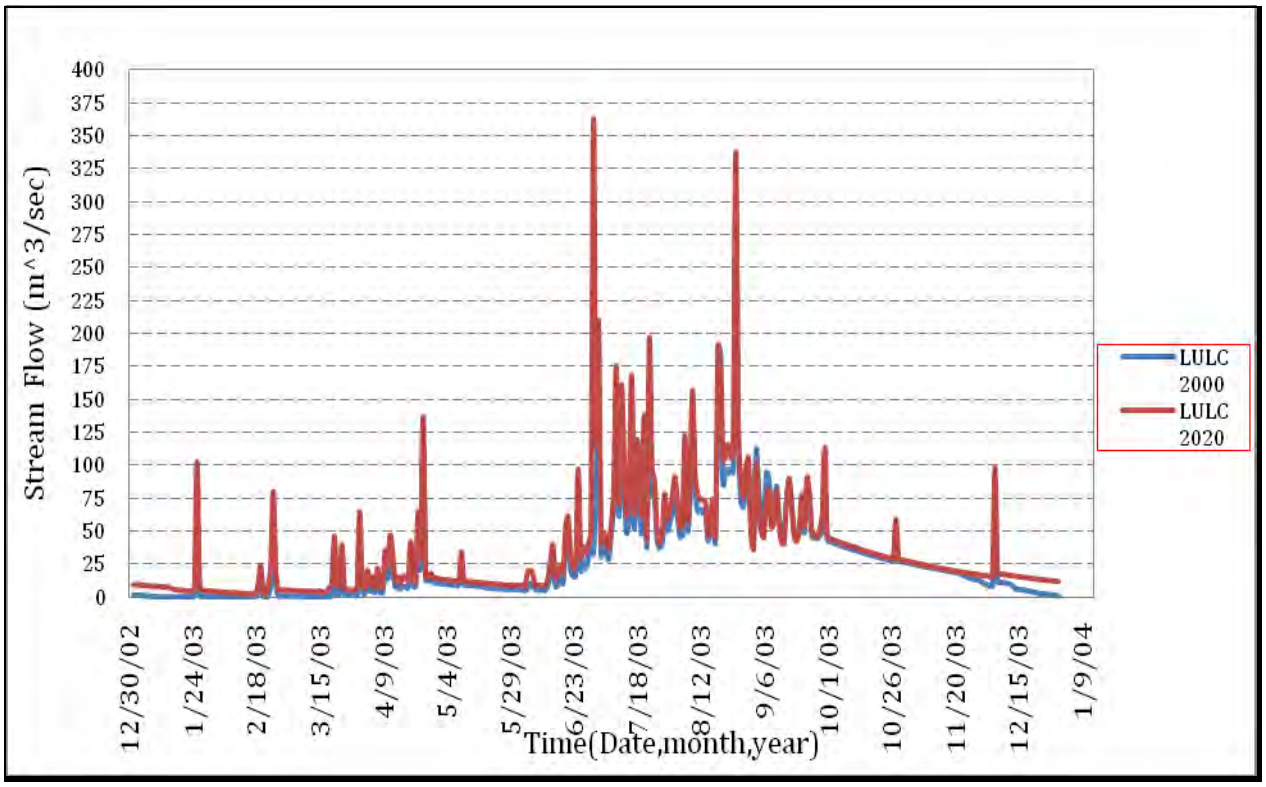

Figure6. 21: Daily stream flow of LULC of 2000 and 2020

The simulation results demonstrate that there are differences in the daily peak flows between the 2000 land cover and 2020 land cover. The hydrograph generated for the 2000 land cover produced the highest daily peak flow of 316.3m^3/s, whereas the 2020 land cover produced the highest daily peak of 363.7m^3/s.

CHAPTER SEVEN

CONCLUSION AND RECOMMENDATION

7.1 Conclusion

In this study, satellite data and GIS were integrated with a hydrological model to evaluate the impacts of land cover change in the hydrology of Akaki catchment of upper Awash basin. Use of GIs and remotely sensed data were found to be helpful tools to detect and analyze spatiotemporal land cover dynamics. The impacts of land cover change on stream flow were analyzed statistically using the physically based, semi-distributed models called SWAT. Based on the results obtained and their analyses, the following conclusions are drawn:

- From the LUCC analysis, it can be concluded that Akaki catchment had experienced a significant change in land use and land cover over the past three decades. The analysis shows that rapid conversion of Forest and Grass land cover to Urban and Cultivated land.

- According to the hydrological analysis carried out, ground water parameters (Alpha base flow (Alpha_Bf), soil available water capacity (SOL_AWC), the threshold water depth in the shallow aquifer for flow (GWQMN), the groundwater Revap coefficient (GW_REVAP), and the saturated hydraulic conductivity (Sol_K), curve number (CN2), Evapotranspiration (soil evapotranspiration factor (ESCO) and sub basin slope are the most sensitive parameters affecting the water flow of the watershed.

- The result of hydrological model calibration and validation indicated that the SWAT model simulates the stream flow appreciably well for the study area. This is proved from model performance criterion used to evaluate the model result such as regression coefficient and the Nash-Sutcliffe.

- From the results of analysis it can be demonstrated that the center sub-watershed areas are dominant in surface runoff generation as compared to upper and lower part of the catchment.

- Future Land use change scenario developed based on past land use trend showed that there will be an increase in annual average streamflow.

7.2 Recommendation

A. The model simulation considered only land use change effect by assuming all other thing constant. But change in climate and soil management activities and other land use variables will also contribute great impact on rainfall runoff process of the watershed.

B. Further study need for detail analysis of land cover in the catchment by taking more ground control point and checking the overall accuracy and Kappa Statistics before interpretation of Satellite image.

C. The reservoirs used as main water source of the city which are found in upper parts of the catchment regulate stream flow need in depth research in the effect of LULC on Water balance.

D. SWAT model calibrated using observed flow data at gauging station. In order to improve the model performance, the weather stations should be improved both in quality and quantity. Hence, it is highly recommended to establish a good network of both hydrometric and meteorological stations.

E. As only river discharges were calibrated and validated, it has to be emphasized that other outputs presented in this study, such as sediment yield, have to be treated with caution. The model could be further tested when data on sediment load is available.

List of References

AAWSA, AAU (2003): Ground water vulnerability mapping of the Addis Ababa Water supply Aquifers, Ethiopia. Report to UNEP/UNESCO/UNHABITAT/ECA

AAWSA, BCEOM (2000) Seureca-Space in association with tropics Engineers): Akaki Ground water model report: Report V. I-IV.

AAWSA, TAHAL (2000) Bathymeteric Survey for the Legedadi and Geffersa Reservoirs and Master plan study for Legedadi Dire and Geffersa Catchment Areas: Final Report AAWSA

access capital (2010): Investing in Ethiopia ,access Report Real State

Ahmed, G., (2001): Mapping a Dry Shrub Forest for Biodiversity Conservation Planning. (A case study in the salt range of Pakistan, using remote sensing and GIS tools) Forest Science Division, the International Institute for Geoinformation Science and Earth Observation (ITC), Enschede, Netherlands. February, 2001.

Arnold, J.G. and Allen, P.M. (1996): Estimating hydrologic budgets for three Illinois watersheds. J. Hydrology 176:57-77.

Arnold, J.G., R. Srinivasan, R.S. Muttiah, and P.M. Allen, (1999): Continental scale simulation of the hydrologic balance. J. Am. Water Resource Association 35(5), 1037-1051

AAMP (2000): Addis Ababa Master Plan Revision Project: Addis Ababa City Administration

Beven, K.J. (ed) (1997). Distributed Modelling in Hydrology: Application of the TOPMODEL concept. Wiley, Chichester, 360 p.

Chase, T.N., R.A. Pielke Sr., T.G.F. Kittel, R.R. Nemani & S.W. Running (2000). Simulated impacts of historical land cover changes on global climate in northern winter. *Climate Dynamics*, 16: 93-105

Chow, V.T., D.R. Maidment and L.W. Mays. 1988: Applied Hydrology McGraw-Hill: New York.

Central Statistical Authority 2007: Summary and statistical Report of the 2007 Population and Housing census. December 2008

Central Statistical Authority 2004: Statistical Abstract 2003. Addis Ababa. January 2004

Central Statistical Authority 1999: The Population and Housing Census of Ethiopia: Results at Country Level. Volume I. Statistical Report. June 1999.

Central Statistical Authority 1995: Population and Housing Census of Ethiopia: Results for Addis Ababa. Volume I – Statistical Report

Cunderlik, 2003: Hyderological model selection for the CFCAS project Assessment of water Resources Risk and Vulnerability change climatic condition, Water Resources Research Report No.046

de Sherbinin, A. (2002): Land-Use and Land-Cover Change, A CIESIN Thematic Guide.

Center for International Earth Science Information Network (CIESIN) of Columbia University, Palisades, NY, USA. http://sedac.ciesin.columbia.edu/tg/guide_main.jsp.

Daniel Gemechu, 1977. Aspects of Climate and Water Budget in Ethiopia. A Technical

Monograph Published For Addis Ababa University. Addis Ababa University Press.

Daniel P. Loucks,(2005):Water Resources systems planning and management ,An introduction to ,models and applications UNESCO publishing.

Dingman, S.L. (2002): Physical Hydrology (2nd ed.), Prentice Hall Inc., USA.

ERDAS Field Guide(2005): User manual of ERDAS IMAGINE ,Leica Geosystems ,Norcross Georgia

FAO (Food and Agricultural Organization) 2002: Major Soils of the World. Land and Water Digital Media Series. FAO Soil Buletin.No (19)

FAO (2006): Irrigation and Drainage paper No 56 Rome Italy.

FAO, (1995): Digital Soil Map of the World and Derived Soil Properties (CDROM) Food and Agriculture Organization of the United Nations,FAO

FAO, (1998): The Soil and Terrain Database for northeastern Africa (CDROM) FAO, Rome.

Fessahatsion Zemuy(2008):Effect of Urbanization on Flood Generation (A Case Study on Addis Ababa City).Arba Minch Univesristy. Arba Minch Ethiopia

Fetter C. W., 1994. Applied Hydrogeology. Prentice Hall, Upper Saddle River, New Jersey.

Githu (2007): Assessing the impacts of environmental change on the hydrology of the Nzoia catchment, in the Lake Victoria Basin Department of Hydrology and Hydraulic Engineering Faculty of Engineering Vrije Universiteit Brussels

Green, W.H. and Ampt, G.A. (1911): Studies in Soil Physics, I: The Flow of Air and Water Through Soils. Journal of Agricultural Sciences 4:1-24.

Halcrow (1989): Awash Master Plan Project MoWR, Addis Ababa, Ethiopia.

JICA and Region 14 Administration (1998) Addis Ababa flood control project Volume V

Lenhart, T., K. Eckhardt, N. Fohrer, H.-G. Frede, (2002): Comparison of two different approaches of sensitivity analysis, Physics and Chemistry of the Earth 27 (2002), Elsevier Science Ltd., 645–654pp

Leica Geosystems (October, 2007) ERDAS Field Guide Volume II, LLC (United States of America)

Liersch S., August (2003):Dew02 Users' Manual, Berlin, 5pp.

Lindström, G., Johansson, B., Persson, M., Gardelin, M., Bergström, S. (1997). Development and test of the distributed HBV-96 hydrological model. Journal of Hydrology 201, pp.272-288.

Lillesand, T.M. and Kiefer, R.W. (1994): Remote sensing and image interpretation. New York: John Wiley and Sons, Inc.

Luzio, M. Di, R. Srinivasan, J.G. Arnold, S.L. Neitsch, (2002): ArcView Interface for SWAT2000 (AVSWAT2000), User's Guide, Grassland Soil and Water Research Laboratory, Blackland Research Center, Texas Agricultural Experiment Station, Texas Water Resources Institute, Texas Water Resources Institute,

Maidment, D.R., editor, (1993a): Handbook of hydrology. New York: McGraw Hill.

Moriasi, D.N, J. G. Arnold, M. W. Van Liew, R. L. Bingner, R. D. Harem,T. L.Veith, (2007):Model evaluation guidelines for systematic quantification of accuracy in Watershed simulations. Vol. 50(3), 850-900pp. American society of Agricultural and Biological Engineers ISSN 0001-235

Morris.M.D., (1991). Factorial sampling plans for preliminary comp experiments. Tecnometrics. Vol.33 nr2

Mustard, J., R. DeFries, T. Fisher & E. Moran (2004). Land Use and Land Cover Change Pathways and Impacts.

Nash, J.E., Sutcliffe, J.V., 1970. River flow forecasting through conceptual models Part I: adiscussion of principles, J. Hydrol., 10, 282-290.

Nathan R.J and T.A McMahon 1990: Evaluation of automated techniques for base flow and recession analysis. Water Resources Research V.26 No 7 pp 1465-1473

Neitsch, S.L. Arnold, J.G., Kiniry, J.R., Srinivasan, R., and Williams, J.R. 2002: Soil and Water Assessment Tool Theoretical Documentation. Texas,Texas Water Resources Institute, Collage Station.

Neitsch, S. L., J. G. Arnold, J. R. Kiniry, R. Srinivasan, and J. R. Williams. (2005): Soil and Water Assessment Tool Input/output File Documentation, Version 2005. Temple, Texas at http://www.brc.tamus.edu/swat College Station, Texas TWRI Report TR-193, 345pp.

Njau E. C., 1996.Generalized Derivation of the Angstrom and Angstrom-Prescott Equations, Renewable Energy, Vol. 7, No. 1, pp. 105-108. Penman, H.L. (1956).

Evaporation: An introductory survey. Netherlands Journal of Agricultural Science 4:7-29.

Piao, S., P. Friedlingstein, P. Ciais, N. de Noblet-Ducoudre´, D. Labat & S. Zaehle (2007). Changes in climate and land use have a larger direct impact than rising CO2 on global river runoff trends. *PNAS*, 104(39): 15242-15247

Refsgaard J.C. (1996) Terminology, modelling protocol and classification of hydrological model codes. In: Abbott MB, Refsgaard JC (Eds): Distributed Hydrological Modelling, Kluwer Academic Publishers, 17-39.

Reid, R.S., Kruska, R.L., Muthui, N., Taye, A., Wotton, S., Wilson, C.J. and Woudyalew

Mulatu (2000). Land-use and land-cover dynamics in response to changes in climatic, biological and socio-political forces: the case of southwestern Ethiopia. Landscape Ecology 15: 339-355

Sahin, V. & M.J. Hall (1996). The effects of afforestation and deforestation on water yields. Journal of Hydrology,178: 293-309.

Shahin, M. (2002): Hydrology and water resources of Africa. Kluwer Academic Publishers, Dordrecht, Niederlande, 659 p.

Soil Conservation Service, (1972): Section 4: Hydrology in National Engineering Handbook. SCS.

Taye Aduna(2009): The impact of land use/ land cover change on catchment hydrology and water quality of Legedad-Dire catchments. Addis Ababa Univesity Addis Ababa Ethiopia

US-ACE (2000). Hydrologic Modeling System HEC-HMS. Technical Reference Manual. US

Army Corps of Engineers, Hydrologic Engineering Center, 149 p.

USDA, Soil Conservation Service (1972): National Engineering Handbook, Section 4: Hydrology. U.S. Government Printing Office, Washington, DC

UN-HABITAT (2007) Situation Analysis of Informal Settlements in Addis Ababa

Van Griensven, A., Meixner, T., Grunwald, S., Bishop, T., Diluzio, M., and Srinivasan, R., 2006. A global sensitivity analysis tool for the parameters of multi-variable catchment models. (Publisher and place of publication)

Ward A.D and W.J Elliot 1995: Environmental hydrological. Lewis Publishers CRC Press, Inc Boca Raton, FL

Williams, J.R. (1969).Flood routing with variable travel time or variable storage coefficients.TransASAE12(1):100103.http://www.brc.tamus.edu/swat/soft_links.html,SWAT(ArcSWAT)website accessedJune,10, 2010

http://www.brc.tamus.edu/swat/soft_links.htl Weather parameter calculator WXPARM (Williams, 1991) and dew point temperature calculator DEW02 programs accessed July, 20, 2010

APPENDIX

Appendix A: Meteorological Locations of the study Area

S. No	Station Name	XPR	YPR	ELEVATION
1	Sendafa	501751.23	1011522.84	2560.00
2	Intoto	496336.15	1013384.28	2205.00
3	Akaki	478060.00	980217.00	2075.00
4	Addis Ababa Observatory	474168.17	993246.95	2225.00
5	Addis Ababa Bole	472306.73	998662.03	2324.00

Appendix-B Weather generator (WGEN) parameters used by the SWAT Model

For Addis Ababa Bole Station

Month	PCP_MM	PCPSTD	PCPSKW	PR_W1	PR_W2	PCPD	tmp_max	tmp_min	hmd	dewpt
Jan.	14.31	2.76	9.41	0.04	0.32	1.92	24.11	8.61	55.43	8.29
Feb.	33.87	4.22	4.78	0.11	0.39	4.46	25.61	8.56	47.36	6.74
Mar.	69.08	6.86	4.53	0.17	0.47	7.65	25.62	10.78	53.91	9.11
Apr.	93.11	7.39	5.08	0.25	0.52	10.92	25.58	11.36	53.04	9.22
May.	74.85	7.00	4.71	0.17	0.53	8.54	25.78	11.49	52.39	9.03
Jun.	122.38	6.81	4.16	0.42	0.69	17.77	23.94	10.95	63.97	11.31
Jul.	234.58	8.16	1.50	0.72	0.81	25.31	21.53	11.3	75.05	12.47
Aug.	238.65	8.38	1.60	0.71	0.79	24.88	21.23	11.45	76.17	12.59
Sep.	133.04	7.08	2.74	0.40	0.63	16.50	22.22	10.74	66.32	10.72
Oct.	31.81	4.45	6.24	0.08	0.35	3.69	23.26	9.05	52.65	6.81
Nov.	3.50	1.10	13.43	0.02	0.16	0.73	23.44	6.98	48.06	5.21
Dec.	4.58	1.83	15.43	0.01	0.23	0.50	23.51	6.88	52.92	6.73

PCP_MM = average monthly precipitation [mm]

PCPSTD = standard deviation

PCPSKW = skew coefficient

PR_W1 = probability of a wet day following a dry day

PR_W2 = probability of a wet day following a wet day

tmp_max = average daily maximum temperature in month [°C]

tmp_min = average daily minimum temperature in month [°C]

hmd = average daily humidity in month [%]

dewpt = average daily dew point temperature in month [°C]

For Addis Ababa Observatory Station

Month	PCP_MM	PCPSTD	PCPSKW	PR_W1	PR_W2	PCPD
Jan.	14.23	2.50	7.54	0.05	0.29	2.00
Feb.	40.24	4.98	5.33	0.10	0.46	4.92
Mar.	70.35	7.07	6.09	0.18	0.48	8.15
Apr.	94.69	7.62	4.53	0.27	0.54	11.65
May.	86.69	7.21	3.57	0.19	0.54	9.69
Jun.	139.21	6.58	2.29	0.45	0.73	19.42
Jul.	269.80	9.14	1.71	0.81	0.85	27.23
Aug.	284.63	9.60	1.89	0.78	0.84	26.92
Sep.	168.46	8.84	2.33	0.38	0.70	17.92
Oct.	38.53	5.03	8.45	0.09	0.51	5.62
Nov.	5.73	1.54	11.08	0.02	0.25	0.92
Dec.	9.32	2.96	14.77	0.03	0.27	1.15

PCP_MM = average monthly precipitation [mm]

PCPSTD = standard deviation

PCPSKW = skew coefficient

PR_W1 = probability of a wet day following a dry day

PR_W2 = probability of a wet day following a wet day

APPENDIX-C Monthly Precipitation Data

Metrological Station – Addis Ababa Bole

Year	Jan.	Feb.	Mar.	Apr.	May.	Jun.	Jul.	Aug.	Sep.	Oct.	Nov.	Dec.	Total Yearly(pcp)
1980	24	27	65	76	45	129	269	215	119	0	0	0	969
1981	0	43	254	82	19	58	277	258	180	25	0	0	1196
1982	27	97	91	49	75	66	222	226	143	19	42	4	1061
1983	12	42	29	114	188	57	218	214	203	37	0	1	1115
1984	0	0	11	12	136	336	317	181	100	0	0	7	1100
1985	34	0	49	133	94	113	210	263	168	31	0	0	1095
1986	0	39	55	218	38	177	168	224	107	31	0	3	1060
1987	0	49	179	86	155	75	158	100	58	17	0	0	877
1988	6	34	7	158	35	96	185	265	189	58	0	0	1033
1989	3	34	58	146	0	89	221	321	151	37	0	8	1068
1990	3	162	60	145	25	49	196	298	146	47	2	0	1133
1991	0	29	136	14	8	106	281	292	125	4	2	0	997
1992	14	28	35	59	55	85	256	226	160	64	2	0	984
1993	12	52	12	170	94	159	213	294	190	24	0	0	1220
1994	0	0	53	70	30	115	243	199	99	0	11	0	820
1995	0	82	72	136	97	79	169	261	93	0	0	30	1019
1996	21	16	136	94	127	294	346	316	212	0	0	0	1562
1997	26	0	13	66	39	104	259	149	95	56	16	0	823
1998	68	40	45	99	200	113	274	240	177	139	0	0	1395
1999	4	0	36	18	30	107	294	274	63	127	0	0	953
2000	0	0	17	88	96	103	194	225	159	20	8	0	910
2001	0	11	176	14	119	170	291	209	115	10	0	0	1115
2002	31	26	81	37	50	115	214	237	74	1	0	33	899
2003	5	42.7	50	112	17	112	207	240	131	4	0	33	953.65
2004	27	12	33	106	7	115	241	229	125	51	1	0	946.88
2005	55	15	43	119	167	160	176	249	77	25	7	0	1093

Metrological Station – Intoto

Year	Jan	Feb	Mar	Apr	May	Jun	July	Aug	Sep	Oct	Nev	Dec
1997	21.2	0	18.6	77.3	27.4	77.2	256	241	89.3	88.3	90	0.2
1998	25.3	25.3	45.2	47	150	149	369	376	205	44.5	0	0
1999	15.8	6.3	34.9	25.4	37	128	283	280	105	58	0.2	0
2000	0	0	5.2	108	91.4	111	304	359	133	17.2	33.5	1.7
2001	20.6	5.5	148	29.8	142	164	286	321	92.5	52.4	0	1.8
2002	17.9	50.4	88.8	67.4	49.2	139	293	263	92.1	10.7	0	28
2003	5.2	47.7	57.1	117	13.9	188	371	249	141	0	6.3	25.6
2004	28.8	31.3	46.7	125	13.8	166	272	335	125	49.7	1.1	1.6

Metrological Station – Addis Ababa Observatory

Year	Jan.	Feb.	Mar.	Apr.	May.	Jun.	Jul.	Aug.	Sep.	Oct.	Nov.	Dec.	Total Yearly(pcp)
1980	23	41.4	46	88	54	126	386	298	111	52	0	0	1225.35
1981	0	76	175	84	4	52	268	324	185	13	0	5	1186
1982	49	81	58	103	115	32	258	259	133	63	43	12	1206
1983	18	21	49	118	241	109	202	246	163	27	0	9	1203
1984	0	8	9	8	129	223	296	296	141	0	4	16	1130
1985	14	0	17	97	85	112	270	330	205	58	3	1	1192
1986	0	37	88	201	127	180	179	273	130	37	0	3.35	1255.69
1987	1	63	250	83	242	92	199	257	117	20	1	0	1325
1988	9	54	5	146	16	108	280	299	232	60	0	0	1209
1989	1	76	76	157	1	122	360	326	189	14	0	7	1329
1990	1	158	61	108	21	90	221	269	185	16	6	0	1136
1991	0	75	109	34	64	205	249	261	126	3	0	49	1175.42
1992	20	33	20	40	52	111	249	294	209	69	0	3	1100
1993	11	67	17	159	100	211	277	428	246	63	0	5	1584
1994	0	0	82	84	64	127	309	226	143	1	14	0	1050
1995	0	69	42	176	69	105	193	315	138	0	0	55.69	1162.69
1996	27	6	107	128	122	258	269	341	294	0	0	3.35	1555.35
1997	39	0	24	51	39	104	273	195	116	63	52	2	958
1998	56	21	49	49	154	126	290	260	213	126	0	0	1344
1999	3	0	29	16	24	117	279	306	90	74	0	0	937.69
2000	0	0	17	47	111	145	248	304	252	47	21	0	1192
2001	0	12	212	26	168	216	427	250	135	15	0	0	1461
2002	15	21	89	57	64	172	256	217	107	0	0	16	1014
2003	11	54	63	100	20	154	291	235	193	1	1	55	1178
2004	25	21	50	141	31	140	238	276	163	76	0	0	1161
2005	47	52	85	161	137	182	248	315	164	104	4	0	1498.7

Metrological Station – Akaki

Year	Jan	Feb	Mar	Apr	May	Jun	July	Aug	Sep	Oct	Nev	Dec
1997	0	0	29.1	93	64.9	100	189	210	124	17.2	23.4	3.8
1998	0	20.7	121	23.6	118	143	258	145	64.9	2.2	0	0
1999	31.1	10.5	87.8	53.9	76.6	108	167	166	52.3	0	0	17.7
2000	19.6	24.8	23.9	114	1.4	125	325	307	113	0	0	40.8
2001	15.6	15.8	61.4	155	15.4	95.2	150	189	80.9	4.8	3.4	0.7
2002	28.8	7.3	47.9	112	141	140	219	231	153	9.1	15.2	0
2003	2.6	44.2	56.3	79.7	22	84.3	276	268	143	38	0	3.2
2004	34.2	24.7	25.6	96.8	64.6	133	254	222	149	14.3	1.3	0

Metrological Station – Sendafa

Year	Jan	Feb	Mar	Apr	May	Jun	July	Aug	Sep	Oct	Nev	Dec
1997	44.5	0	29.4	60	44.8	150	304	251	84.7	72	34.6	0
1998	28.9	23.3	5.8	27	38.2	68.8	359	290	152	98.9	0	0
1999	0	1.2	56.3	11.8	25.4	145	442	365		79.6	0	0
2000	0	0	35.5	44	87.9	166	352	373	114	5	10	0
2001	0	35.3	154	9.2	135	150	336	277	27.4	9.8	0	0
2002	21.2	3.4	67.2	20.6	60.9	144	247	289	85.4	0	0	27.4
2003	75.5	0	29.7	123	1.7	121	304	373	122	0	0	19.7
2004	15.2	7.1	2.2	119	0	69.8	315	319	30.6	0	0	0

Appendix D: Double mass curve plots

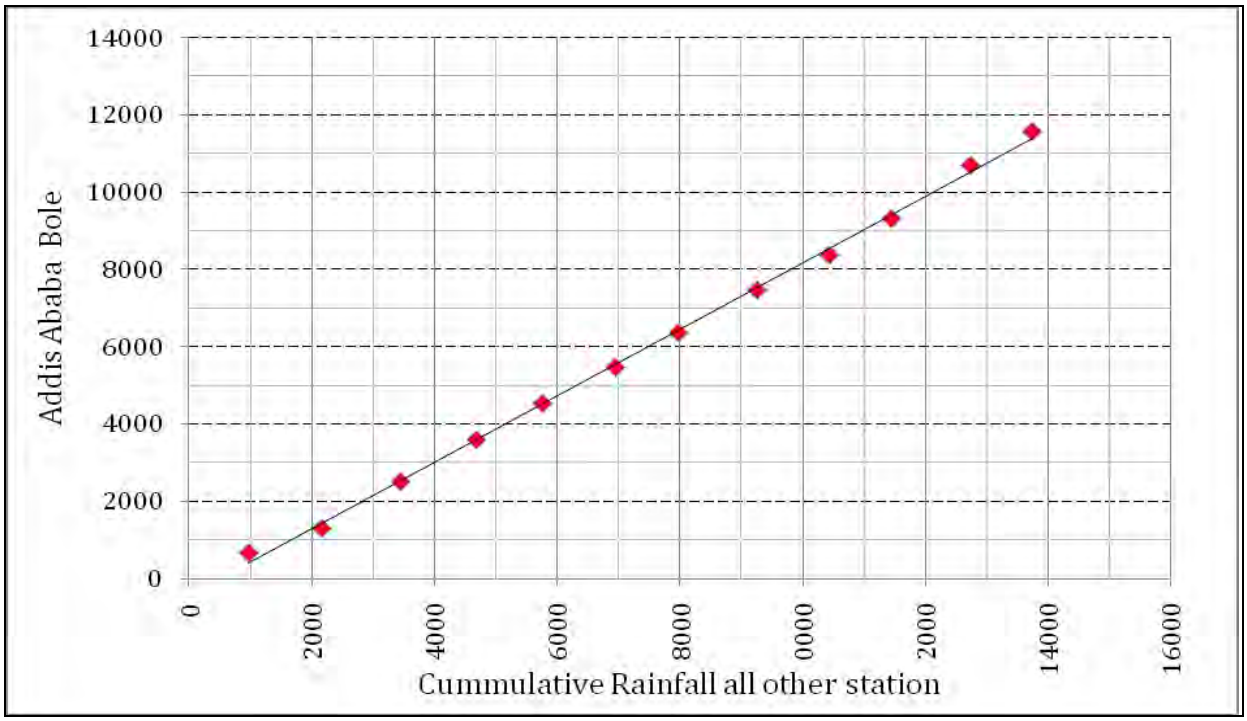

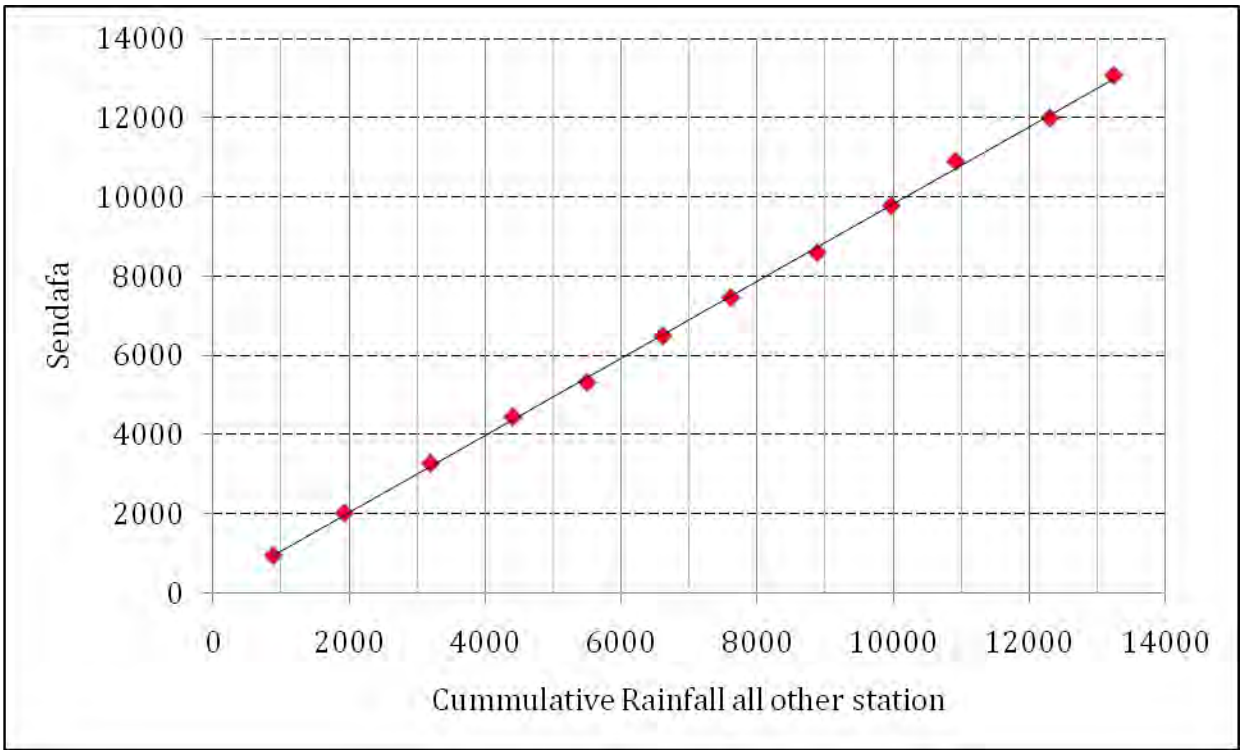

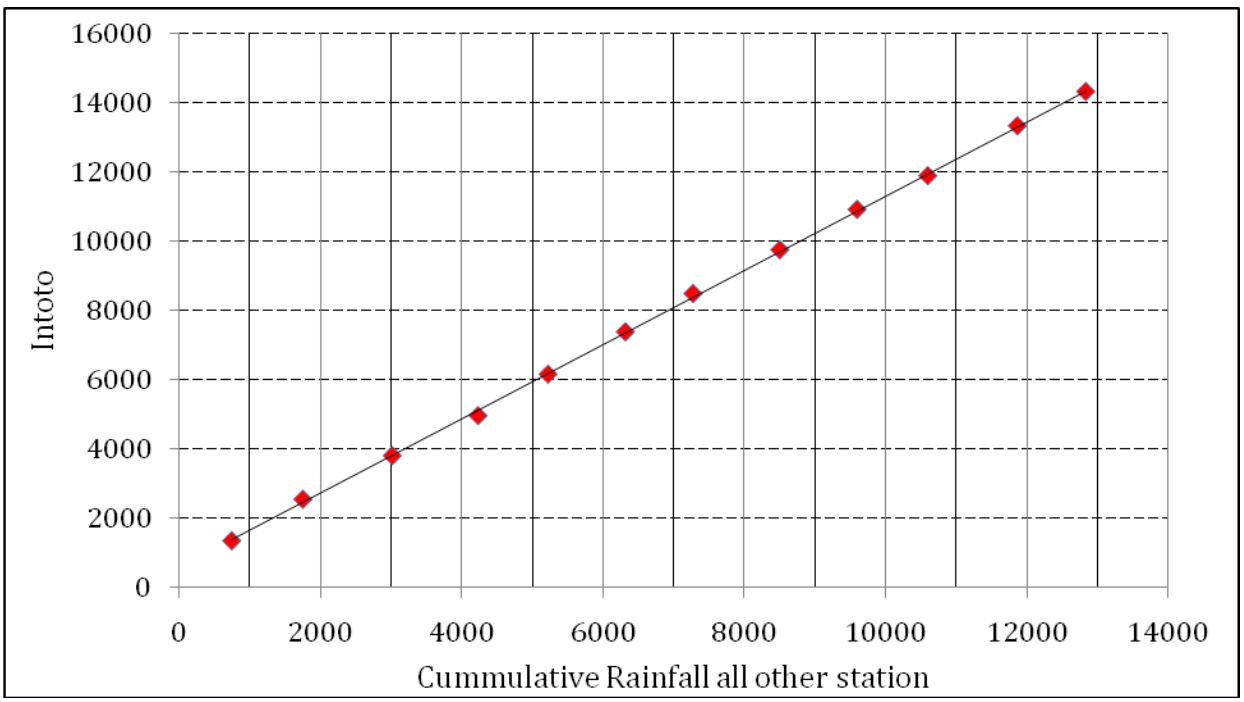
16000
14000
12000
10000
8000
6000
4000
2000
0
Intoto
0
2000
4000
6000
8000
10000
12000
14000
Cummulative Rainfall all other station

Appendix E: Model Output for the Reservoirs

Variable name	Definition
RES	Reservoir number **Note (Our case……..** **1-Dere and** **2-Legedadi Reservoirs**
MON	Daily time step: the julian date, Monthly time step: the month (1-12), Annual time step: four-digit year
VOLUME	Volume of water in reservoir at end of time step (m3 H2O).
FLOW_IN	Average flow into reservoir during time step (m3/s H2O).
FLOW_OUT	Average flow out of reservoir during time step (m3/s H2O).
PRECIP	Precipitation falling directly on the reservoir during the time step (m3 H2O).
EVAP	Evaporation from the reservoir during the time step (m3 H2O).

RES	YEAR	MON	VOLUME(m^3)	FLOW_OUTcms	FLOW_INcms	PRECIP(m^3)	EVAP(m^3)	EVAP(m^3)
1	1997	Jan-97	19050000	0	0.00203	8512	30970	0.03097
1	1997	Feb-97	18200000	0	0.005244	0	25300	0.0253
1	1997	Mar-97	17270000	0	0.004991	18420	30730	0.03073
1	1997	Apr-97	16410000	0	0.02034	14920	24430	0.02443
1	1997	May-97	15520000	0	0.01572	23690	27710	0.02771
1	1997	Jun-97	14820000	0	0.06201	66730	25400	0.0254
1	1997	Jul-97	16060000	0	0.7333	219600	15920	0.01592
1	1997	Aug-97	17770000	0	0.9077	226000	19090	0.01909
1	1997	Sep-97	18350000	0	0.5445	88820	23120	0.02312
1	1997	Oct-97	18160000	0	0.2559	86360	32180	0.03218
1	1997	Nov-97	18030000	0	0.2762	89720	29400	0.0294
1	1997	Dec-97	18510000	0	0.5372	0	30770	0.03077
1	1998	Jan-98	18610000	0	0.3912	9245	27820	0.02782
1	1998	Feb-98	18080000	0	0.1295	25380	28270	0.02827
1	1998	Mar-98	18000000	0	0.3114	44890	31050	0.03105
1	1998	Apr-98	17640000	0	0.2011	47270	27840	0.02784
1	1998	May-98	19970000	0	1.501	152900	31960	0.03196
1	1998	Jun-98	19970000	0.4401	1.735	164100	21090	0.02109
1	1998	Jul-98	19970000	4.814	4.995	403700	19060	0.01906
1	1998	Aug-98	19970000	9.24	8.22	410300	20610	0.02061
1	1998	Sep-98	19970000	6.157	7.677	226500	24430	0.02443
1	1998	Oct-98	19970000	3.731	4.07	48140	29040	0.02904
1	1998	Nov-98	19970000	1.288	1.647	0	27610	0.02761
1	1998	Dec-98	19950000	0.1576	0.5089	0	31630	0.03163
1	1999	Jan-99	19470000	0	0.1736	16270	29260	0.02926
1	1999	Feb-99	18740000	0	0.05512	6251	26800	0.0268
1	1999	Mar-99	17950000	0	0.04966	36600	29110	0.02911
1	1999	Apr-99	17170000	0	0.04741	24170	25460	0.02546
1	1999	May-99	16380000	0	0.04944	34220	29210	0.02921
1	1999	Jun-99	16750000	0	0.4533	116700	25050	0.02505
1	1999	Jul-99	19970000	2.133	3.559	293100	19380	0.01938
1	1999	Aug-99	19970000	6.746	5.778	315800	21510	0.02151
1	1999	Sep-99	19970000	3.078	4.633	116000	30680	0.03068
1	1999	Oct-99	19970000	2.501	2.833	64550	29720	0.02972
1	1999	Nov-99	19970000	0.834	1.193	0	27200	0.0272
1	1999	Dec-99	19860000	0.05692	0.372	0	23990	0.02399
1	2000	Jan-00	19210000	0	0.1156	0	29270	0.02927
1	2000	Feb-00	18370000	0	0.02518	0	28880	0.02888
1	2000	Mar-00	17430000	0	0.001957	8216	28560	0.02856
1	2000	Apr-00	16830000	0	0.1035	65300	27620	0.02762
1	2000	May-00	18200000	0	0.8453	48630	19580	0.01958
1	2000	Jun-00	19730000	0	0.8982	116800	12410	0.01241
1	2000	Jul-00	19970000	4.087	4.356	391600	13990	0.01399
1	2000	Aug-00	19970000	7.991	6.911	334800	9254	0.009254
1	2000	Sep-00	19970000	3.834	5.477	145500	22010	0.02201
1	2000	Oct-00	19970000	3.006	3.356	17500	22760	0.02276
1	2000	Nov-00	19970000	1.142	1.483	37200	23610	0.02361
1	2000	Dec-00	19970000	0.2517	0.6079	1094	24860	0.02486
1	2001	Jan-01	19780000	0	0.2794	22880	30780	0.03078
1	2001	Feb-01	19280000	0	0.1514	6477	25470	0.02547
1	2001	Mar-01	19080000	0	0.251	80610	31190	0.03119
1	2001	Apr-01	19440000	0	0.4852	33040	28360	0.02836
1	2001	May-01	19600000	0	0.387	90870	32410	0.03241
1	2001	Jun-01	19970000	1.117	1.531	180200	24430	0.02443
1	2001	Jul-01	19970000	3.349	3.569	314000	19820	0.01982
1	2001	Aug-01	19970000	8	6.965	353400	23100	0.0231
1	2001	Sep-01	19970000	3.694	5.306	101700	22300	0.0223
1	2001	Oct-01	19970000	2.28	2.616	57990	30760	0.03076
1	2001	Nov-01	19970000	0.9002	1.26	0	27510	0.02751
1	2001	Dec-01	19900000	0.08825	0.4188	2188	28730	0.02873
1	2002	Jan-02	19410000	0	0.1659	19580	19390	0.01939
1	2002	Feb-02	19210000	0	0.2535	52340	30730	0.03073
1	2002	Mar-02	19970000	0.6018	1.204	98950	29920	0.02992
1	2002	Apr-02	19970000	1.076	1.4	74400	23050	0.02305
1	2002	May-02	19970000	0.7493	1.082	54700	21580	0.02158
1	2002	Jun-02	19970000	0.6787	0.9661	153200	19160	0.01916
1	2002	Jul-02	19970000	3.287	3.502	318400	13640	0.01364
1	2002	Aug-02	19970000	6.601	5.548	291000	21900	0.0219
1	2002	Sep-02	19970000	3.592	5.246	102800	21530	0.02153
1	2002	Oct-02	19970000	2.233	2.587	12030	26230	0.02623
1	2002	Nov-02	19970000	0.5193	0.8773	0	24150	0.02415
1	2002	Dec-02	19790000	0.016	0.303	30500	23060	0.02306

RES	YEAR	MON	VOLUMEm^3	FLOW_INcms	FLOW_OUTcms	PRECIPm3	EVAPm3
2	1997	Jan-97	20200000	0.01495	0	254.9	726.7
2	1997	Feb-97	17210000	0.01337	0	0	815.4
2	1997	Mar-97	13940000	0.01696	0	800.7	1207
2	1997	Apr-97	11020000	0.1037	0	1967	2187
2	1997	May-97	7918000	0.07166	0	3010	3399
2	1997	Jun-97	6352000	0.6065	0	30390	8087
2	1997	Jul-97	18380000	5.584	0	419300	28270
2	1997	Aug-97	23400000	4.703	1.843	687800	57150
2	1997	Sep-97	23340000	1.92	0.8089	268600	70980
2	1997	Oct-97	23340000	1.168	0	298000	99680
2	1997	Nov-97	23390000	1.536	0.3555	351000	113500
2	1997	Dec-97	23350000	1.553	0.3105	0	125300
2	1998	Jan-98	22110000	0.7816	0	40750	121600
2	1998	Feb-98	19950000	0.3356	0	115500	127100
2	1998	Mar-98	17920000	0.4558	0	211500	146300
2	1998	Apr-98	15560000	0.3017	0	232200	134200
2	1998	May-98	16110000	1.343	0	449100	91820
2	1998	Jun-98	18450000	2.023	0	436400	55540
2	1998	Jul-98	23390000	14.62	11.91	1068000	50040
2	1998	Aug-98	23400000	20.63	19.81	1091000	54220
2	1998	Sep-98	23400000	16.48	15.48	874600	103500
2	1998	Oct-98	23390000	10.02	8.811	218500	129900
2	1998	Nov-98	23390000	3.607	2.353	0	123500
2	1998	Dec-98	23240000	1.554	0.3559	0	132500
2	1999	Jan-99	21600000	0.6243	0	74500	132300
2	1999	Feb-99	19100000	0.2168	0	29800	124800
2	1999	Mar-99	16040000	0.07793	0	178800	143500
2	1999	Apr-99	13140000	0.109	0	124100	128000
2	1999	May-99	10110000	0.0927	0	113200	95970
2	1999	Jun-99	13360000	2.427	0	380300	81250
2	1999	Jul-99	23390000	17.02	12.31	827200	53250
2	1999	Aug-99	23400000	21.85	20.94	857500	56560
2	1999	Sep-99	23400000	13.68	12.57	458900	125000
2	1999	Oct-99	23390000	8.97	7.778	293000	133000
2	1999	Nov-99	23390000	3.97	2.717	0	121700
2	1999	Dec-99	23350000	1.72	0.4874	0	110400
2	2000	Jan-00	21900000	0.7156	0	0	133400
2	2000	Feb-00	19360000	0.2373	0	0	132600
2	2000	Mar-00	16180000	0.05912	0	40590	141000
2	2000	Apr-00	14040000	0.3722	0	335700	145400
2	2000	May-00	14510000	1.385	0	147900	62850
2	2000	Jun-00	21050000	3.672	0	329300	35780
2	2000	Jul-00	23390000	16.72	14.98	1037000	36920
2	2000	Aug-00	23400000	21.31	20.42	877400	25340
2	2000	Sep-00	23400000	13.4	12.32	588000	86350
2	2000	Oct-00	23390000	7.296	6.065	79460	103200
2	2000	Nov-00	23390000	3.182	1.969	168900	105800
2	2000	Dec-00	23230000	1.522	0.3347	4966	113100
2	2001	Jan-01	21680000	0.6542	0	104300	138400
2	2001	Feb-01	19900000	0.5115	0	29800	116200
2	2001	Mar-01	18990000	0.8501	0	358400	145500
2	2001	Apr-01	19010000	1.231	0	154000	130900
2	2001	May-01	19020000	1.18	0	257100	91330
2	2001	Jun-01	23390000	3.892	1.119	486700	65390
2	2001	Jul-01	23390000	13.76	12.82	835600	52000
2	2001	Aug-01	23400000	18.91	18.02	954500	61160
2	2001	Sep-01	23400000	11.24	10.12	349300	87650
2	2001	Oct-01	23390000	4.998	3.799	263200	137600
2	2001	Nov-01	23390000	2.324	1.07	0	123300
2	2001	Dec-01	22660000	1.008	0.02936	9933	128700
2	2002	Jan-02	20750000	0.5141	0	89400	88620
2	2002	Feb-02	18980000	0.471	0	248300	142900
2	2002	Mar-02	21010000	1.929	0	456900	135800
2	2002	Apr-02	23390000	2.264	0.1636	337700	104400
2	2002	May-02	23390000	1.965	0.7704	173200	61210
2	2002	Jun-02	23390000	3.928	2.835	412600	52740
2	2002	Jul-02	23390000	11.12	10.19	835900	36050
2	2002	Aug-02	23400000	16.51	15.56	786600	59420
2	2002	Sep-02	23400000	11.81	10.69	354600	88390
2	2002	Oct-02	23390000	5.615	4.375	54630	120400
2	2002	Nov-02	23390000	2.256	1.007	0	103900
2	2002	Dec-02	22720000	1.026	0.02421	139100	104700

Appendix F. Graphical Representation of Model Out Put for Legedadi and Dere Reservoirs